SCUOLA NORMALE SUPERIORE

PH. D. THESIS

Precursor and mature Nerve Growth Factor trafficking in neurons through a novel site specific labeling strategy

Teresa De Nadai

ADVISOR

Prof. Antonino Cattaneo

2015

To my grandmothers, Antonia and Teresina,
who've been a rock of stability throughout my life,
and whose loving spirit sustains me still.

Foreword

This thesis is the result of my research activity at the NEST and at BioLab laboratories of Scuola Normale Superiore in Pisa: I began my studies on Nerve Growth Factor in 2010, motivated by the strong interest in Neurotrophins that Prof. Antonino Cattaneo inherited directly from Prof. Rita Levi Montalcini and transmitted to me. This research was carried out in the framework of a PhD program sponsored by Scuola Normale Superiore.

Table of Contents

List of Figures and Tables

List of Abbreviations

AD	Alzheimer's disease
Amp	Ampicillin
BDNF	Brain-derived neurotrophic factor
CD	Chopper domain
CNS	Central nervous system
CoA	*Coenzima A*
CRD	Cystein-rich domain
DD	Death domain
DRG	Dorsal root ganglion
IgL-D	Immunoglobulin-like domain
LB	Luria broth
LRR	Leucine-rich domain
MN	Motor neuron
NGF	Nerve growth factor
NT3	Neurotrophin-3
NT4-5	Neurotrophin-4/5
NTs	Neurotrophins
$p75^{NTR}$	p75 neurotrophin receptor
PDB	Protein Data Ban
SCG	Superior cervical ganglion
SFP Synthase	4´-phosphopantetheinyl transferase
TKD	Tyrosine-kinase domain
Trk	Tropomyosin receptor kinase

Introduction

The peculiar architecture and morphology of neurons requires unique mechanisms for intracellular communication. Specialized strategies have evolved through which signals emanating from the axon tips are transmitted to the soma of neurons, where an appropriate response is mediated. Neurotrophins exploit this strategy.

Neurotrophins are essential for proper neuronal subtype specification, synapse and circuit formation, and in helping neurons to respond to axon injury. The most studied neurotrophin is the Nerve Growth Factor (NGF). Latest findings highlighted the fundamental importance of proNGF, NGF precursor, known to be the most abundant form of this factor in the brain. In fact, proNGF can either act as an intracellular or secreted precursor for mature NGF or remain unprocessed, respectively activating survival/differentiation or apoptosis pathways. Moreover, the different biological function of NGF and proNGF is proved by the observation that, when administered separately or together in target cells, they activate distinct and peculiar gene expression patterns. Evidences report that the reciprocal levels of NGF and of its unprocessed precursor proNGF play a crucial role in regulating the survival/death balance of several neuronal populations in physiopathological conditions. The disruption of this balance leads to neurodegeneration, as it is demonstrated by the increase of proNGF levels versus NGF in the brain cortex in patients affected by Alzheimer's disease. Thus, describing the signaling mechanisms that link NGF and proNGF cellular trafficking to their specific biological function is of crucial importance. In particular, the question whether pro-neurotrophins retrogradely move along axons like their mature counterparts has remained so far almost unexplored.

Chemically labeled NGF has been previously used to study axonal transport of the neurotrophin. Those studies have provided valuable information on NGF trafficking. However, these suffer from the substantial impossibility to control the exact number and site of conjugated probes, so that heterogeneous and not fully reproducible labeled protein populations are obtained. Similar approaches are not recommended for labeling proNGF, whose pro-domain has been reported to have features of an intrinsically unfolded protein, nor for a precise comparison of the trafficking of NGF and proNGF.

In this context, this PhD thesis presents a novel toolbox designed for the non-invasive, site-specific labeling of NGF and proNGF. The employed strategy allows to monitor and to study the trafficking of NGF and proNGF in living cells. The obtained labeled NGF is fully functional compared to recombinant wild-type NGF. The approach presented herein holds many advantages over the other chemical non-specific strategies previously adopted: (i) it yields a precise control of stoichiometry and site of label conjugation; (ii) the used tags can be functionalized, in principle, with any small probe; (iii) the technique is versatile, and can be generally applied to all (pro-) neurotrophins; (iv) overall, it makes possible to image and track interacting molecules at the single-molecule level in living systems; (v) it allows for the production of "homologous" fluorescent NGF and proNGF, eliminating heterogeneous labeled protein populations and assuring high experimental reproducibility.

Thanks to the labeled method developed in this PhD work, the trafficking of a nearly-native form of NGF was studied. Also, proNGF transport in neurons was characterized for the first time, showing that it is retrogradely transported as its mature counterparts. Fluorescence microscopy experiments performed on compartmentalized living cultures of rat dorsal root ganglion (DRG) neurons, in which fluorescent proNGF and NGF were administered either separately or together, allowed the comparison between the trafficking of precursor and mature neurothrophin forms.

The results presented in this thesis unveil new details of neurotrophin neuronal trafficking and represent a starting point for the study of proNGF *versus* NGF signaling mechanisms in the nervous system.

Furthermore, the labeling technique described here constitutes a novel method to obtain structurally nearly-native labeled neurotrophins for a number of applications.

Chapter

1

Nerve Growth Factor

A Long-range signaling molecule in the nervous system

Neurons are highly polarized cells with long axons extending over thousand times the length of their cell bodies. Their peculiar architecture and morphology require unique mechanisms for intracellular communication to detect, analyze, decipher and respond to different kinds of stimuli. In fact, such stimuli can either involve receptors present on the plasma membrane of cell soma, or they can originate very far from it. Specialized mechanisms of intracellular communication have evolved through which signal emanating from the farthest tip of the axon can be transmitted to the neurons cell body where an appropriate response can be mediated. As a result, neurons rely on active axonal transport for all the materials needed to be carried from synaptic terminals to cell bodies and *vice versa*, including neurotrophins, receptors, synaptic proteins, ion channels, lipids, and mitochondria.

Neurotrophins are known to be required for proper neuronal subtype specification, synapse and circuit formation, and in helping neurons to respond to axon insult and injury. After a brief historical account, this first chapter will briefly summarise the

role of the first neurotrophin discovered, Nerve Growth Factor (NGF), in brain physiology and will summarize recent findings regarding mechanisms of NGF signals propagation in the nervous system. The important role emerging for the unprocessed NGF precursor (proNGF) in brain physiology will be emphasized and I will describe how reciprocal levels of NGF and proNGF are fundamental in regulating the survival/death balance of several neuronal populations in physiopathological conditions. In this context, an over view will be provided on the crucial importance of signaling mechanisms that link NGF and proNGF cellular trafficking to their specific biological function. The methods previously used to label NGF and to study its axonal transport will be discussed, and I will illustrate why similar approaches are not well suited to the purpose of labeling proNGF.

1.1 The Neurotrophic Factor Hypothesis

More than 60 years ago, the discovery of the target-dependent nature of developing neurons by Viktor Hamburger and Rita Levi Montalcini led to the formulation of the "*Neurotrophic Factor Hypothesis*"[1,2]. This hypothesis states that target tissues have an important role in neuron development by producing a limited amount of growth factor specific for the innervating neuronal population. Developing neurons are initially overproduced, and those successfully acquiring adequate amount of this growth factor will survive, whereas the other die.

These findings were described in late 1940s, in the context of experiments defining the interaction between developing neurons and their innervation targets. It was shown that the changing of the target tissue produces modification in the size of the corresponding neural center (i.e., ganglia or neuronal nuclei). Thus, removing a limb bud resulted in hypoplasia of the developing neural center, whereas transplanting an extra limb bud produced hyperplasia[3]. Hamburger and Levi-Montalcini discovered that cell death occurred normally during development and that the hypoplasia of neural centers, following limb bud extirpation, was associated with increased degeneration of neurons in the centers, that would normally supply the surgically removed limb. Significantly, during normal development, neurons died at the time that their processes entered the target. These studies were important because they identified the target as a key role in neuronal development. Moreover, they suggested that the target determined the size of its neural center (i.e., the number of neurons present) by regulating death of these neurons. These experiments demonstrated that the target plays a key role in neuronal development by regulating life and death of neurons. In Rita Levi Montalcini early studies, conducted after she joined Victor Hamburger's laboratory, she found that when a mouse tumor was transplanted into a chick embryo, it produced a diffusible agent that promote and stimulated nerve growth, demonstrating the extrinsic nature of factors controlling the innervation process. Using cell culture, Montalcini and coworkers were able to demonstrate that a chemical factor, of tumoral origin, induced nerve growth. Following these findings, Hamburger and Montalcini proposed a "metabolic exchange between the neurite and the substrate in which it grows", where the nature of this "metabolic exchange" should have been a soluble diffusible agent, that acted on neurons travelling from the axon tip to the cell soma to promote neuronal

survival. With the collaboration of the biochemist Stanley Cohen, they were able to determinate that this factor is a protein and to identify, purify, characterize it. This factor was called Nerve Growth Factor [2,4].

Moreover, Rita Levi Montalcini predicted, in the early 60's, that different neuronal populations might be responsive to different neurotrophic factors of the same nature[5].

NGF was the first neurotrophin discovered, followed by other members of this family: brain-derived neurotrophic factors (BDNF)[6], neurotrophin-3 (NT3)[7], and neurotrophin-4/5 (NT4-5)[8]. As neurotrophic factors, they support the growth, differentiation, and survival of neuron, thanks to their binding to specific membrane receptors called tropomyosin receptor kinases (TRKs) and low-affinity p75 receptor.

Important aspects of their signaling biology were well described by the *Neurotrophic Factor Hypothesis*, that has grown to the status of a true paradigm. This model describes that neurotrophins, that act locally at the axonal terminals, send their signals to the cell body for subsequent actions on gene transcription, exploiting their function thanks to the retrograde signalling. This mechanism is important for neuronal physiology, development and growth, and also for helping neurons to respond to axon insults and injury.

Moreover, recent studies have shown that the mechanisms by which neurotrophic factors act are more complex. It was described that in addition to target derived delivery, autocrine and non-target derived paracrine models exist. BDNF, for example, acts in adult DRG neurons via an autocrine loop[9]. Furthermore, neurotrophins besides moving from the axon tip to cell soma in a retrograde way, can also move anterogradely along axons[10]. However, the *Neurotrophic Factor Paradigm* remains the central theme of neurotrophin signaling.

1.2 The Nerve Growth Factor

Since its discovery in the 1950s, Nerve Growth Factor is clearly the best–characterized neurotrophic factor. It plays a fundamental role in the sensory and autonomic nervous system and in central nervous system (CNS). NGF acts on sympathetic and neural crest-derived sensory neurons and on basal forebrain cholinergic neurons in the CNS[4]. Moreover, NGF has been found to be important not only for the nervous system, but also for additional non neuronal NGF-responsive cells that include lymphocytes, mast cells, eosinophils, other ectodermal-derived cells such as keratinocytes and melanocytes, and cellular elements of the endocrine system[11].

The mature NGF, as all other neurotrophins, derives biosynthetically from the proteolytic cleavage of its precursor form called proNGF[12,13](Fig.1.1). NGF and proNGF are important proteins for growth, maintenance, and survival of neurons, having fundamental roles during development and in adult life (owning both pro-apoptotic and neurotrophic properties)[14]. NGF is generally synthesized at a considerable distance from the cell body of the NGF-sensitive neurons by peripheral target tissues (that are typically non-neuronal cells) or target neurons, which are contacted by axons. To mediate its response, NGF must have the ability to reach the cell soma where it transduce a series of complex signalling events.

1.2.1 Biosynthesis of NGF: from Precursor to Mature Neurotrophin

The amino acid sequence of the NGF was determined by Angeletti and Bradshaw[15] in 1971. Its determination provided invaluable information on its primary structure and it was instrumented for the identification of NGF cDNA. The cloning of mouse, human, bovine, and chick genes, demonstrated their high degree of homology[4].

The human NGF gene is located on the proximal short arm of chromosome 1[16] and codes for a large polypeptide of 307 amino acid residues, which, upon cleavage, yields a mature NGF protein with 118 amino acids[4].

NGF is encoded by a single gene that is over 45 Kbases in length, that yields two major alternatively spliced transcripts. From those, NGF protein is translated to

produce 34 and 27 kDa pre-pro species. Removal of the signal sequence reduces these translation products to two proNGF species of 32 and 25kDa respectively. ProNGF contains three potential glycosylation sites, two in the pro-segment (that contribute to efficient protein expression) and one in the mature sequence. Glycosylated NGF precursors have been identified both *in vitro* and *in vivo*, however, many tissues contain the unglycosylated proNGF (Fig.1.2)[14].

The long precursor, pre-proNGF contains the signal peptide for protein secretion (pre-peptide), that is cleaved upon translocation into the endoplasmic reticulum to produce the precursor homo-dimer proNGF. proNGF can be either secreted outside the cells or cleaved intracellularly into mature NGF[17,18]. Generally, secretion of NGF occurs as a mixture of proNGF and mature NGF. Both mature NGF and proNGF exist in their active forms as homodimers.

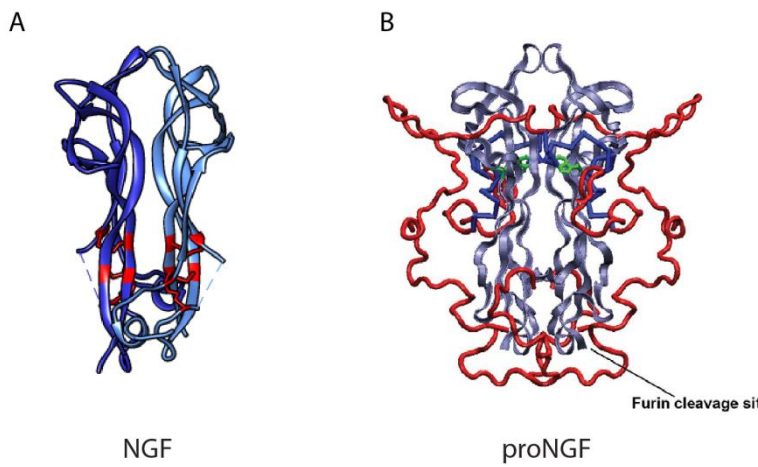

Fig. 1.1 NGF and proNGF structures. (A) Mature NGF structure where the cysteine knot is highlighted in red (PDB code 1WWW). (B) Model of proNGF structure built according to SAXS data. Mature NGF is shown in blue, the pro-peptide domain in red. Figure adapted from *Paoletti et al*., 2011[19].

The pro-sequence composed of 103 amino acids (represented in dark red in the left panel of Fig. 1.1) can be processed both intracellularly and extracellularly,

resulting in the release of the mature NGF dimer of about 26 kDa. The extracellular cleavage is performed by proteases, such as plasmin and metalloproteases[17], while the intracellular one is made by furin convertase (at a highly conserved dibasic amino acid site) in the trans-Golgi network[18].

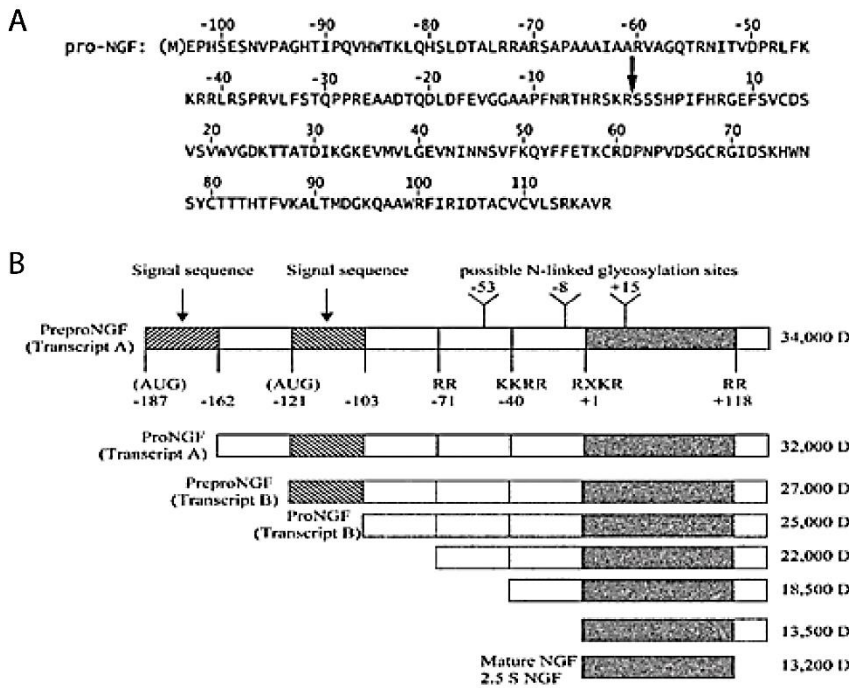

Fig. 1.2. Primary structure of proNGF. (A) The amino acid are represented in one-letter code. The arrow represents the cleavage site between the pro and the mature region[20]. (B) Intermediates in NGF biosynthesis. 'Y' represents potential glycosylation sites. The figure is not on scale. Figure taken by *Fahnestock et al*., 2004.[14]

The longest isolated form of mature NGF polypeptide contains 118 amino acids with 3 intrachain disulphide bonds, as represented in figure 1.1A. However, shorter chains, truncated at both termini, were also identified (generally these shorter forms are produced by removal of the amino-terminal octapeptide and/or the C-terminal arginine residue)[21].

While the amino acid sequence of NGF was determined more than 40 years ago[15], the 3-dimensional structure has been achieved[22] in 1991, showing a dimeric protein characterized by cysteine knot structure made up of beta strands twisted around each other and linked by disulphide bonds (Fig. 1.1). This tertiary structure based on a cluster of 3 cystine disulfides and 2 extended and distorted β-hairpins, identifies NGF as the prototype of the neurotrophins family.

1.2.2 Nerve Growth Factor receptors

It is now well known that NGF, like other neurotrophins, bind specific receptors, both at the soma and at the neuronal distal compartments. The binding of NGF and its receptors gives rise to an activated complex that acts both locally (where it controls growth cone motility), and distally, moving retrogradely through long axons up to distant cell bodies (where it promotes gene expression and survival).

It is common knowledge that NGF binds mainly two types of membrane receptors: the tropomyosin receptor kinases, Trks and the p75 neurotrophin receptor, p75NTR (Fig. 1.3) [23,24,25].

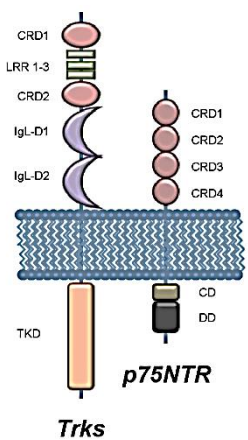

Fig. 1.3. Schematic picture of Trks and p75NTR receptors. Structure of the two receptors: the intracellular (on top) and extracellular (on bottom) domains are highlighted. The following abbreviations are used: CRD (cystein-rich domain); LRR (leucine-rich domain); IgL-D (immunoglobulin-like domain); TKD (tyrosine-kinase domain); CD (chopper domain); DD (death domain). Figure adapted from *Marchetti et al*. 2015[25].

Trk receptors belong to the tyrosine kinase (RTK) family of growth factor receptors, which are traditionally known to dimerize upon ligand binding, thus activating the trans-phosphorylation of the intracellular kinase domains and further phosphorylation of intracellular effectors[26]. For the Trks, these mechanisms ensure most neurotrophic and survival responses[27]. Figure 1.3 shows that the extracellular domain of Trk consists of a cysteine-rich cluster followed by three leucine-rich repeats, another cysteine-rich cluster and two immunoglobulin-like domains. The Trk spans the membrane once, and is terminated with a cytoplasmic domain consisting of a tyrosine kinase domain. Different neurotrophins exhibit specificity in their interactions with the three members of the Trk receptor family (TrkA-TrkB-TrkC): NGF binds to TrkA receptors[27]. The major site at which neurotrophins interact with the receptors is in the highly conserved membrane-proximal immunoglobulin-like domain. In particular, the three-dimensional structure of NGF bound to the TrkA Ig domain has been determined, showing that the two elongated β sheet region of NGF dimer interact with the immunoglobin-like domains D2 of two TrkA receptors[28] (Fig. 1.4).

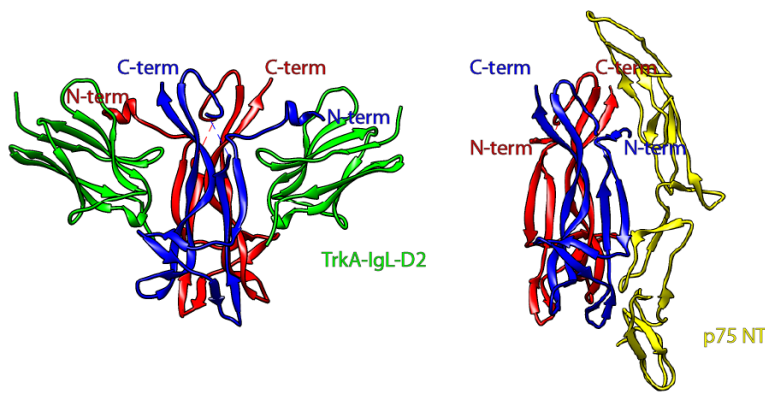

Fig. 1.4. NGF and its receprtors. (*Left*) Ribbon diagram representing the crystal structure of the complex between NGF and IgL-D2 of TrkA (PDB code 1WWW)[29]. The NGF monomers are depicted in red and blue, and the two copies of TrkA -IgL -D2 are shown in green. (*Right*) Structure of NGF complexed with p75. p75 binds along one side of the NGF homodimer. Backbone representation of NGF monomer are coloured in red and blue, and p75in yellow (PDB code 1SG1)[30].

On the other hand, p75NTR is a member of the tumour necrosis factor receptors (TNFR) superfamily. It has no intracellular enzymatic activity, but it interacts with several proteins that transmit signals important for the regulation of neuronal survival, differentiation and synaptic plasticity, as well as for mediating neural cell death during development and in the adult following injury[31,32,33]. p75NTR is characterised by an extracellular domain that includes four cysteine-rich motifs, a single transmembrane domain and a cytoplasmic domain that includes the "death" domain characteristic of other members of this family (Fig. 1.3). The three-dimensional structure of the extracellular domain of p75NTR in association with an NGF dimer revealed that each cysteine-rich domains participates to NGF binding[34] (Fig. 1.4).

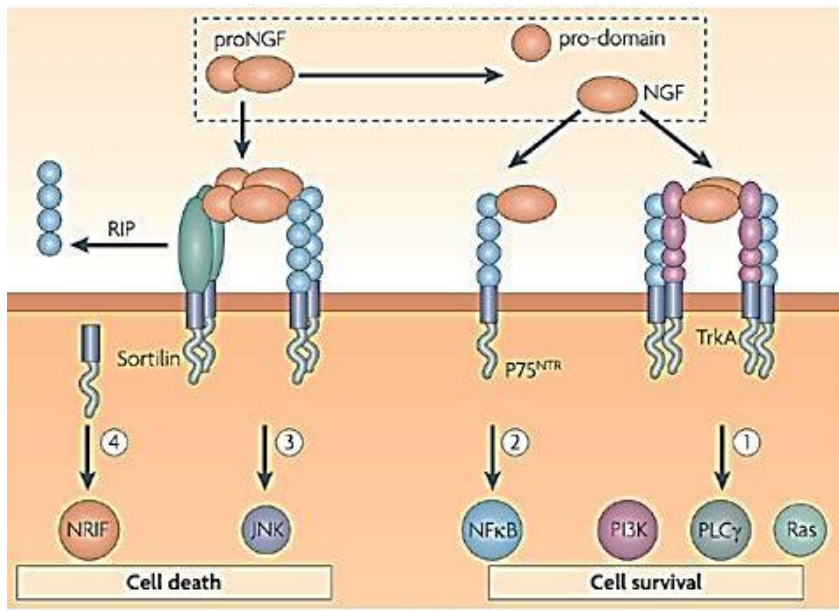

Fig. 1.5. proNGF and NGF activate distinct signaling pathways. The binding of NGF to TrkA stimutate PI3K, PLCγ and Ras pathways, promoting cell survival. The binding of proNGF to Sortilin-p75 complex activates cell death. Figure adapted from *Willnow et al*., 2008[35].

Several studies have been performed to understand the functional and structural interplay between NGF, TrkA and p75NTR.

In the past years, the existence of a ternary TrkA/NGF/ p75NTR complex has been proposed[36]. It was described that TrkA and p75NTR form a complex on the cell membrane, both with and without the presence of NGF[37], and that, when p75NTR is co-expressed with TrkA, mature NGF binds to the receptors complex with higher affinity than that measured for the p75NTR alone[38]. However, the existence, on the cell surface, of direct extracellular interactions between these three proteins is still a matter of controversy, due to the difficulty of interpreting the structural data of ligand-receptors complexes[28,34]. Two main models regarding the interaction between NGF, TrkA and p75 p75NTR have been proposed. The first, defined the 'ligand-passing model', reports that p75NTR and TrkA bind NGF in different orientations, giving rise to a ''NGF sandwich'' and that they are able to "pass" the ligand one another[39]. In the second model, it is described that NGF oligomerizes giving rise to a heteromeric structure (composed by two NGF dimers) defined 'dimer of dimers', and that the NGF/receptors complex exists as heterocomplex composed of TrkA/NGF/p75NTR ligand/receptors molecular assembly with a (2:4:2) stoichiometry [40].

Moreover, p75NTR was found to bind the also to the unprocessed NGF, proNGF, resulting in dramatically different consequences, such as apoptosis and cells death, with respect to those that follow ligand engagement by Trk receptors[41,42] (Fig.1.5). It was discovered that proNGF creates a signalling complex following to its simultaneous binding to p75NTR and sortilin, a member of the family of Vps10p-domain receptors. The pro-region of NGF was shown to make contacts with sortilin and the mature part with p75NTR[43,44,45](Fig 1.5), demonstrating a direct binding of sortilin and p75NTR to proNGF. The presence of sortilin is required to observe apoptosis following engagement of p75NTR.

Furthermore, p75NTR has been shown to promote retrograde transport of several neurotrophins by suppressing TrkA ubiquination (delaying TrkA receptor internalization and degradation) and promoting TrkA endocytosis[27].

Therefore, while physiologically TrkA and p75NTR co-exist, at various reciprocal expression levels, in different neurons and during different stages of neuronal development[46], the ratio of p75NTR to Trks is linked to the decision between survival and death among NGF-responsive neurons[47]. Furthermore, since proNGF

displays a much higher affinity for p75NTR than the respective mature NGF, and induces p75NTR-dependent apoptosis in cultured neurons at a much lower dose than that of the respective mature neurotrophins and with minimal activation of TrkA-mediated differentiation or survival signalling[43], this proposes a more complex scenario (as will be illustrated in the next section).

1.3 ProNGF: a neurotrophic or apoptotic molecule?

It is now widely accepted that pro-neurotrophins play a fundamental active role in regulating several biological processes[48], but initially, besides the demonstration that the pro-sequence assists the proper folding of the neurotrophin[49,20] and regulates neurotrophin secretion (defining their constitutive or regulated secretory pathways)[43], no specific biological role was attributed to the proNGF. However, sequence comparison of relevant regions of neurotrophins pro-domains shows that they are conserved, suggesting that they may mediate additional biological actions (although less conserved than their mature counterparts).

For a long time, it was believed that NGF was secreted from cells only in its mature forms and that it was the only one possessing a biological function. About ten years ago, it was found that proNGF is the most abundant form of NGF in the brain, and that its level are increased in brains from Alzheimer's disease patients[50]. In addition, it was demonstrated that also proNGF is released by cells in the extracellular space, and that its release is activity-dependent[17]. It was described that the maturation of proNGF to NGF and its degradation can take place after cell secretion and depends on the action of enzyme regulators (plasminogen activator, plasminogen, neuroserpin, precursor metalloproteinase 9, MMP9, and tissue inhibitor metalloproteinase 1).

The first demonstration proving that also proNGF has its own role, distinct by the one of mature NGF, comes from a study conducted by Lee and co-workers in 2001[43]. The work was performed on a mutated form of proNGF that is cleavage-resistant. It was shown that, in primary sympathetic cervical ganglion (SCG) neurons and smooth muscle cells, a furine-resistant proNGF form acts preferentially activating apoptosis via p75 receptor instead of promoting survival via TrkA receptor, as the mature form does. Moreover, it was measured that treatment of SCG neurons with proNGF results in cell death and that proNGF bind to p75 with five times greater affinity than mature NGF. Authors suggested also that the regulated activity of proteases (plasmin or MMPs) may further define the pro-apoptotic or pro-survival action of neurotrophins[43]. Later on, it was established that sortilin is an important receptor targeting the pro-domain of proNGF with high affinity, that it is required to activated proNGF signalling via p75 and that it facilitates the formation of a signaling complex comprising p75, sortilin and proNGF[44]. Controversially to

Lee et al., Fahnestock and co-authors reported a neurotrophic activity of proNGF[14]. In their study, the authors analysed the effect of another type of cleavage-resistant form of proNGF, demonstrating that proNGF exhibits neurite outgrowth activity on both SCG neurons and PC12 cells, with a specific activity of proNGF in stimulating neurite outgrowth approximately five-fold lower than that of mature NGF[14]. It was then deduced that the difference between their results and those obtained by *Lee et al.* were probably due to the different proNGF cleavage resistant form utilized in the two works and that the neurotrophic activity might also be induce by the mature NGF proteolytically produced in the culture.

Most recently, Wang and co-workers proved that proNGF promotes the death of different cell types including primary neurons, and that its toxicity is mediated by p75 receptor[51]. They showed that proNGF has the opposite role, compared to NGF, of retarding neurite growth, causing a significant reduction in cell viability of aged neuron *in vitro*. In the same framework, another group of researchers analysed the neurotoxic and neurotrophic roles of proNGF showing that the precursor neurotrophin induce neurites outgrowth in young sympathetic neurons and cell death in old sympathetic neurons[52]. These finding highlighted the different role played by proNGF in neurons of different age, that is probably mediated by sortilin.

From these data, controversies emerge on the nature of the activity exhibited by full-length native proNGF in comparison to mature NGF, which have not yet been fully characterized and resolved.

Finally, published data suggest that secretion of proneurotrophins is increased following to brain injury or degeneration. Since proNGF was identified in some studies as neurotoxic,[43] or significantly less neurotrophic[14] than mature NGF, an increase in proNGF levels may lead to neuronal loss in injury and disease neurons[27]. In fact, it was suggested that proNGF contributes to neurodegeneration in the adult nervous systems. Thus, Fahnestock and co-workers proposed the existence of a switch mechanism in adulthood of the predominant available form of NGF protein from the mature to the precursor. Indeed, proNGF has been found to be present at high levels in several areas of adult brain [53], in Alzheimer Disease (AD) brain [54] and in injured adult CNS[55,52]. Also, a selective imbalance of proNGF versus NGF, induce by a mature NGF-specific anti NGF antibody, was found to cause the progressive Alzheimer-like neurodegeneration in the brain of anti NGF expressing

transgenic mice[56,57]. Finally, proNGF overexpressing mice were found to display a severe neurodegeneration[58].

Thus the need to understand the mechanisms of proNGF induced neuropathy is compelling and therefore, it is of huge interest to understand the mechanism of proNGF transport and signaling, in comparison to that of its mature counterpart.

For example, it is not clear whether proNGF and NGF are both internalized and transported by cells or whether they are internalized at the same rate. The study and the characterization of different aspects of precursor and mature NGF trafficking would help to better understand their function and physiology.

1.4 NGF Transport and Trafficking

As previously described in the *Neurotrophic Factor Paradigm*, neurotrophins, that act locally at the axonal terminals, must send their signals to the cell body for subsequent actions on gene transcription. Retrograde signalling is important for neuronal physiology, development and growth, and also for helping neurons to respond to axon insults and injury.

In the past, different approaches have been tested to understand how the NGF signal is transmitted through neuron and several data were collected, but, to the best of my knowledge, there are no studies regarding proNGF long range transport and trafficking in neurons.

Direct evidences of mature neurotrophins retrograde transport are present in the literature since 1970s. Different aspects and properties have been analysed and observed.

The first demonstration of retrograde transport of NGF was accomplished by injecting ^{125}I-NGF into the anterior eye chamber of the adult mice and rats[59], and intraocularly in chicks[60]. After injection, NGF was found to accumulate selectively in the superior cervical ganglion from the nerve terminals of the iris[59]. It has been calculated that this transport occurs at a similar rate, in different species (at least rats and mice), of about 2.2-2.5 mm/h (≈0,6 μm/s)[59].

Moreover, subsequent studies, demonstrating that NGF injected into the cytoplasm is not active, have led to the notion that internalized and/or retrogradely transported NGF resides in the lumen of membrane-bound organelle[61].

With the advancing of years and the improvement of new techniques, the understanding of NGF transport mechanism became more profound and exhaustive.

For example, the use of compartmentalized culture system allowed the neurons to growth under a carefully controlled NGF administration. By using this type of device (later defined as Campenot chamber), in the ’80s, Campenot and co-workers have analysed the transport of ^{125}I-NGF in sympathetic cervical ganglia neurons[62]. The presence of a retrograde NGF transport along axon has been shown with an average velocity of approximately 0,83 μm/s[62]. It has been reported that ^{125}I-NGF starts to be internalized from axon after 1 hour form neurotrophin administration,

and that NGF endosomes move only in a retrograde and not anterograde (from cell bodies to distal axon) manner. Moreover, it has been established that ^{125}I-NGF, when supplied to the distal axon, accumulates with its receptor in the cell body or in the proximal axon[63], demonstrating that neurons are capable of taking up NGF at the distal axon and transporting it to the cell body.

More recently, fluorescent NGF (Cy3-NGF) has been used to investigate neurotrophin trafficking in a single-molecule imaging study. Tani and co-workers in 2005[64] presented a work where they studied NGF movement upon endocytosis on dorsal root ganglia (DRG) growth cone. It was demonstrated that within 1 min after NGF administration growth cones responded expanding their lamellipodia, that the NGF-receptor complex shifts its movement from a diffusion type to a vectorial mode of transport directed toward the central region of the growth cone and that this movement is actin-driven. This movement was suggested to precede the NGF-receptor complex internalization in the vicinity of the central region of the growth cone, and actin-driven clustering of the NGF receptor complex on the plasma membrane was thus proposed to be an essential step for the accumulation and endocytosis of NGF at the growth cone and for the initiation of the retrograde transport of NGF towards the cell body.

Furthermore, neurotrophin motion and transport was also investigated in PC12 cells. In a work, published in 2011 by *Nomura et al.*[65], Cy3.5-NGF was used together with a GFP fusion of TrkA (TrkA-mSEGFP). The two complementary probes were used in simultaneous imaging experiments along neurites of PC12 cells. A mobile and immobile population of recorded trajectories was registered. It was shown that ≈60% of fluorescent NGF dots moved along PC12 neurites, while the rest of the dots showed non-directional motions. Among all moving dots, half were found to move retrogradely and half anterogradely, with a wide range of velocities between 0.1–3 μm/s. Upon NGF application TrkA-mSEGFP was found to undergo increased directional (both anterograde and retrograde) movements. Interestingly, the average speed of TrkA-mSEGFP dots associated with Cy3.5-NGF (anterograde velocity peaks: 0.45-1.50 μm/s; retrograde velocity peaks: 0.45-1.23 μm/s) was remarkably higher than that of TrkA-mSEGFP dots without Cy3.5-NGF (anterograde velocity peaks: 0.30-1.10 μm/s; retrograde velocity peaks: 0.18-0.45 μm/s). Co-localization of TrkA-mSEGFP with Cy3.5-NGF was found to occur more frequently in retrogradely moving vesicles than in anterogradely moving ones.

Moreover, the bidirectional movement of NGF was also confirmed in another work, where NGF conjugated to Quantum Dots (QD-NGF) was used to study NGF trafficking properties whit single particle tracking experiment performed on neurite-like process of differentiated PC12 cells. NGF-receptor complex was found to move for ~70% of the time and the ~60% of this movement was found to be retrograde (with a mean velocity of ~0.15μm/s). The velocities in the two directions (retrograde and anterograde motion), found to be microtubule-dependent, were very similar and characterized by frequent and short pauses [66].

Additionally, *Lalli and Schiavo* described that, in primary motor neurons (MNs), NGF labelled with Alexa Fluor is transported only in a retrograde manner and that this transport is mediated by p75 receptor only (TrkA receptor is not present)[67].

Five years later, *Cui et al*. described QD-NGF transport in axon of DRG neurons plated in a microfluidic chamber. They acquired moving endosomes trajectories of NGF filled vesicles, demonstrating an active transport characterized by rapid, unidirectional movements, that exhibited 'stop and go' retrograde motion (90% of the recorded trajectories) with an average speed of ~1.31 μm/s. Moreover, each endosome was found to contain about only a single NGF dimer[68].

These observations support the idea of the existence of an active ligand-receptor signaling complex that transmit the neurotrophin signal by physically transporting the neurotrophin along the axons. This concept is represented by the "*Signaling Endosome model*" (Fig. 1.6).

Moreover, indirect measurements of NGF trafficking were performed studying TrkA movements. QD-TrkA vesicle complex moving in an anterograde and retrograde direction were transported at velocities that ranged from 0.03 to 0.67 μm/s in PC12 neural processes[69]. These velocities are similar to estimates reported in other works: in 2003, *Jullien et al*. described TrkA-GFP trafficking induced by NGF in PC12 cells to have an estimated moving anterograde velocity of 0.46±0.09 μm/s and a retrograde one of 0.48±0.07 μm/s[70]. In 2000, a previous article showed both anterograde and retrograde movements of TrkA-CFP transporting vesicles in neurites of PC12 NGF-differentiated cell, with a mean velocity of 0.2±0.03 μm/s and 0.3±0.05 μm/s respectively[71].

NGF retrograde transport was found to be dependent of an dynein-microtubule system, since the pharmacological disruption of microtubules or the inhibition of dynein activity results in its impairment[72,73].

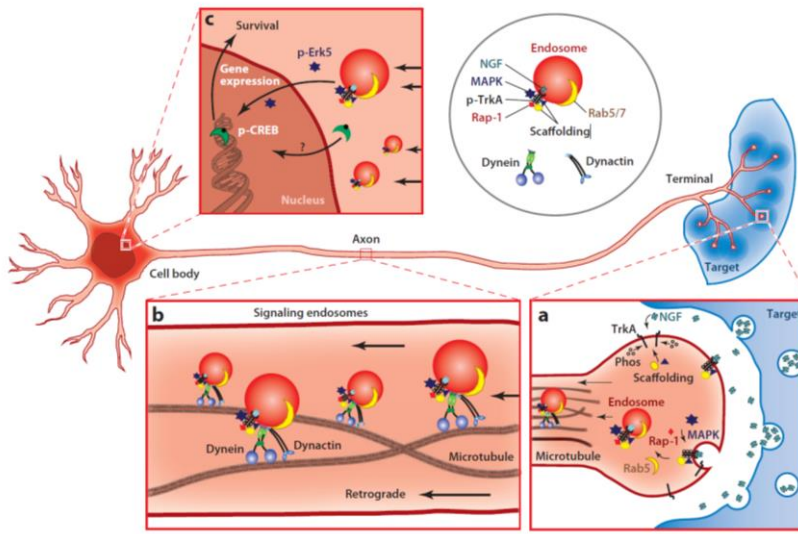

Fig. 1.6. Transport of signaling endosomes. Neurotrophins released by target tissues bind to their receptors at the axonal terminals, giving rise to signaling endosomes. Subsequently, signaling endosomes are retrogradely transported toward axon, driven by the dynein-microtubule system, to the cell body, where they regulate gene expression. Figure taken by *Chowdary et al.*, 2012[74].

Therefore, a vast literature reporting NGF binding, internalization and trafficking process exist, which is however characterised by a large and sometimes dishomogeneus amount of data (Table 1.1). The reason for this variability will be discuss below. Moreover, such knowledge does not exist at this time for the traffic of the precursor NGF. It is worth noting that pro-neurotrophin trafficking in neurons is currently an unresolved topic, and elucidation on the mechanisms used to transmit proNGF signal from the axons terminals to cell bodies is yet to be fully defined.

Cell type	NGF transport direction	Velocity	Ref.
anterior eye chamber of the adult mice and rats	retrograde	0,6 µm/s	59
sympathetic cervical ganglia neurons		0,83 µm/s	62
dorsal root ganglia neurons	retrograde motion (90% of the recorded trajectories)	~1.31 µm/s	68
neurites of PC12 cells	retrograde and anterograde	0.1to3 µm/s	65
		0.15 µm/s	66
		0.03 to 0.67 µm/s	69
		0.46-0.48 µm/s	70
		0.2–0.3 µm/s.	71

Table 1.1. Modality of NGF signal transmission through different kind of cell. The recorded velocities are reported for each study.

1.4.1 NGF *Signaling Endosome Model*.

The *Signaling Endosome Model* defines that long range signaling in neurons is accomplished by the compartmentalization of signaling complexes and accessory factors in membrane-bound organelles, which are transported along axons in the retrograde direction towards the soma[75].

This way is mainly used by neurotrophins, but also several molecules has been found to follow this route. In fact, the "*signaling endosome*" is a main gateway for the entry of various neurotoxins into neurons. Thus, virulence factors such as neurotoxins and pathogens toxins hijack the neurotrophin axonal trafficking routes to gain access into the CNS[76,77].

The mechanism regulating this phenomenon, is composed on a multi-step process present in neurons. The first step takes play in the membrane of the axon terminal and is composed by the interaction of neurotrophins with their receptors giving rise to the ligand-receptor complex. This process allows the internalization of the newly formed complex in an endosome, called "*signaling endosome*". This step is followed by the maturation and the sorting of the signaling endosome defining its nature and destination. Next, the signaling endosomes is translocated along the microtubule tracks toward the cell body, where the signalling pathway is activated (Fig.1.7)[78].

In the first step, after the interaction between the neurotrophins and their receptors, signaling effectors are activated. After its binding to its receptor TrkA, NGF activates three major early downstream effectors PI3K–AKT, ERK and PLCγ. Of these, the PI3K and PLCγ pathways have an active role in receptor internalization. PI3K activity is important in regulating the binding and the action of several proteins (including dynamin, RAS-related protein Rab5, AP2 and synaptotagmin) implicated in different steps of Trk-mediated endocytosis, like pinching off the endocytic vesicle from the plasma membrane, participating in vesicle coat formation and vesicle targeting, and contributing to NGF–TrkA internalization and retrograde transport[74]. On the other hand, PLCγ, a multifunctional enzyme that acts as interacting partner for additional receptor tyrosine effectors, is linked to dynamin regulation fundamental for receptor internalization[79].

There are different endocytic routes that a membrane receptor bound to its ligand can choose: macropinocytosis, clathrin-mediated endocytosis, caveolae-mediated

endocytosis and clathrin- and caveolae-indipendent endocytosis. Regarding the mechanism of NGF signaling endosomes internalization, there are evidence that support both clathrin dependent[80] and clathrin independent (pinocytosis mediated by Pincher) mechanism[81] (upper panel Fig.1.7) .

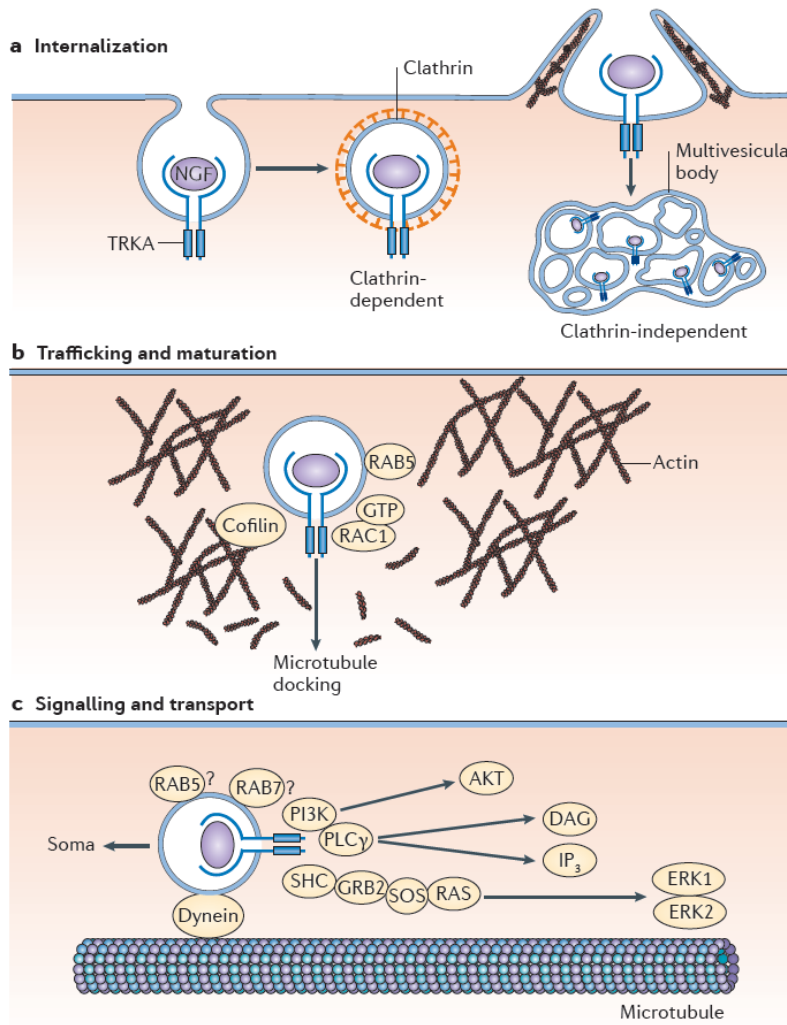

Fig. 1.7. Mechanisms of neurotrophin internalization, signaling and retrograde transport. Different phases of the endosome trip. Figure taken by *Sharma et al*., 2010[78].

In the case of the first endocytic route, activated TrkA bound to NGF complex was found in clathrin-coated vesicles along with components of the key downstream signaling of the ERK pathway[82]. Moreover, also the binding of NGF to p75 was found to induce internalization of the complex via clathrin-coated pits into early endosomes and this process has been found to possess a rate approximately three times slower than that of NGF-TrkA complexes in the same cells (PC12 cells), suggesting that such endosomes may be temporally and spatially distinct from those containing trk receptors[83].

Moreover, the inhibition of clathrin-dependent endocytosis stops the retrograde transport of neurotrophin signal when this is added to the distal axons[73], showing the importance of clathrin-dependent mechanism in NGF trafficking. Furthermore, TrkA internalization was found to depend on dynamin, a GTPase known to mediate the uncoating of the clathrin-coated vesicles[84].

On the other hand, other studies support the clathrin independent macropinocytosis mechanism. This mechanism involves the formation of plasma membrane protrusions that fuse together and engulf large volumes of membrane and extracellular fluid. Recently, Pincher, an NGF-upregulated GTPase involved in macropinocytosis-like mechanism, was identified as membrane trafficking protein that mediated endocytosis of NGF-TrkA complex[85]. This complex is processed into multivesicular bodies (MVB) that escape lysosomal degradation guaranteeing a long-lasting signaling. RNAi-mediated inhibition of Pincher severely attenuates the retrograde transport-mediated survival response of neurons to neurotrophins[85,86,74].

Thus, clathrin and Pincher appear to promote the formation of endosomal vesicles that differ in their stability and signalling potential, with Pincher promoting the formation of endosomes, which are preferentially recruited for retrograde signalling[27].

However the relative contributions of both endocytosis pathways for the internalization of TrkA and initiation of the NGF retrograde signal in neurons *in vivo* are currently unknown.

In any case, once the signaling endosome is formed, the next step is its maturation. It was shown that, in this process, a crucial role is played by actin cytoskeleton. When the NGF-receptor complex is internalized, it is associated with actin. Moreover, it was established that, in order to guarantee the docking with microtubules, the ability to successfully overcome the F-actin barrier is an essential

step, allowing for trafficking and long distance transport of the complex. For this purpose, the actin disassembly that allows the release of actin-bound endosome is fundamental[87].

Finally, the last step (when the endosome is ready for the transport) involves motor proteins, allowing the endosomes to move along microtubules from the axon to the cell soma. There is substantial evidence that axonal transport of signaling endosomes is dependent on cytoplasmic dynein, as showed also for other types of retrogradely transported cargoes. In fact, microtubule depolymerization inhibits the retrograde transport and the cell body accumulation of neurotrophins [72].

However, we currently lack a precise molecular understanding of the "*signalling endosomes*". In particular, the question whether the molecular composition and identity of traffic and signaling endosomes are dependent on the transported cargo is totally open.

1.5 Labeled NGF

The majority of the studies regarding NGF transport and trafficking presented so far is based on the use of various kinds of labelled-NGF. The scheme of Figure 1.8 illustrates all the principal techniques reported by literature and shows that they can be essentially reconducted on 2 main classes: a first class, composed by chemical non site-specific methods, and a second one, more recent, composed by a site specific labelling approaches.

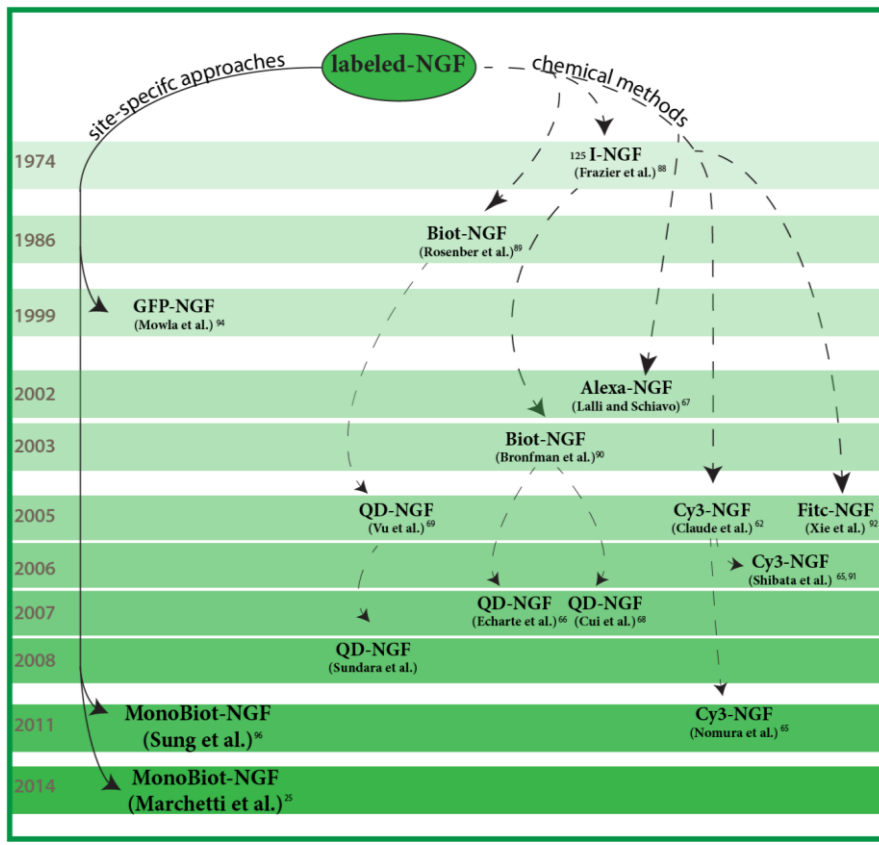

Fig. 1.8. Schematization of the papers reported in literature regarding labelling methods applied to NGF in a chronological order.

Regarding the first class, including strategies derived from old studies, the first approach to label NGF was presented by *Frazier et al*.[88] in 1974. NGF was radioactively labelled with ^{125}I to analyse its interaction with the receptor(s) present on the plasma membrane of sympathetic and sensory neurons isolated from chick embryo. This work was the progenitor of all the successive studies regarding ^{125}I-NGF, like those of *Hendry et al*.[59] published in 1974, *Max et al* in 1978[60], *Sutter et al* in 1979[24], *Claude et al* in 1982[62] and many others. All these works allowed to obtain loads of information regarding NGF trafficking: they represented the first evidence of the retrograde axonal transport of NGF in the neurons of the sympathetic nervous system[59,60]. However, this kind of labeling strategy had some limitations, being unsuitable for analyses that require high spatial and temporal resolution.

More than ten years later, a new kind of labeled-NGF was reported in the literature. This was a biotinylated NGF obtained with chemical non-specific strategy in which biotin ligands were randomly bound to a set of free carboxylic groups exposed on NGF protein. This technique, first reported by *Rosenberg et al*. in 1986[89] and then by *Bronfman et al.*in 2003[90], is the base of all studies that use QD-NGF. This biotinylated NGF is subsequently conjugated with streptavidin-QDs or streptavidin-fluorophores. Such approaches have produced heterogeneous results in neurotrophin trafficking. In fact, these methods give rise to heterogeneous NGF proteins labelled in different positions, and covalently conjugated to large size cargos (QD ~15-20 nm of diameter compared to 2-3 nm of NGF), which can clearly alter the diffusion and the real physiology of the neurotrophin. Moreover, these processes reported a very low yield [66,68].

In the same years when QD-NGF was used to study NGF dynamics, another types of fluorescent-NGF (Texas Red NGF[67] and Cy3-NGF[91,65]) were used for the same purpose. Texas Red-NGF and Cy3-NGF are a chemically labelled NGF in which a reactive organic dye is bound to some of the free amino and carboxyl groups, respectively, of NGF surface. Also other approaches, based on chemical labeling between amino groups and fluorescein isothiocyanate (FITC), were reported[92].

All these approaches have been the most widely used to label NGF, however both of them suffer of allowing almost no control in number and type of modified sites of the target proteins, so that mixed and not reproducible populations of labelled proteins are obtained.

Labelling strategy	Ratio of probes per NGF molecule	Cell type	Ref.
^{125}I-NGF	n.d.	Sympathetic neurons	88,24 60,59.
Biotinylated NGF (NGF-b)	~ 3 biotin molecules per NGF subunit	PC12	89
NGF-b /Streptavidin Alexa647	~ 9 biotins per NGF molecule; 20 nM NGF-b is given to the cells and further detected with Streptavidin Alexa647	PC12 and PC12nnr5	90
NGF-b /streptavidin Qdot	≤ 3 biotins per NGF subunit; NGF-b is conjugated to streptavidin-Qdot at a molar ratio of 1 NGF: 1 QD.	PC12	93
	~ 1 biotin was bound per NGF molecule; 2nM NGF-b is given to the cells and further detected with 50-500 pM streptavidin-coated Qdot	Differentiated PC12	66
	~ 3 biotins per NGF dimer; NGF-b is conjugated to streptavidin-Qdot at a molar ratio of 1 NGF: 1 QD.	Rat DRG neurons	68
Cy3-NGF or Cy3.5-NGF	~ 1.0-1.1 ratio between fluorophore and NGF	Chick embryonic DRG neurons; PC12	91,65
GFP-NGF	GFP fused to the C-terminal region of NGF	hippocampal neurons	94,95
Mono-biotinylated NGF via chemical tag	AVI-tag fused at NGF C-terminus; NGF-b is obtained transfecting the construct in HEK293FT cells together with the biotinylating BirA enzyme; NGF-b is conjugated to streptavidin-Qdot at a molar ratio of 1 NGF: 1 QD.	Rat DRG neurons	96

Table 1.2. Modality of NGF labelling strategies. The ratio of probes per NGF molecule and the cell type (where fluorescent neurotrophins are studied) are reported for each study.

The second class of NGF-labeled technique is represented by the approaches where the number of the probes and the site of the labeling are controlled. The first example of this group is reported by constructs coding for GFP fused to the C-terminal region of NGF[94,95] .

These methods were followed in 2011 by a new technique: a site specific labeling technique where the sequence of a chemical tag is fused to the sequence of NGF[96]. In their article, Sung and co-workers, used an AVI-tag (15 amino acids) fused at NGF C-terminus in order to biotinylate NGF (NGF-b) thanks to the biotinylating BirA enzyme. NGF-b was than conjugated to streptavidin-Qdot at a molar ratio of 1 NGF: 1 QD. Compared to the previous approaches, the latter has the remarkable advantage of allowing a site-specific labeling and of ensuring a 1:1 stoichiometry between QD and NGF. Nevertheless, the conjugation to NGF of a large size probe like a QD (7-70 orders of magnitude larger than the native protein) can easily influence the neurotrophin dynamics.

A versatile labelling strategy allowing for a higher yield of labelled neurotrophin with minimal structural modification and easily applicable also to precursor neurotrophin, is still lacking. In particular, it is necessary to consider that none of these different labelling techniques have been applied to proNGF. No study regarding labelled proNGF has been reported so far. It can be argued that the lack of knowledge on proNGF trafficking may be also due to a lack of a proper technique useful to label precursor neurotrophins.

1.6 The need for a new approach to study neurotrophins signaling.

proNGF and, generally, precursor neurotrophins are emerging as crucial actors in the physiology of the nervous system. However, for many years, the attention in the neurotrophic factor field has been given only to the study of the mature form of neurotrophins, because for long time they were the only believed to possess an active function[40,41]. This common belief has determined that the majority of information regarding neurotrophin properties is restricted to mature neurotrophins.

Before 2001, the majority of the studies regarding NGF has been performed on its mature form and little has been reported on proNGF mechanism of action. There are still no studies regarding proNGF trafficking in neuron.

Furthermore, since a primary and fundamental characteristic of all neurotrophins is to travel through neurons to trigger their response, the analysis of such a basic property provides important information regarding neurotrophins physiology. This is the reason why many studies have been conducted to analyze NGF transport, but unfortunately some of them report contrasting information (see table 1.2). Moreover, at the best of my knowledge, there are not such information regarding proNGF trafficking. I think that one of the reason for both this discrepancy and this lack of information could be due to the lack of a good labeling strategy applicable to both precursor and mature neurotrophins.

Thus, during my PhD studies, I focused my attention to develop a technique to fluorescently label precursor and mature NGF with minimal and controlled structural modification. The approach I developed is based on a site-specific insertion of a short amino acid tag into the sequence of proNGF; this tag is here used to covalently conjugate a label-substituted arm of a coenzyme A (coA) substrate by phosphopantetheinyl transferase enzymes (PPTases). This tag system allows to label proteins with many different chemical compounds. Thanks to this approach a site-specific biotinylation, as well as fluoro-labeling, of the purified recombinant tagged neurotrophin can be successfully achieved. Importantly, the resulting labelled NGF is fully functional, compared to recombinant wild-type NGF (see chapter 3 for more details). It should pointed out that this strategy guarantees

precise control over stoichiometry and site of conjugation. Importantly, this technique allows to obtain both precursor and mature labeled NGF.

These overall advantages allowed me to study in details proNGF trafficking in neuron and to compare it with that of mature NGF (see chapter 4). To this end, as it will be described in detail in the next chapters of this thesis, fluorescence microscopy experiments have been performed on DRG neurons grown in compartmentalized living cultures, in which fluorescent proNGF and NGF have been administered either separately or together.

Chapter

2

Development of new techniques and methods, and experimental procedures

In this section, I will describe the techniques that were developed in order to synthesize and to label precursor and mature NGF with fluorescent probes.

In the first paragraph (2.1.1), the insertion of amino acid tag sequence in the cDNA of human proNGF is described. In the second one (2.1.2), the protocols to express, refold and purify both proNGF-tag and NGF-tag are reported. Further on, the procedure to label the tagged neurotrophins is reported (paragraph 2.2), and finally, the physiological tests performed to study the retention of both tagged and fluorescent neurotrophins are illustrated.

To conclude this chapter, the microscopy procedure and protocols developed to perform the study of neurotrophin trafficking, both in terms of single particle tracking and analysis of the number of molecules per vesicles, are reported (paragraphs 2.4, 2.5 and 2.6).

2.1 Synthesis of fluo-NGF and fluo-proNGF

In this work, the 'short peptide tag insertion technique[97] has been used to label both precursor and mature NGF.

I have compared 4 different tags (spanning from 8 to 12 amino acids; namely: YBBR, A4, A1, and S6; their sequence are reported in the next paragraph), previously described in the literature[98,99,100], to identify the best to be inserted into proNGF sequence (the one that ensures an optimal yield of both neurotrohin production and labeling, as well as the retention of neurotrophin physiological activity). All these tags contain a specific serine residue, which is specifically conjugated to the phosphopantetheinyl (Ppant) arm of coenzyme A substrates by PP transferase enzymes (PPTases).

The four different short amino acidic tags have been inserted into the C-terminus of NGF. The method to insert each amino acid tag sequence in the cDNA of human proNGF is described in the following paragraph.

2.1.1 Plasmid preparation

Human proNGF cDNA was cloned in pET11 vector and was used as template. The cDNA coding sequences of YBBR (DSLEFIASKLA), A4 (DSLDMLEW), A1 (GDSLDMLEWSLM) and S6 (GDSLSWLLRLLN) tags were inserted at the C-terminus of proNGF. The protocol described in *Marchetti et al*. 2014[101] was used.

Briefly, the scheme of a standard site-directed mutagenesis has been followed, except for two main modifications. The first one is the use of a two-step PCR program in which, during the first step, amplifications with forward and reverse primers were kept separate. The second one is the splitting of the amino acids to be introduced in two sequential PCR reactions (Fig. 2.1).

The reasons to keep the forward and reverse primers separated during the first step amplifications is that in a PCR reaction when long primers are attempted, the mutagenesis efficiency drastically decreased. This is due to the high tendency of

primer to dimerise with each other (since thy are 100% complementary) instead to prefer the primer-template annealing (i.e., due to the multiple mismatches).

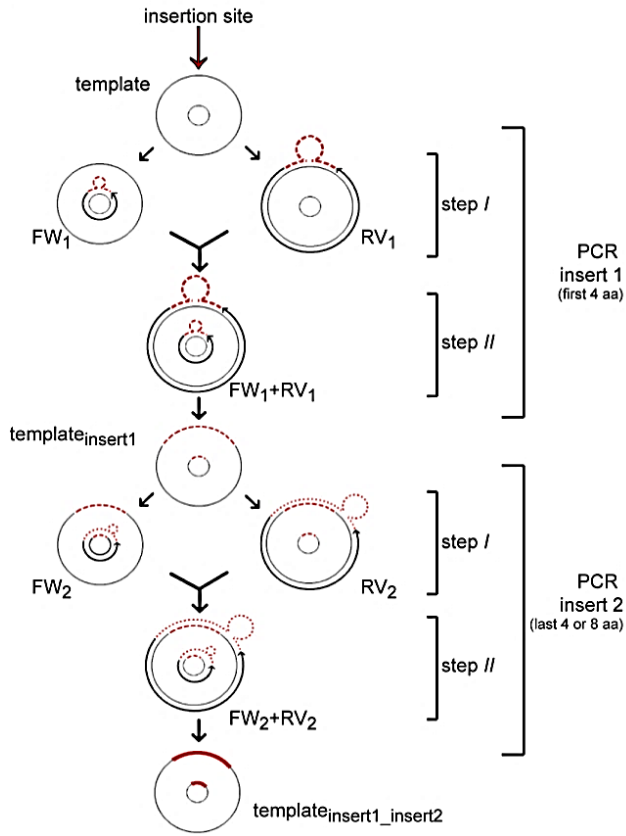

Fig. 2.1. Schematic overview of the insertional mutagenesis method.

Moreover, the splitting of the amino acids tag sequence in two primers and the performing of two sequential PCR reactions allows to avoid classical cloning techniques, and to speed up the insertional process.

All primer pairs were purchased from Sigma-Aldrich, purified by PAGE, and are listed in Table 2.1.

primer name	**Sequence (5'→ 3')**
YBBR-insert1-FW	G CTC TCT AGA AAG GCT GTG AGA GAT TCT CTT GAA TGA TAA GGA TCC GGC TGC TAA C
YBBR-insert1-RV	G TTA GCA GCC GGA TCC TTA TCA TTC AAG AGA ATC TCT CAC AGC CTT TCT AGA GAG C
YBBR-insert2-FW	G GCT GTG AGA GAT TCT CTT GAA TTT ATT GCT AGT AAG CTT GCG TGA TAA GGA TCC GGC TGC TAA C
YBBR-insert2-RV	G TTA GCA GCC GGA TCC TTA TCA CGC AAG CTT ACT AGC AAT AAA TTC AAG AGA ATC TCT CAC AGC C
S6-A1-insert1-FW	G CTC TCT AGA AAG GCT GTG AGA GGA GAT TCT CTT TGA TAA GGA TCC GGC TGC TAA C
S6-A1-insert1-RV	G TTA GCA GCC GGA TCC TTA TCA AAG AGA ATC TCC TCT CAC AGC CTT TCT AGA GAG C
S6-insert2-FW	CT GTG AGA GGA GAT TCT CTT TCG TGG CTG CTT AGG CTT TTG AAT TGA TAA GGA TCC GGC TGC TAA C
S6-insert2-RV	G TTA GCA GCC GGA TCC TTA TCA ATT CAA AAG CCT AAG CAG CCA CGA AAG AGA ATC TCC TCT CAC AG

A1-insert2-FW	CT GTG AGA GGA GAT TCT CTT GAT ATG TTG GAG TGG TCT TTG ATG TGA TAA GGA TCC GGC TGC TAA C
A1-insert2-RV	G TTA GCA GCC GGA TCC TTA TCA CAT CAA AGA CCA CTC CAA CAT ATC AAG AGA ATC TCC TCT CAC AG
A4-insert-FW	CTC TCT AGA AAG GCT GTG AGA GAT TCT CTT GAT ATG TTG GAG TGG TGA TAA GGA TCC GGC TGC
A4-insert-RV	GCA GCC GGA TCC TTA TCA CCA CTC CAA CAT ATC AAG AGA ATC TCT CAC AGC CTT TCT AGA GAG
A4-insert1-FW	G CTC TCT AGA AAG GCT GTG AGA GAT TCT CTT GAT TGA TAA GGA TCC GGC TGC TAA C
A4-insert1-RV	G TTA GCA GCC GGA TCC TTA TCA ATC AAG AGA ATC TCT CAC AGC CTT TCT AGA GAG C
A4-insert2-FW	G GCT GTG AGA GAT TCT CTT GAT ATG TTG GAG TGG TGA TAA GGA TCC GGC TGC TAA C
A4-insert2-RV	G TTA GCA GCC GGA TCC TTA TCA CCA CTC CAA CAT ATC AAG AGA ATC TCT CAC AGC C

Table 2.1. List of insertional primers used for construct preparation. The inserted sequence coding for YBBR, A4, A1 or S6 tags are reported. Each FW and RV pair is formed by complementary primers.

Each insertion was obtained by performing the following PCR reaction in 50 µl reaction: 1.5X Turbo DNA Polymerase Buffer, 250 ng insertional Primer, 1 mM dNTPs, 3 µl Quick Solution, 1 µl Turbo DNA Polymerase and 15 ng DNA template. To avoid primer self-annealing artifacts, each PCR run consisted of two steps, as reported in Table 2.2 and depicted in Fig. 3.3. In the first step (10 cycles), two independent 50 µl PCR reactions were run for the same template, one containing only the FW insertional primer, the other one containing only the corresponding RV insertional primer. In the second step (18 cycles), the two separate reactions were mixed and two tubes containing each 25 µl of FW and 25 µl of RV reaction were supplemented with 0.75 µl Turbo DNA Polymerase.

Afterwards, each 50 µl PCR reaction was subjected to digestion with 1 µl DpnI (New England Biolabs), at 37°C for 2-3h in the presence of the specific DpnI buffer to eliminate parental DNA template. The final 100 µl reaction was recovered and purified using the QIAquick PCR Purification Kit (Qiagen), eluted in 25 µl EB buffer and ~1/5 of recovered DNA was transformed into chemically competent XL10 Gold bacteria.

To obtain YBBR-, A1- and S6- tagged proNGF two sequential PCR reactions with two partially overlapping primer pairs were performed to introduce the first 4 (*insert1*, see Table 2.1) and the other 7-8 amino acids (*insert2*, see Table 2.1). Each PCR run was followed by DpnI digestion, PCR cleanup and transformation in XL10 Gold bacteria. Bacteria transformed with *insert1* reaction were grown in 5ml LB medium supplemented with antibiotic overnight at 37°C; next morning DNA was mini-prep extracted, quantified and used as template of the *insert2* PCR run. Bacteria were plated for screening only after transformation of *insert2* reaction. Colonies were picked and positive clones screened by DNA sequencing.

For the insertion of A4 tag downstream the sequence of proNGF, both the insertion of the complete tag (8 amino acids) with a unique primers pair and the sequential insertion of 4+4 amino acids was performed.

For the two strategies, the measured insertion yields was 33% and 17%, respectively. These values were measured counting the number of positive clones, after their screening by DNA sequencing, and comparing this value with the total amount of clones picked.

PCR program		**Temperature**	**Time**
Initial Denaturation		95°C	60 s
Step 1 (10 cycles)	**Denaturation**	95°	60 s
	Primer annealing	55°	90 s
	Extension	68°C	60 s per Kb DNA template
Step 2 (18 cycles)	**Denaturation**	95°	60 s
	Primer annealing	55°	90 s
	Extension	68°C	60 s per Kb DNA template
Hold		4°C	∞

Table 2.2. Scheme of the PCR program used for the insertional mutagenesis.

2.1.2 Expression, purification and refolding of proNGF and NGF.

To express and to purify the proNGF and tagged-proNGF (proNGF-tags), I used this protocol adapted from a previous one published for the purification of recombinant human proNGF[20] and modified according to *Paoletti et al.*[102]. A schematic representation of all the entire process is represented in Figure 3.3 of the following chapter.

- **Protein Expression**

ProNGF/proNGF-tagged cDNA were cloned in the prokaryotic expression vector pETM11, where the expression is regulated by the T7 promoter and induced by IPTG (Isopropil-β-D-1-tiogalattopiranoside) during the phace of bacterial growth.

The protein expression was performed in the BL21(DE3) strain of *E. coli*, transformed with 30-100 ng of plasmid pET11a containing the gene of human proNGF or proNGF-tags. The cells were plated on agar plates containing Luria broth (LB) medium added with ampicillin (amp) overnight at 37°C.

After the overnight growth, one colony was inoculated in 20 ml of LB supplemented with Amp and grown overnight at 37°C with shaking at 250 rpm.

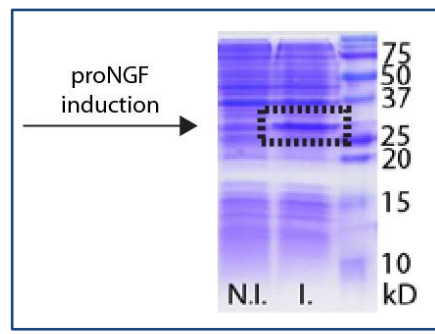

Fig. 2.2. A typical SDS-PAGE (15% acrylamide gel) analysis of cell culture of BL21(DE3) strain of *E. coli* transformed with pET11a plasmid containing the gene of human proNGF or proNGF-tags before protein induction (N.I.) and after protein induction (I.). Coomassie Blue stained. Last lane represents the molecular standard weights (MW).

The day after, 18 ml of this culture were inoculated in 1 L of LB + Amp at 37°C at 250 rpm to reach an OD_{600nm} of about 1, in order to obtain a considerable cell mass, before induction of protein expression with 1 mM IPTG. The protein

induction was checked by SDS-PAGE, where a small amount of culture, before and after the protein induction, were compared (Fig 2.2).

- **Inclusion Bodies Purification**

After 5 hours, cells were centrifuged at 6000 rpm 4°C for 10 min. The obtained pellets were first resuspended in 20 ml of lysis buffer (10 mM TRIS HCl pH 8, 1 mM EDTA pH 8 and 1mg/ml lysozyme), then sonicated (3 times of 45" on 60" off at 4°C), and finally 50 ug/ml DNase was added to isolated inclusion bodies.

After 30 minutes, the solution was harvested at 13000 rpm 4°C for 30 min and then washed twice with 50 mM TRIS HCl pH7.5 and 1 mM EDTA. Next, it was harvested once again, solubilized with 5 ml of 6M guanidinium, 100 mM TRIS HCl pH 8, 1 mM EDTA and 100 mM DTT, and left one night to dialyze in a 6M guanidinium pH 3.5 buffer.

At this point the inclusion body were solubilized. Each step was controlled through a SDS-PAGE (Fig. 2.3).

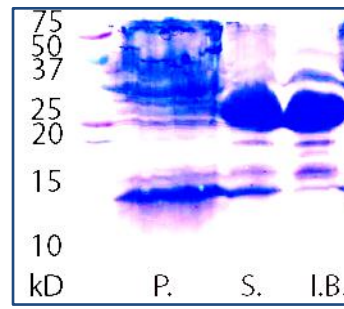

Fig. 2.3. A typical SDS-PAGE (15% acrylamide gel) analysis of the pellet before (P.) and after (S.) the sonication and of solubilized inclusion bodies (I.B.). Coomassie Blue stained. The first lane is the MW standard.

- **Protein Refolding**

To allow the correct folding of the neurotrophin, protein concentration was measured whit Bradford assay, followed by a drop by drop addition of 5mg solubilized inclusion body in 100 ml of refolding buffer (1 M Arginine, 100 mM TRIS HCl pH 9,3, 5 mM EDTA pH 8, 5mM GSSG and 5 mM GSH).

- **proNGF Purification**

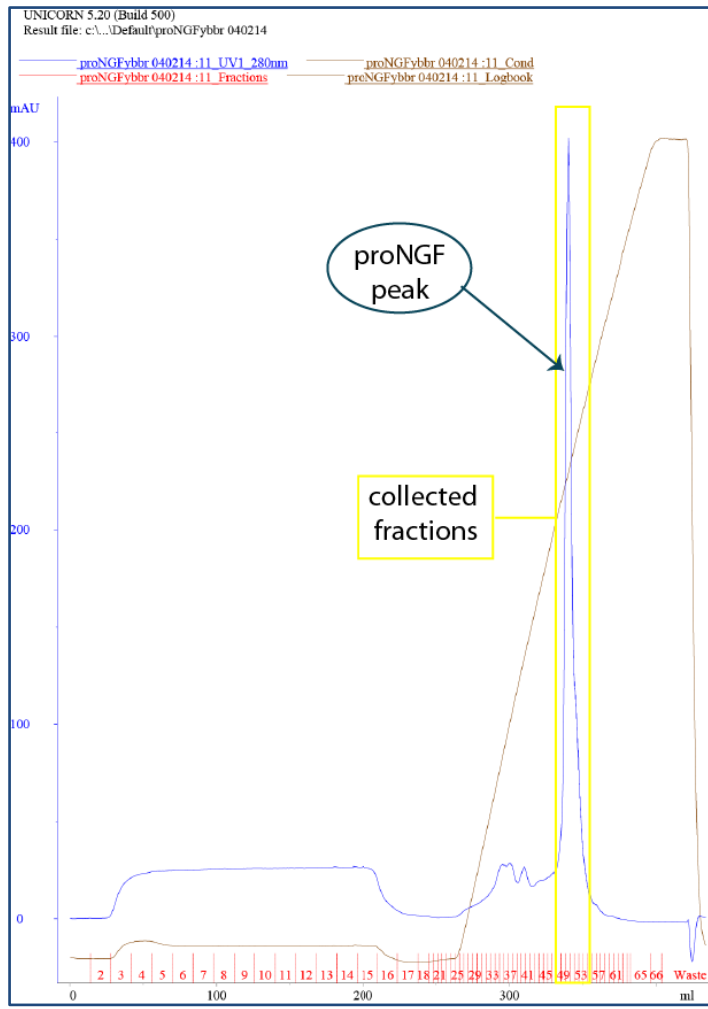

Fig. 2.4. Chromatographic profile of proNGF purification. The aliquot of filtered (0,22µm) proNGF solution was applied to a HiLoad 16/10 SP Sepharose 1 (20 ml) 17-1137-01 (5-ml) column preequilibrated with the phosphate buffer 50mM, pH 7.4. The fractions were eluted at a flow rate of 1 ml/min, with a linear gradient of 0–1 M NaCl. Fractions (1-5 ml) were collected, and a 20 µl aliquot from each fraction was assayed in a SDS-page. FPLC ion-exchange chromatography graph of proNGF purification.

After an overnight dialysis in phosphate buffer, native proNGF and proNGF-tags were purified via FPLC ion-exchange chromatography (Fig. 2.4). Before the purification each aliquots were filtered with 0,22 µm nitrocellulose filter membrane.

ProNGF was collected, fraction by fraction, as reported in the FPLC graph (Fig. 2.4). Each fraction was controlled by SDS-PAGE, as show in Figure 2.5.

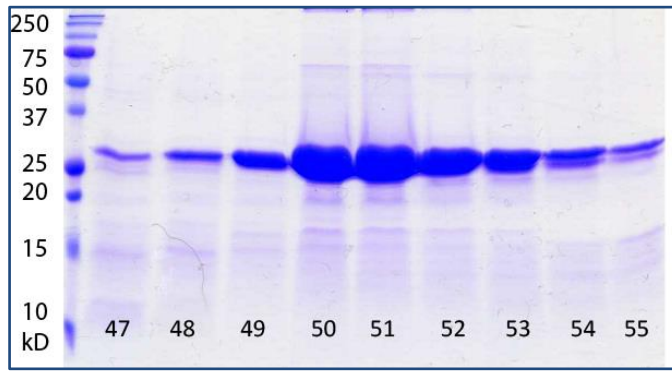

Fig. 2.5. SDS-PAGE (15% acrylamide gel) analysis of the fractions (20µl) collected from FPLC during proNGF purification. Coomasie Blue stained. The first lane is the MW standard.

- **proNGF Cleavage**

Mature NGF and NGF-tags protein were obtained upon proteolysis of the purified proNGF or proNGF-tags, using trypsin protease (1µg enzyme: 100-200 µg of neurotrophin).

In both cases, mature protein were obtained after a non-specific cleavage of the pro-peptide domain from the C-terminal up to the N-terminal of the mature NGF. This process was always followed with SDS-page experiment in a time-course, to check the correct time and enzyme concentration needed to reach the proper cleavage (Fig. 2.6).

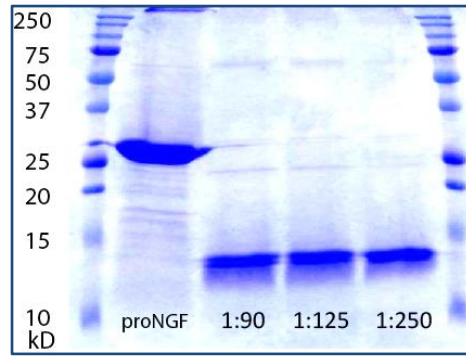

Fig. 2.6. SDS-PAGE (15% acrylamide gel) analysis of the proNGF enzymatic cleavage. The first and last lane are the MW standard. The second lane (proNGF) corresponds to proNGF before the incubation with trypsin; the following lane correspond to proNGF incubated overnight 4° with trypsin in the proportion of 1 µg of enzyme for 90 µg of pro-neurotrophin (1:90), or 1 µg of enzyme for 150 µg of pro-neurotrophin1 (1:125), and 1 µg of enzyme for 250 µg of pro-neurotrophin. Coomassie Blue stained

To verify that, during proNGF-tags incubation with trypsin, the covalent linked amino acid tag was not cleaved, a SDS-PAGE to confront *wt* NGF and NGF-tags was performed. The SDS-page demonstrates the higher molecular weight of NGF-tag respect to that of *wt* NGF (Fig. 2.7).

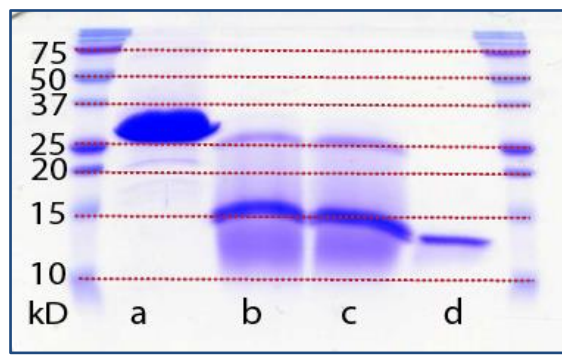

Fig. 2.7. SDS-PAGE (15% acrylamide gel) analysis of the NGF-tag compared to the wt NGF. The first and last lane are the MW standard. The second lane (a) corresponds to proNGF-YBBR before the incubation with trypsin; the following lanes (b and c) correspond to NGF-YBBR and the last lane (d) correspond to wt NGF. Coomassie Blue stained.

- **NGF Purification**

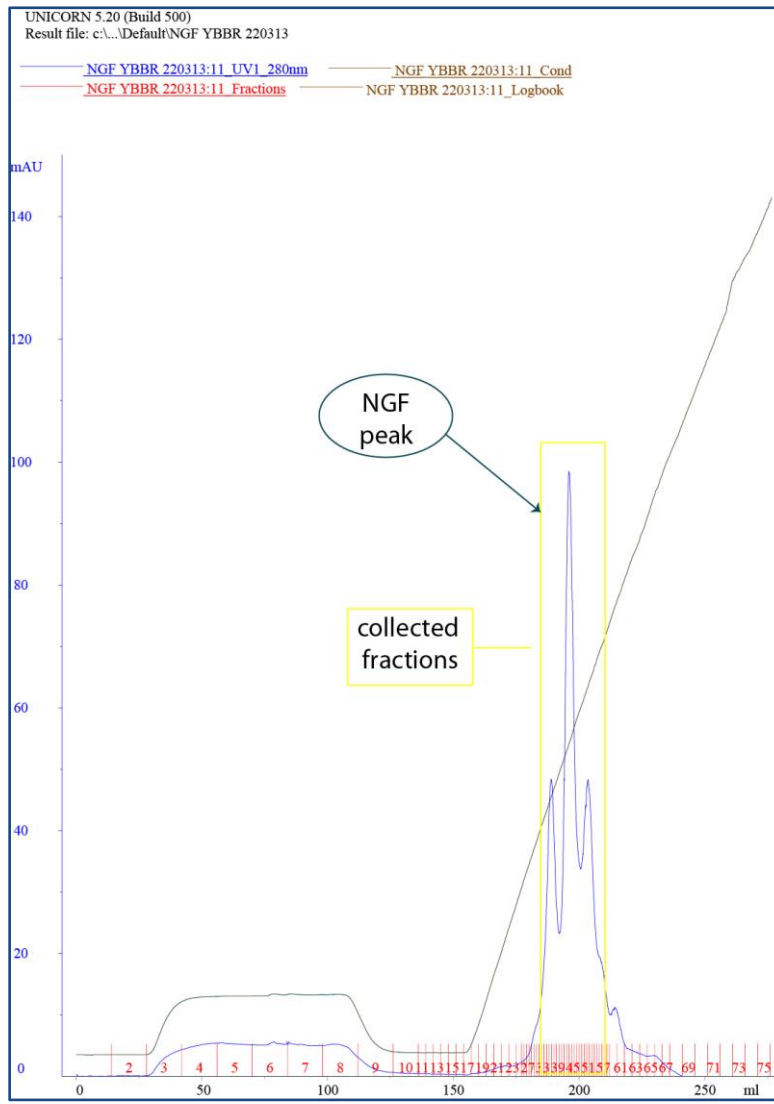

Fig. 2.8. Chromatographic profile of NGF purification. The aliquot of proNGF solution reacted with trypsin was applied to a HiLoad 16/10 SP Sepharose 1 (20 ml) 17-1137-01 (5-ml) column preequilibrated with the phosphate buffer 50mM, pH 7.4. The fractions were eluted at a flow rate of 1 ml/min, with a linear gradient of 0–1 M NaCl.

After proNGF cleavage, another step of ion exchange FPLC chromatography was used for the purification of mature neurotrophin from fragments arising from the multiple cleavage of the pro-peptide domain (Fig 2.8).

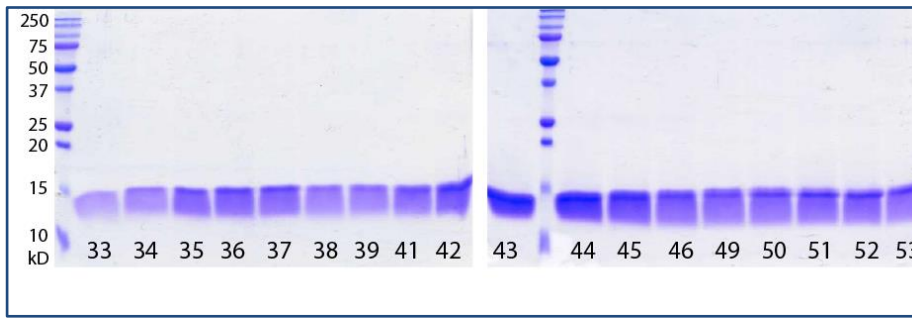

Fig. 2.9. SDS-page (15% acrylamide gel) analysis of the fractions (20µl) collected from FPLC during NGF purification. Coomassie Blue stained. The first lane and the 12th are the MW standard.

Fraction were collected and were controlled by SDS-page assay, as shown in Figure 2.9.

2.2 Labeling of tagged proNGF and NGF.

2.2.1 Biotin-NGF and biotin-proNGF

To obtain proNGF and NGF labeled with biotin, equal amounts (10 µg) of purified, tagged NGF and precursor proNGF were incubated for 30 minutes at 37°C with a reaction mix (10 mM $MgCl_2$, 10 µM CoA-biotin and 2 µM Sfp Synthase (SfpS) or Acp Synthase (AcpS) (New England Biolabs), or no enzyme as control in phosphate buffer up to 30 µl final volume. Untagged proNGF and NGF were subjected to the same reaction, as controls.

- **NGF and proNGF biotinylation analysis**

In order to quantify proNGF and NGF biotinylation reaction yields, 2 µl of all NGF/proNGF biotinylation reactions were treated under denaturing conditions (100°C, 8 minutes in 2X Laemmli Sample Buffer), loaded on two gels (1 µl for each gel; 4–12% Criterion™ XT Bis-Tris Gel, BioRad) and electrotransferred to two PVDF membranes respectively. These were blocked in TBST + 5% w/v BSA, then one of them was blotted with anti-NGF antibody (sc-549, Santa Cruz Biotechnology) (1:2000), while the other one was incubated with HRP-conjugated streptavidin (Zymed®) 1:10000 diluted in blocking solution.

2.2.2 Fluo-NGF and fluo-proNGF

For the fluorolabeling, 10 µg of proNGF-YBBR or NGF-YBBR were incubated for 30 minutes at 37°C at 300 rpm with a reaction mix (10 mM $MgCl_2$, 10 µM CoA-alexa488 or CoA-alexa 647 and 2 µM Sfp Synthase (SfpS) (New England Biolabs), in phosphate buffer up to 250 µl final volume. This step was immediately followed by an ion exchange HPLC chromatography in order to remove the non-fluorescent form from the labeled specie (see Fig. 3.8 of next chapter). Purified fluorescent neurotrophins were stored up to three weeks in pre-coated (BSA 1%) tubes at 4°C.

- **Determination of labeling yield.**

In order to determine NGF-YBBR fluorolabeling yield, the integral of the 280 nm peak of fluo-NGF has been compared to that of the non-reacted NGF. This required a correction of fluoNGF absorbance at 280 nm for the contribution of Alexa488 fluorophore. Briefly, the correction factor (CF), defined as A_{280nm}/A_{488nm}, was calculated from the value obtained by the HPLC analysis of Alexa488 fluorophore alone. FluoNGF absorbance at 280 nm was then subtracted of CF multiplied for fluoNGF absorbance at 488 nm.

2.2.3 Synthesis of CoA- conjugate.

The synthesis and HPLC purification of CoA-biotin and CoA-fluorophore conjugates were conducted as described in *Marchetti et al.*, 2014[103].

Briefly, for the synthesis of CoA-biotin and CoA-Alexa488/647, Coenzyme A (10 nmol), dissolved in DMF (2 ml), was mixed with the appropriate maleimido derivative (20 nmol) in DMF (10 mM). The solution was stirred at 35˚C for 4 hours. The product was purified by RP-HPLC (column: Phenomenex Fusion 15064.6. Solvents: ammonium formate 5 mM/acetonitrile).

2.3 Characterization of fluo-NGF and fluo-proNGF physiology

2.3.1 Cell culture

- **PC12 cells**

PC12 cells are a NGF responsive cell line, derived from a rat pheochromocytoma. PC12 cells project long neurites in response to NGF: by one week's exposure to NGF, PC12 cells cease to divide and begin to extend processes similar to those produced by neurons in primary cell cultures[104]. In this thesis, I used PC12 cells to perform qualitative analysis on NGF and NGF-tags and fluo-NGF, to verify their retention of biological functions (Fig. 3.6A and Fig. 3.8C)

PC12 (ATCC, CRL-1721) cells were maintained at 37°C, 5% under CO_2 in RPMI1640 medium supplemented with 10% horse serum, 5% fetal bovine serum and 1% penicillin/streptomycin (Gibco). To induce PC12 differentiation, cells were maintained at 37°C, 5% CO_2 in RPMI1640 medium supplemented with 1% horse serum, 0,5% fetal bovine serum and 1% penicillin/streptomycin (Gibco) and were treated with 50 ng/ml *wt* NGF or recombinant NGF-tags or NGF-biot or NGF-Alexa. As controls non treated PC12 cells were used. Cells were observed after five days at a Leica DM6000 microscope capable of transmission DIC imaging.

- **TF1 cells**

TF-1 cells (ATCCLGC Standards, Teddington, UK) are a factor-dependent human erythroleukemic cell line, that express TrkA receptor.

To verify whether NGF-tags and fluo-NGF retained all the physiological characteristics of *wt* NGF, I performed studies to analyse NGF ability to induce cells proliferation. NGF administration causes cells proliferation in this cell line. The chromogenic substance MTT (3-(4,5-Dimethyl-2-thiazolyl)-2,5-diphenyl-2H-tetrazolium bromide) is added after the NGF has stimulated TF1 cells, to conduct a colorimetric analysis on a micro plate reader[105]. In this work, this test has been

performed in order to estimating the bioactivity of *wt* NGF compared to that of NGF-tags (Fig. 3.6 B). This method represent a quantitative NGF assay.

TF1 cells were cultured in RPMI 1640 medium, 10% fetal bovine serum and 1% penicillin/streptomycin (Gibco), supplemented with 2 ng/ml recombinant human GM-CSF (R&D Systems Inc.). The TF1 proliferation assay was performed in 96 wells microtiter plates by incubating 15,000 cells per well in the presence of several doses of either wild type hNGF and NGF-YBBR or NGF-A4, ranging between 50,000 and 5 pg/ml. Cells were seeded 1 h before treatment. A MTT Cell proliferation assay (ATCC kit) was employed to evaluate cell response: after a 40-hour culture period, MTT solution was added for an additional 4 hours incubation. The intensity of each colorimetric signal was measured at 570 nm in a microtiter plate reader, 16 hours following addition of detergent reagent. In all experiments, each different treatment was done in triplicate.

- **Rat Dorsal Root Ganglion Neurons**

Rat Dorsal Root Ganglion Neurons (R-EDRG-515 AMP, Lonza) were maintained in a humidified atmosphere at 37°C, 5% CO_2 in Primary Neuron Basal medium (PNBM, Lonza) supplemented with L-glutamine, NSF-1 (2% final concentration) and antibiotics. For the survival of DRG neurons, 50-100 ng/ml of NGF were added to the media. The media was replaced every 4-5 days with a pre-warmed fresh one. When neurons were plated in microfluidic devices, this procedure has to be performed being careful to always leave the main channels filled with media. Moreover, a NGF gradient, performed leaving the soma compartment with 50 ng/ml of NGF while the axon compartment in the presence of 100 ng/ml, was used to induce DRG axons to grow in the channel compartment and to reach the axon compartment.

  - **Compartmented Cultures**

For compartmented cultures, a microfluidic device (Xona Microfluidics, RD 450) was sealed to willCo-wells (WillCo-dish "Series GWSt-3522) with a with a plasma sterilizer/cleaner. The device was coated with a solution of poly-L-Lysine (0.01%, sterile-filtered, P4832, Sigma) and Laminin (5µg/ml, 23017-015,Gibco, Invitrogen) overnight in a humidified incubator at 37 °C. DRG neurons were plated into the soma chamber (SC). Axons crossed the channel barrier (CC) into the central

chamber and reached the axon chamber (AC) within 3–6 days, as previously described[106]. DIV8-15 cultures of DRG neurons were used in all experiments.

2.3.2 NGF signal transduction effectors analysis

To study the signal transduction effectors, PC12 cells were cultured in P100 petri dish to reach confluence, starved overnight (o.n.) in a serum-free medium and then incubated with native NGF, tagged NGF, biot-NGF and fluo-NGF (150 ng/ml) at 37°C. After 15 min cells were washed in ice-cold PBS and lysed in RIPA buffer supplemented with proteases and phosphatases inhibitors. 50 µg of each clarified lysate were loaded on a gel (4–12% Criterion™ XT Bis-Tris Gel, BioRad) and electrotransferred to PVDF membranes. These were first blotted using the antibody anti-phospho-PLCγ1 (#2821, Cell Signaling Technology;1:1000), anti-phospho-p44/42 MAPK (#9106, Cell Signaling Technology;1:2000) and anti-phospho-Akt (#4060, Cell Signaling Technology;1:2000). The primary antibody was detected by using an anti-mouse or rabbit secondary antibody HRP-conjugated (Biorad; 1:1000) diluted in blocking solution. The membranes were then stripped and re-blotted with respectively anti-PLCγ1 (#5690, Cell Signaling Technology;1:2000), anti- p44/42 MAPK (#4695, Cell Signaling Technology;1:1000) and anti-Akt (#4691, Cell Signaling Technology;1:2000). The detection was performed as above described. Presented images have been subjected to linear contrast enhancement after image analysis.

2.4 Microscopy Measurements.

All microscopy measurements have been conducted using a wide field microscope (Leica DM6000 equipped with the Leica TIRF-AM module) at 37°C, 5% CO_2. Light has been collected with a HCX PL APO 100x NA 1.47 oil immersion objective (Leica Microsystems) and recorded by an EMCCD camera (Hamamatsu C9100-13). An additional -0.7x lens was mounted in front of the camera chip and a complete field of view of 117 µm x117 µm was obtained.

To measure PC12 differentiation, transmitted light imaging has been performed in Differential interference contrast (DIC) configuration.

- **Acquisition settings**

To record fluo-NTs transport in neurons by epi-fluorescence microscopy, two solid state lasers at 488nm and 633nm (present in the Leica Microsystems TIRF-AM module) have been used, in order to excite Alexa488 and Alexa647 respectively.

In single-color experiments, Alexa488 fluorescence light has been separated by a dichroic mirror lw_t502lpxr (Leica) and it has been filtered by a Semrock FF01-525/45 band pass filter (Leica). The exposure has been set to 0.1 s and a 10 Hz frame rate has been obtained.

In two-color experiments, sequential excitation at 488nm or 633 nm was applied and fluorescence light has been separated by the Quad ET TIRF MC filtercube for Laser line 405/488/561/632 No 11523026 (Leica). Light from Alexa488 has been additionally filtered by the Semrock FF01-525/45 band pass filter (in addition to the bandpass capability 525/36 of the Quad filtercube), for the emission for Alexa647 the 705/72 bandpass of the Quad filtercube was sufficient. The exposure time has been set to 0.05 s for each channel and a 6 Hz repetition rate has been obtained.

2.5 Single Particle Tracking.

Single Particle Tracking analysis has been performed by custom made Matlab scripts following the approach previously described by Raghuveer Parthasarathy[107].

In brief, vesicle sub-pixel localization has been achieved by an analytic, non-iterative calculation of the best-fit radial symmetry center, method that allow to find the center of each vesicle. This localization method has been selected because it provides a very fast localization (up to 180000 frames for each experiment has been analyzed) .

For each acquired fluorescence image sequence, the channel area has been manually selected, then vesicles localization and trajectories reconstruction has been achieved by means of Matlab code distributed by Raghuveer Parthasarathy. Vesicle trajectories shorter than 10 µm have been discarded in order to minimize the impact of artefacts due to wrong linking.

A variable number of trajectories (between ~1000 and ~6000) have been measured for each selected condition.

In order to characterize vesicle dynamics, a particle displacement was measured as the displacement that each vesicles had from the initial position to the end of its movement. For measurements in the channel compartment, the sign of the displacement modulus is positive for retrograde transport and negative for anterograde transport. For the measurement in the soma compartment just positive sign was used.

Since the measured trajectories were mostly straight, the average vesicle speed is determined by a fit of displacement versus time (if necessary, along x and y directions, with the two results quadratically combined).

- **Characterization of the stop and go motion**

Due to the characteristic stop and go motion exhibited by endosomes, the average vesicle speed doesn't fully describe the movement properties. Thus, in order to better characterize vesicle motion, each trajectories was divided in subtrajectories where the vesicle was moving anterogradely, moving retrogradely, or mostly immobile.

Thus, after a moving average filter of 5 frames on the particle position, were considered as immobile the region of each trajectory with an instantaneous speed below 1.25 μm/s. This threshold was empirically determined by visual inspection of some hundreds of trajectories: the speed on parts that were undoubtedly in a "go" phase was almost always in the 2-3μm/s range (so the threshold was chosen to be half of the mean of this range), with rare cases of "steps" with higher speed (up to 3.7μm/s), and no case of "go" motion with speed below 1.25μm/s. Moreover, the minimum length of each subtrajectory has been set to 0.5 s and thus shorter segment were assigned with the same class of the neighbors subtrajectories. As example, a region considered as immobile was rejected if shorter than 0.5 s and it was labeled as anterograde if in between two anterograde regions or as retrograde if in between two retrograde regions. Furthermore, if a subtrajectory shorter than 0.5 s was found between two different classes of motion is was assigned to the region with the more similar speed. As example, a region of anterograde motion shorter than 0.5 s found between an immobile and a retrograde step has been considered as immobile. Finally, the results with the chosen parameters described above were satisfactorily checked on some tens of trajectories.

Moreover, in order to avoid the choice of a somewhat arbitrary threshold, the distribution of times required to move 1 μm was also measured. This quantification allows reducing the impact of stop region in the estimation of the speed. In fact, many vesicles spend several seconds immobile before starting to move again and this behavior greatly reduces the average speed.

In brief, particle displacement for each measured trajectory was divided in steps of 1 μm length. For each step, the time delay required to the particle in order to shift 1 μm was measured (the total number of measured time delays corresponds therefore to the total measured displacement in μm). Each measured time delay is used to estimate the speed in the 1 μm related displacement.

The final distributions were obtained by the histogram of all time delays for all measured trajectories. The mode of the time distribution was estimated by a Gaussian interpolation of the 4 highest bins. Such estimated time was used to quantify the modal speed during active movement.

In the case of colocalizing trajectories, they were estimated by visual inspections of extracted trajectories in the green and red fluorescence channels, after an initial automatic selection based on the average time and positions of each trajectory in each microfluidic channel.

All statistical comparisons were performed by GraphPad Prism (GraphPad).

2.6 Quantification of neurotrophins number inside vesicles.

The trajectories recorded by single particle analysis (between ~1000 and ~6000 for each selected condition) were further investigated in order to measure the average number of fluorophores contained in each spot (number analysis).

This analysis is allowed by the 1:1 fluorophore:neurotrophin monomer stoichiometry, and by the identical excitation and emission configuration for all the single fluorophores, which allow to measure the number of fluorophores in each spot by the intensity of the spot.

In order to correct for particle movement in the axial direction and for variable background, the integral of emitted fluorescence was quantified by a Gaussian interpolation of intensity spots (as it is represented in Fig. 4.11 of the 4th chapter). Thus, to allow a smooth convergence of the interpolation algorithm we performed a procedure that includes a re-centering step followed by a moving average filter.

In brief, in order to re-center each recorded vesicle, a 3 μm square selection has been applied in each frame around the particle position and moved frame by frame according to the recorded trajectory. In fact, in the image sequence obtained in this way, the recorded vesicle was fixed in the center. Thus, a moving average filter of 20 frames could be applied, in order to reduce the noise, before a Gaussian interpolation was used to quantify the integral of fluorescent light of the selected vesicle.

Fitted intensities corresponding to a Gaussian waist more than 600 nm (about twice the optical resolution) were discarded, in order to avoid erroneous brightness estimation due to background and proximity of other vesicles.

The obtained intensities were then normalized by the average value measured with the same algorithm applied to pseudo-immobilized fluorophores contained in a 10% agarose gel. The average value measured for single fluorophores has been further verified by occasional blinking or photobleaching single steps of fluorophores immobilized in the used gel (Fig. 2.10).

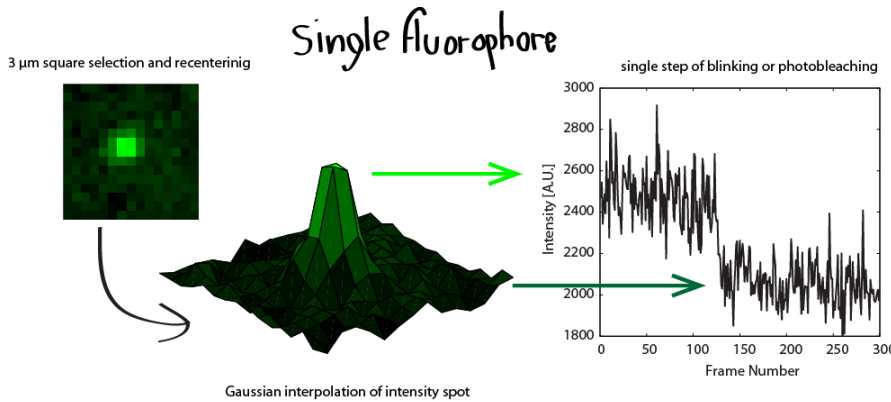

Fig. 2.10. Emitted fluorescence of a single fluorophore. Schematization of the analysis for the quantification of brightness derived from a single fluorophore.

Summarizing, the comparison between the emitted fluorescent coming from each single vesicle was compared to that coming from a single fluorophore, in order to estimate the number of neurotrophin carried by vesicles.

Chapter

3

Site-specific labeling of mature and precursor NGF forms

In this chapter I will present the toolbox that I have designed for the site specific labeling of NGF and proNGF. By means of a suitable insertional mutagenesis method, the insertion of a short amino acid tag into the sequence of NGF will be shown. This tags is covalently conjugated to a label-substituted arm of a coenzyme A (CoA) substrate by phosphopantetheinyl transferase enzymes (PPTases). I will present that a site-specific biotinylation, as well as fluoro-labeling, of the purified recombinant tagged neurotrophin can be achieved, in both the immature proNGF and mature NGF forms. The resulting labelled NGF is fully functional, compared to recombinant wild-type NGF. I will describe the process to obtain the enzymatic labeling of neurotrophins as an alternative to their chemical, non-site-specific labeling.

The present strategy has several main advantages. First of all, it yields precise control over stoichiometry and site of label conjugation. Second, the tags used can be functionalized with virtually any small probe that can be carried by coA substrates, besides (and in addition to) biotin and fluorophores. Third, the toolbox can be applied, in principle, to all the mature neurotrophins and their precursor. Fourth, it makes possible to image and track interacting molecules at the single-molecule level in living systems (topic analyzed in the next chapter).

3.1 Tagged NGF and proNGF

3.1.1 The strategy: the use of short amino acid tags

In order to obtain fluorescent NGF and proNGF, I have designed and adopted a two-step labeling technique schematized in Figure 3.1A. The strategy is composed of a first phase where a short peptide tag has been introduced into the protein sequence (as indicated in Fig. 3.1B and represented as a red arm in Fig. 3.1A), and a second step where a site-specific enzymatic reaction has been exploited to covalently link a biotin or a small organic fluorophore to a residue of the inserted tag. Since both the unprocessed and mature forms of NGF are homodimeric proteins, this labeling procedure allows to get one precisely label per neurotrophin monomer (represented in green in Fig. 3.1A).

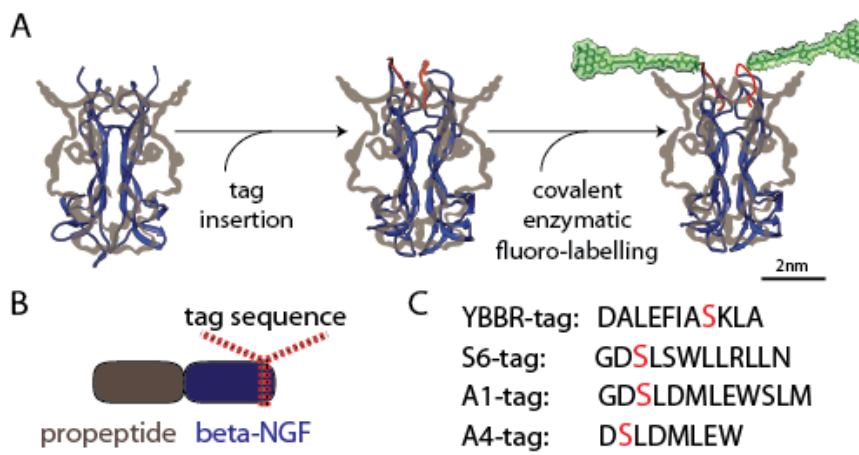

Fig. 3.1. Tagged and fluorescent NGF and proNGF. (A) Schematic cartoon depicting the two-step of the applied labeling strategy. Crystal structure of NGF (blue ribbon, PBD 1SG1) with the overlay of pro-peptide domain schematized in grey as one representation of the possible conformation (*Left)*; schematized proNGF-tag where in red is pictured the tag sequence (*Middle*), and fluo-proNGF where the green shadow overlay the fluorophores (*Right*). (B) Representation of proNGF sequence where the tag insertion site is highlighted by a dashed red arrow. (C) Tags sequence. For each sequence, the serine residue involved in the bound with the fluorophore is highlighted in red.

This kind of labelling approach has been inspired by a sector of the literature describing the methods for modifying proteins site-specifically with small synthetic molecules. Several investigators have described different methods: short peptide sequences with a tetracysteine motif were found to react with biarsenical fluorophores in living cell[108]; the *Escherichia coli* biotin holoenzyme synthetase, BirA was used to catalyse transfer of biotin to the 15-residue acceptor peptide (AP)[109], and then to catalyse transfer of ketone isotere of biotin specifically conjugated to functionalized molecules[110]; acyl and peptide carrier proteins (ACP and PCPs) were found to label protein with small molecules by Sfp phosphopantetheinyl transferase [111]. Regarding the latter methods, target proteins were expressed as fusions to the PCP (small peptide, 80 amino acids) and a Sfp phosphopantetheinyl transferase was used to label PCP site-specifically with small molecule phosphopantetheinyl (Ppant) conjugate (when the small molecules were attached to CoA via thioester, thioether, or disulfide linkages).

I took advantage of the previous demonstration in the laboratory that TrkA can be successfully labeled with ACP-tags methods and that, exploiting this strategy, single particle tracking has been performed[112].

In this work, short peptide tags, derived from *in vitro* evolution studies[100,113] aimed to the shortening of the acyl and peptidyl carrier protein (ACP and PCP) tags[98], have been used. I have compared 4 different tag sequences (spanning from 8 to 12 amino acids; named: YBBR, A4, A1, and S6; Fig. 3.1C) to identify those ensuring an optimal yield of both neurotrohin production and labeling, as well as the retention of neurotrophin physiological activity. Like PCP tag, all tags contain a specific serine residue (highlighted in red in the sequences of Fig. 3.1C), which is specifically and covalently conjugated to the phosphopantetheinyl (Ppant) arm of coenzyme A substrates by PPTases, as represented in Fig 3.2. The reason to choose this kind of tag was that these are versatile in that differently substituted CoA substrates can be used in the labeling reaction (e.g. biotin-CoA, fluorophore-CoA), leading to differently labeled neurotrophins. Moreover, they offer the advantages of a short length, which promises little modification of the NGF structure with reference to the wild type form. In principle, with this approach any small-molecule probe can be easily site-specifically attached to tag fused to the target protein in one simple step within 30 min.

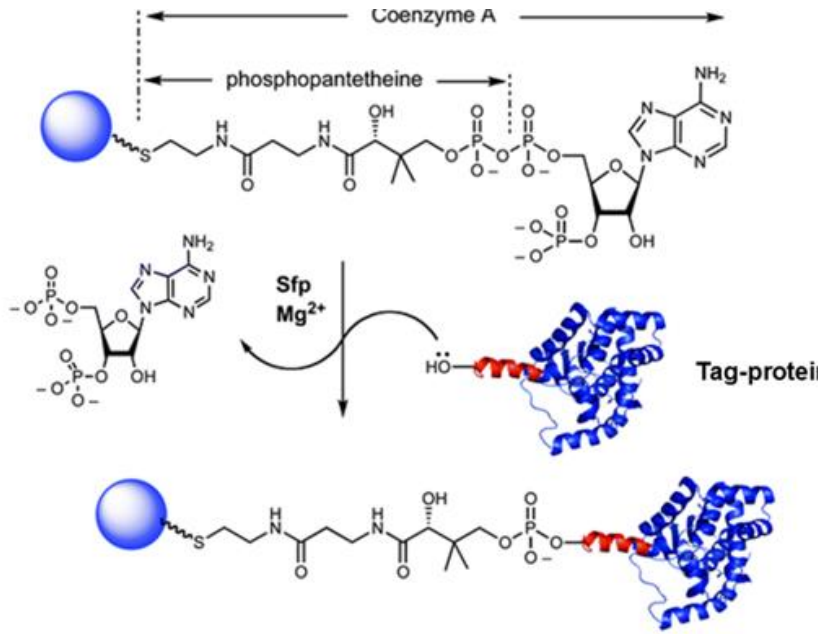

Fig. 3.2. Peptide labeling reaction Sfp- or AcpS- catalyzed. Small-molecule-CoA conjugates are used as the donor of the small-molecule-Ppant group to a specific serine residue in the peptide tags.

3.1.2 The insertional mutagenesis method

The tags have been inserted through an insertional mutagenesis method, based on a modification of the standard site-directed mutagenesis protocol, that allows to speed up the tag insertion procedure. The four different recombinant constructs encoding NGF-tags have been prepared by insertion, one at the time, of the short amino acidic tags into the C-terminus of neurotrophin sequences (Fig. 3.1B). The C-terminus of the neurotrophin was chosen as the best site to insert the tags, because in this position NGF does not interact neither with TrkA nor p75, as it is represented in Figure 1.4 of the first chapter of this thesis.

The insertional mutagenesis procedure used herein has been described in detail in the second chapter of this thesis[101] (see 2.1.1 section).

3.1.3 NGF-tag expression and characterization

For both the native and tagged NGF expression, constructs of human *wt* and tagged proNGF have been expressed and produced in *E. coli*. I followed a method adapted from a protocol previously reported by *Rattenholl et al.*, 2001[114] and modified by *Paoletti et al.*[102]. Briefly, the inclusion bodies have been collected, refolded and purified by FPLC ion exchange chromatography. Purified precursor neurotrophins have been then digested by trypsin and further purified by FPLC ion exchange chromatography in order to obtain mature native and tagged NGF (Fig. 3.3). For more details, see paragraph 2.1.2.

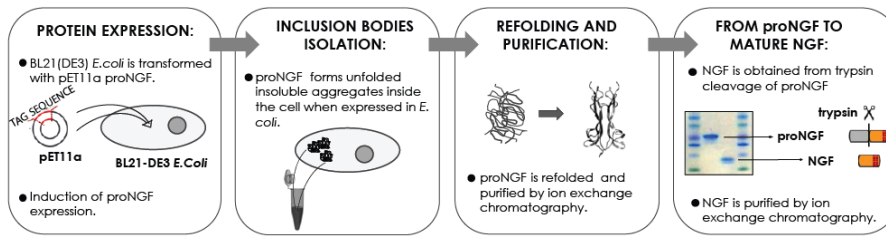

Fig. 3.3. Schematization of different steps in proNGF and NGF synthesis and purification protocol.

The production yields have been measured for all four tagged neurotrophins and compared to those obtained for the untagged counterparts. Figure 3.4 reports the total amount, reported in mg, of precursor and mature *wt*/tagged neurotrophin obtained from one liter of bacterial culture, and shows that tag insertion influences neuropeptide production leading to different yields of protein. In the case of precursor neurotrophins, all tagged constructs have been successfully purified, although with different yields: YBBR>A4>A1>S6. In the case of the mature form, only two of the tags, YBBR >A4, allowed to obtain measurable amounts of purified protein.

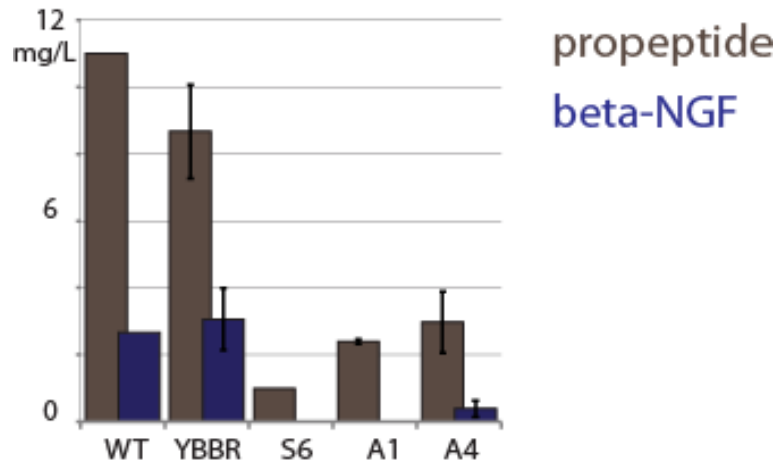

Fig. 3.4. Purification yields of tagged neurotrophin, both as immature proNGF-tag and mature NGF-tag, compared to *wt* NGF.

Accordingly, NGF-YBBR and NGF-A4 have been further characterized in this work.

In order to verify if the tagged neurotrophin still maintains their biological function, I performed a qualitative bioassay to test neurotrophin ability to induce PC12 differentiation. PC12 cells endogenously express NGF receptors TrkA and P75NTR and, when incubated with NGF, undergo neuronal differentiation which manifests morphologically as a neurite network. PC12 cells were incubated with purified *wt* NGF, NGF-YBBR and NGF-A4. I found that both NGF-YBBR and NGF-A4 induce PC12 differentiation to a similar extent of *wt* NGF. These data prove that the modified neurotrophin retains its biological activity to induce neurite growth (Fig. 3.5 A).

In another comparison study using native NGF, NGF-A4 and NGF-YBBR, I checked if the tag insertions interferes with NGF property to induce cell proliferation. The Human erythroleukaemia TF1 cell line express in their surface TrkA receptor, which when bound to NGF, causes the cell proliferation[115]. This allows to have a more quantitative bioassay to determine the potency of different NGF proteins variants. The MTT assay requires adding a chromogenic substance to cells after NGF treatment. The results, performed on cells incubated with *wt* NGF

and NGF-tags (NGF-YBBR and NGF-A4), show that the dose/response obtained values are substantially similar in the three cases (Fig. 3.5 B).

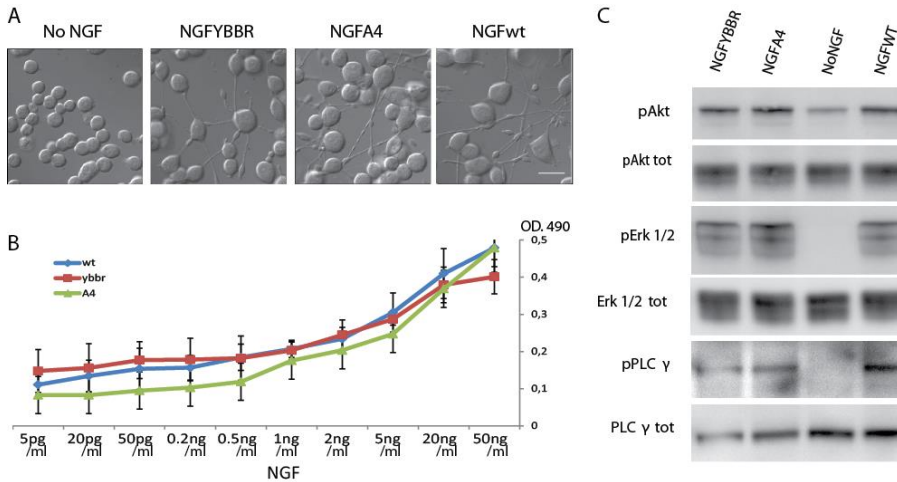

Fig. 3.5. NGF-tag characterization. (A) Typical Nomarski images obtained performing the differentiation assay in PC12 cells using equimolar amounts of wt NGF, NGF YBBR and NGF A4. Cells were observed after five days from the neurotrophin administration. Untreated cells are represented as control. Scale bars represent 20 µm. (B) TF1 factor-dependent human erythroleukemic cells proliferation assay performed administrating wt NGF, NGF YBBR and NGF A4. (C) Western blot analysis of phosphorylated Akt (pAkt), phosphorylated Erk 1/2 (pErk1/2) and phosphorylated PLCγ (pPLCγ) protein levels in PC12 cells in response to wtNGF, NGF-YBBR and NGF-A4 ; protein levels of untreated cells (NoNGF) are used as control.

To complete the analysis of the biological activity of the NGF-tags, I carried out the study of the major signal transduction pathways, activated by NGF in PC12 cells, like phosphorylated Erk1/2, PLC-γ and AKT proteins. Western blot analysis shows no difference between the native and the tagged neurotrophin, demonstrating that NGF-A4 and NGF-YBBR are able to activate TrkA and p75NTR signal transduction pathways similarly to the wild type protein.

Taken together these data demonstrate that NGF-tags are fully functional and they retain all the physiological properties of the native neurotrophin.

3.1.4 Labeling reaction

Subsequently, in order to measure the yield of NGF labeling reaction for the two tagged constructs, I have incubated purified precursor or mature YBBR and A4 constructs with CoA-biotin substrate and Acp- or Sfp-synthase PPTases (Fig. 3.6). As a control, the same biotinylation reaction was performed without enzyme, or on untagged neurotrophins.

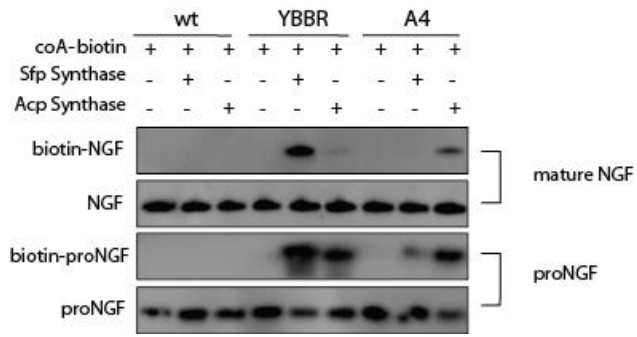

Fig. 3.6. Western blot for the analysis of the biotinylation reaction of purified NGF-YBBR and NGF-A4 using CoA-biotin substrate and AcpS or SfpS PPTases. The same biotinylation reaction is performed in parallel using untagged wt NGF as negative controls. Streptavidin-HRP is used for biotin detection. The anti-NGF blot is the loading control.

Western blot analysis of all biotinylation reactions demonstrates that a specific biotin labeling is achieved for NGF-YBBR and proNGF-YBBR in the presence of both enzymes, with a higher labeling yield provided by the reaction with Sfp-synthase. In the case of NGF-A4 and proNGF-A4, significant labeling is displayed mostly in presence of Acp-synthase, but with a lower yield than in the case of NGF-YBBR reacting with Sfp-synthase.

In literature, A1 and S6 tags are described to possess orthogonal labeling properties[101]. However, figure 3.6 shows that this property is retained in the case of YBBR and A4 tags inserted into NGF but not into proNGF and labeled using Sfp and Acp synthase, respectively.

Based on these data, YBBR sequence has been identified to be the best tag for NGF and proNGF labeling. In fact, NGF-YBBR exhibits the best yield in protein production comparable to native protein and shows the best labeling yield as proved by the biotinylation assay. Thus, all the experiments presented in this and in the next section have been performed using NGF and proNGF tagged with the YBBR tag.

3.2 Fluorescent NGF and proNGF

Next, I have exploited YBBR tag insertion to produce fluorescent precursor and mature neurotrophins, hereafter referred as fluo-proNGF and fluo-NGF. To this purpose, purified proNGF-YBBR or NGF-YBBR have been incubated with CoA-Alexa488 (or CoA-Alexa647) substrate in the presence of Sfp-synthase (see second chapter, paragraph 2.2.2).

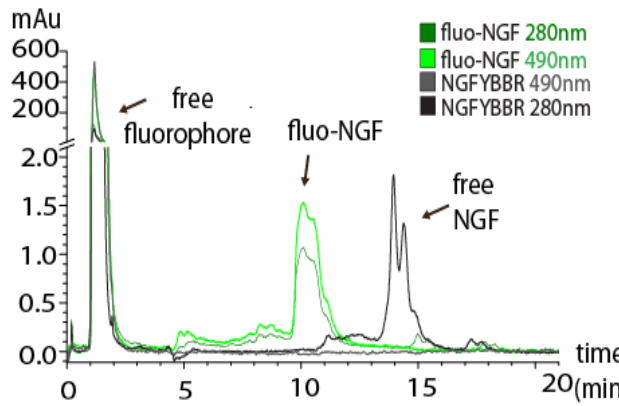

Fig. 3.7. Fluorescent NGF and proNGF purification. Ion exchange chromatogram of fluo-NGF and NGF YBBR shows the different retention times of fluorescent and non-fluorescent neurotrophin (ProPac SCX-20 column, Dionex, Thermo Fisher Scientific).

In order to obtain a pure population of molecules upon labeling, composed exclusively of fluorescent neurotrophins, fluo-proNGF and fluo-NGF have been purified by ion exchange chromatography to remove both the free fluorophore and the non-reacted neurotrophin (Fig. 3.7). Notably, comparing the integrals of the various peaks in the chromatogram allowed to estimate a high labeling yield in the order of 80%.

3.2.1 Fluo-NGF and fluo-proNGF functionality

In order to test if fluo-NGF and fluo-proNGF retain their biological outcome, several biological assays were tested.

On a fist stage, the retention of fluorescent neurotrophins ability to induce their physiological response was verified with a qualitative test: fluo-NGF was shown to retain the capacity to induce PC12 cells differentiation, inducing morphological changes and neurite outgrowth typical of differentiation to the same extent as *wt* NGF (Fig. 3.8A).

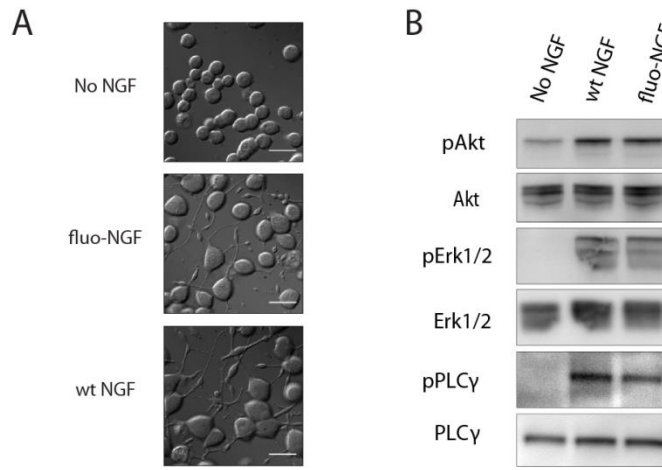

Fig. 3.8. Fluorescent NGF and proNGF functionality. (A) Nomarski images obtained performing the differentiation assay in PC12 cells using equimolar amounts of wt NGF, fluo-NGF. Untreated cells are the control. Scale bars represent 20 μm. (B) Western blot analysis of phosphorylated Akt (pAkt), phosphorylated Erk1/2 (pErk1/2) and phosphorylated PLCɣ (pPLCɣ) protein levels in PC12 cells in responce to wt NGF and fluo-NGF; protein levels of untreated cells (No NGF) are used as control.

Furthermore, a robust activation of the downstream signaling effectors involved in NGF-signaling pathways, like phosphorylated Erk1/2, PLC-ɣ and AKT proteins, was proven for fluo-NGF (Fig. 3.8B).

These data indicate that fluo-NGF is biologically active and induces physiological responses comparable to the native protein.

Moreover, I showed that mature NGF-tag can be efficiently obtained through proteolytic cleavage of the *in-vitro* refolded precursor proNGF-tag. The former retains

the biological properties of native mature NGF, meaning that the tag addition does not substantially modify the folding of the mature and, by extension, of the precursor neurotrophin. For this reason, it is reasonable to assume that also proNGF-tag retains the physiological properties of the native non-tagged precursor neurotrophin (proNGF).

In order to directly study fluo-proNGF ability to interact with its receptor, PC12 cells were incubated with 2 nM fluo-proNGF for 2 h at 37°. Alternatively, as control, cells were incubated with a mixture of unlabeled proNGF and free fluorophores (Fig. 3.9).

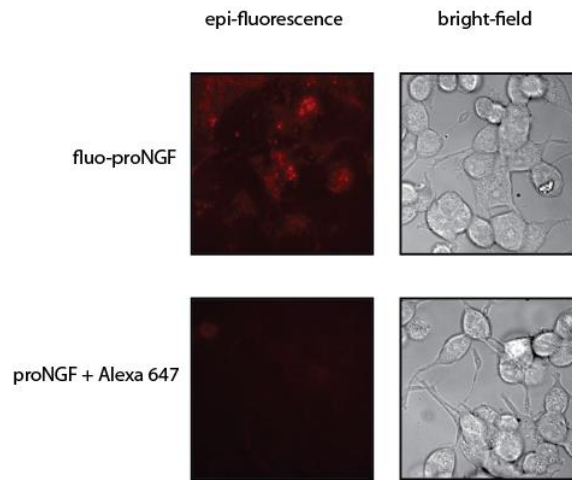

Fig. 3.9. Selective uptake of fluo-proNGF in PC12 cells. PC12 cells were treated with 2 nM fluo-NGF or fluo-proNGF for 1-2 h at 37°, showing internalization of the neurotrophins. While treatments with the same concentration of proNGF and Alexa647 (mixture on the same conditions results in no fluorophore uptake or membrane staining.

Live fluorescence imaging showed a bright fluorescence signal inside cells treated with the fluorescent proNGF, while this was virtually absent in the second case (Fig. 3.9), demonstrating that the fluo-proNGF retains its capability to interact with its receptors and to be internalized (for more discussion on this point see paragraph 3.3).

3.2.2 Tag stability

Even if the amino acid tag is covalent linked to proNGF and NGF, tag stability was tested, in order to complete the characterization of fluorescent and tagged neurotrophins.

Ideally, a good approach to test fluo-NGF stability, would be to analyze the integrity of fluorescent neurotrophin after its incubation with different cell line for different time. For this reason, the fluorescent neurotrophin was incubated with brain extract, for different time periods (Fig. 3.10), in view of a possible use of the fluorescent proteins to follow the biodistribution after labeled neurotrophins injection in the brain or administration to neurons in in-vitro experiment.

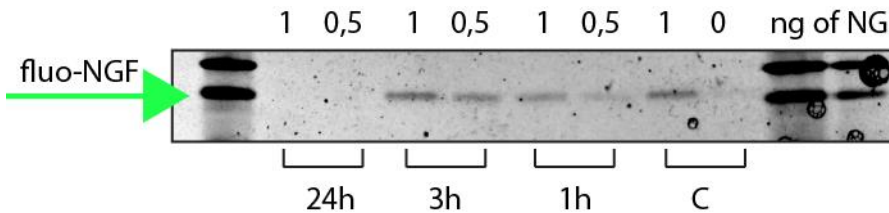

Fig. 3.10. fluo-NGF stability during brain lysate incubation. Immunoprecipitation of fluo-NGF incubated for 24h, 3h, 1h or 0h (control, 'C') with brain lysates. The same amount of fluorescent neurotrophin was used in all the time windows: 1 or 0,5 ng (or 0 as control) of fluo-NGF was incubated with 100 ul of brain lysate or 100 ul of PBS (as control, 'C'). Dynabeads protein G (life technologies) bind to αD11 antibody were used. The amounts coming from each incubation were loaded on a gel for SDS-PAGE and imaged using a Image Quant LAS4000 (GE Healthcare) instrument equipped with a narrow bandwidth Leds lamp for detection of Alexa fluorescence.

The comparison between fluo-NGF incubated for 3 and 1 hours in brain lysates with the one incubated in PBS, demonstrates that there is no loss of signal after the incubation, indicating that during these time windows the tag is still conjugated with the neurotrophins. Instead, the situation is different in the case of fluo-NGF incubated for 24 hours in presence of brain extract, where the signal coming from the fluorescent neurotrophins is completely absent, most likely due to neurotrophins or tag degradation.

These results, demonstrating that within 3 hours from the administration, fluorescent neurotrophin is still conjugated to its tag, and so, to the fluorophores.

Thanks to these result, all the trafficking experiment performed in this thesis were conducted within 3 hours from neurotrophins administration to neurons.

3.2.3 Fluorescent proNGF stability

proNGF can be cleaved both intracellularly[18] and extracellularly[17] by several proteolytic enzyme, giving rise to the mature protein NGF.

In this paragraph, I report the analysis of dynamics of proNGF cleavage.

A time course of proNGF cleavage upon additions to cells was performed, over the three-hours' time range. (Fig. 3.11). For this reason, fluo-proNGF (2nM) was administered in fresh medium for different time to differentiated PC12 cells.

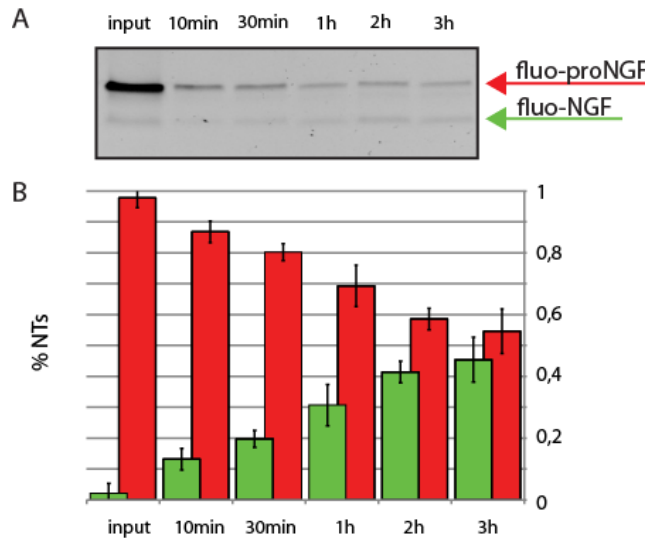

Fig. 3.11. fluo-proNGF intracellular cleavage. Fluo-proNGF is represented in red, and fluo-NGF in green. (A) SDS-PAGE of PC12 cells lysate after fluo-proNGF administration. 10 min, 30 min, 1h, 2h and 3h represent the period of incubation. The input represents the signal of fluo proNGF spiked into untreated PC12 cell lysate. (B) Quantification of the percentage of precursor and mature fluorescent neurotrophins after 0 min (input), 10 min, 30 min, 1h, 2h and 3h of incubation. Data derive from the average of two different experiments. The error bars derive from the standard deviation of the data by standard propagation of uncertainties.

The amount of fluo-NGF generated at the end of the first, second and third hours of incubation is about 30%, 41% and 45% respectively (Fig. 3.12B). These data will be used in the next chapter to analyse and interpret proNGF axonal transport properties.

3.3 Open questions: Is tagged/fluorescent proNGF functional?

In this chapter, it has been assumed that fluo-proNGF retained all the physiological characteristics of the native one since:

1) it has been shown that it was able to interact with its receptor on the plasma membrane of PC12 cells (Fig.3.9);

2) the tagged mature NGF, obtained from the tagged precursor proNGF after *in vitro* trypsin cleavage, has been shown to induce PC12 differentiation, TF1 proliferation and to activate the major signaling transduction pathways identically to the native protein (see chapter 3, section 3.1.3).

However, it is still unclear if this evidence is indeed sufficient to affirm that fluo-proNGF is biologically indistinguishable from the *wt* proNGF.

Unfortunately, the literature does not provide any simple, robust and quantitative assay to test proNGF biological activity in a conclusive way. Previous reports were based on the study of PC12 differentiation. However, this assay did not allow to exclude the presence of a fraction of cleaved precursor neurotrophins, that could be present in the cell medium after the long period of incubation needed for PC12 differentiation[116].

Another assay reported in the literature was based on monitoring DRG or SCG neuron death after they incubation with proNGF. However, the same death response could arise also without administering any kind of neurotrophins (or also an inactive proNGF) to the neurons[117].

Indeed, a reliable and conclusive test to study the biological outcome of proNGF is still lacking. For purpose, a good test would ideally possess a readout dependent only on the precursor neurotrophin, and not on its mature counterpart.

I would like to suggest Muller retinal cells to test proNGF activity. In fact, it has been reported that under proNGF and not NGF treatment these cells increase the production of TNFα protein[118]. The readout upon treatment of Muller cells with *wt* proNGF and mutated/tagged/fluorescent proNGF could indeed represent a solid test to evaluate proNGF action.

3.4 Advantages of a site-specific, stoichiometry controlled labeling technique

Thanks to the development of the labeling strategy presented in this chapter, biotin and fluorophores have been successfully conjugated to NGF and its precursor proNGF. It has been demonstrated that upon insertion of short amino acids tags, a site-specific labelling of the purified recombinant neurotrophin is achieved. Moreover, the data reported here show that the insertion of such tags in the chosen sites has no measurable impact on NGF functionality.

It is important to underline that the strategy presented fulfills all the recommended criteria for the specific labeling of proteins. First of all, the used tag is small, being a reduced version of the ACP and PCP tags. YBBR tag fused to NGF is 11 amino-acid long. Second, this approach of tag site-specific insertion minimizes any interference with recombinant-protein folding and function, compared to chemical labeling. Finally, the insertion site for the tags were chosen in order to lie as far as possible from residues involved in the formation of NGF-receptor complexes (see paragraph 1.2.2) and amino acid tag insertion in this site has been already reported to lead to functional NGF proteins[96].

Generally, non-site-specific labeling of proteins is achieved by chemical conjugation of reactive label derivatives to amine, thiol or carboxyl groups of proteins, as represented in Figure 3.12. The main disadvantage of this approach is the lack of control in number and type of labeled sites of the target proteins. Generally, a mixed populations of labeled proteins are obtained with these chemical approaches. This problem can potentially lead to impairment of physiological activity and loss of experimental reproducibility. Example of similar methods are reported in the literature, where neurotrophins have been chemically coupled to biotin[68,66,69] and organic fluorophores[90,65,91,119]. Indeed, in such cases the approaches followed led to mixed populations of labeled neurotrophins (containing 3-9 small probes per neurotrophin, depending on the experimental procedure used; for more details see paragraph 1.6 of the first chapter).

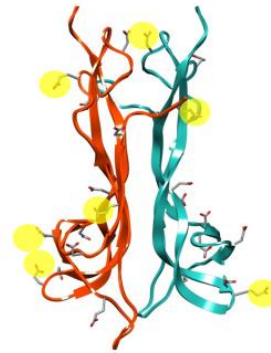

Fig. 3.12. Cartoon depicting the structure of NGF where the carboxylic group are shown. Each carboxylic group can be the site of a chemical labeling reaction. The yellow circles highlight a random set of carboxylic group that can be involved in a non-site-pecific chemical labeling reaction.

Our strategy, relying on labeling NGF with 1:1 stoichiometry, yields reproducible results and it is very well suited for single-molecule imaging, where experimental study of neurotrophins trafficking and their precursor requires methods to label them independently, simultaneously, and with controlled stoichiometry. In this context, the methods adopted here could be similar to what recently reported for NGF-AVI tag construct (AVI (AP) tag/biotin ligase system)[96], even if it owns one relevant advantage: indeed, any substituted Ppant arm of CoA substrates can be conjugated to the protein of interest[120]. Moreover, the approach presented here possess a vast spectrum of applications, from standard biochemistry to single-molecule imaging and counting, from electron microscopy to NMR studies depending on the probe used for NGF labeling.

Also, the relevance of the present approach not only for its specific application to NGF, but also in general to all neurotrophins, should be emphasized.

To conclude, the application of these nanoprobes allow for the investigation of trafficking of NGF and proNGF in living cells. This topic will be discussed in the next chapter of this thesis.

Chapter

4

Precursor versus mature Nerve Growth Factor axonal transport in live neurons

The previous chapter presented a site-specific method to label precursor and mature NGF forms with a controlled stoichiometry. It was shown that proNGF and NGF can be covalently conjugated at their C-terminus to, in principle, any kind of molecules, and that after the labeling with biotin or fluorophores, the neurotrophins retain all the physiological characteristics of the native protein. The labeling method used herein has several advantages, compared to the chemical ones previously reported in literature, and one of the most important is that it allows for the production of "homologous" fluorescent NGF and proNGF, guaranteeing higher experimental reproducibility. In this chapter, I have exploited this feature to study for the first time to my knowledge, the dynamics of proNGF trafficking in neurons, in comparison to that of NGF.

In this contexts, chemically labeled NGF has been previously used by many groups[68,66,69,90,65,91,119] to analyze axonal transport of the mature neurotrophin, showing its importance for survival, differentiation, and maintenance of central and peripheral target neurons. However, even if recent studies reveal the important role played by proNGF, known to be the most abundant form of this factor in the brain[50], a detailed description of its signaling and transport mechanisms, that link proneurotrophin cellular trafficking to its biological function, is still missing. In this chapter, thanks to the labeling method

described in the previous section, proNGF transport in neurons will be characterized in comparison to that of NGF.

To this end, fluorescence microscopy experiments were performed on compartmentalized living cultures of rat dorsal root ganglion (DRG) neurons, in which fluorescent proNGF and NGF (fluo-proNGF and fluo-NGF) were administered either separately or together. In the following paragraphs, I will first explain the basics and potential benefit of microfluidic devices and then report their application in fluorescent proNGF and NGF trafficking study.

4.1 Compartmentalized living cultures of DRG neurons

4.1.1 Microfluidic cell culture platform

Microfluidics is a multidisciplinary field, emerged in the late 1970s, dealing with the design of systems in which small volumes of fluids are handled. Microfluidics allows to control and manipulate cellular microenvironments. Microfluidics devices guide the growth of neurons and allow separated-controlled microenvironment for cell bodies and axon termini.

In 1977 Campenot and co-workers presented for the first time a multicompartment culture for neuritis isolation. The presented device, later defined as Campenot chamber, was made of Teflon. In their work, they used the device to analyze the transport of neurotrophic factors along axons[121]. This kind of chamber is still used because it creates different environments to separate distal axons from their cell bodies. However, it has a huge fluorescent background that prevents any single molecule study, and it is made on plastic, that not allow high resolution microscopy.

Twenty-six years later, *Taylor et al.* reported the application of a microfluidic chamber, fabricated with poly dimethylsiloxane (PDMS), to culture neurons[122]. PDMS is a biocompatible, silicon-based organic polymer, adapted for the fabrication of neuronal culture devices: it is optically transparent in the visible range, it is compatible with fluorescence microscopy and it also forms water-tight seal to the glass substrate of the petri dishes. The designed device was composed of two compartments interconnected by microchannels that separated both physically and chemically the axon termini from their cell bodies.

In this thesis, PDMS compartmentalized microfluidic chambers (RD450, Xona Microfluidic), similar to that described by Taylor in 2003, have been employed to study purified fluorolabeled proNGF and NGF axonal transport in living DRG neurons. The selected device is designed to divide neuron cultures in two fluidically isolated compartments[106]: a soma chamber (SC), where neurons are plated and an axon compartment (AC) where neurons spread their axon tips; these two compartment are connected by a channel compartment (CC), where neurons extend theirs axons through micrometer channels. The soma and axon compartments are made of tiny channels with dimensions of tens to hundreds of micrometers that are large enough to culture a few

thousand neurons in well-controlled microenvironments. The channel compartment, that separates axons from soma, is composed by micrometer-sized grooves (Fig. 4.1).

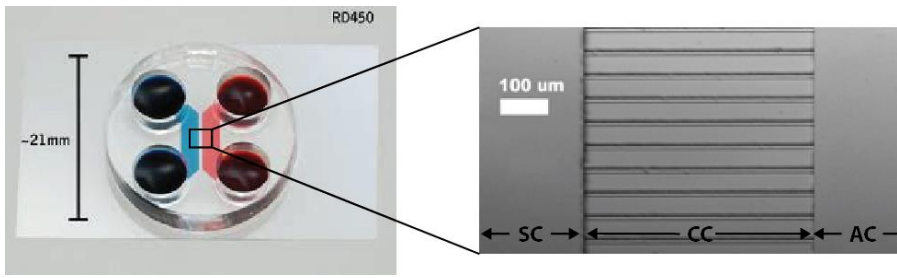

Fig. 4.1. The microfluidic platform consist of a PDMS (Polydimethylsiloxane) **device composed of a SC and an AC** (1,5 mm wide, 7mm long, 0,1 mm high) **connected by microchannels CC** (10µm wide, 3 µm high, 450 µm long). Figure adapted from http://www.xonamicrofluidics.com/products.html

Neurons, plated into the soma compartment, extend their axons across the barrier through the microgrooves reaching the axon compartment. A small gradient of neurotrophic factor was used to help axons to reach and grow into the axon compartment. The device is designed in order to obtain fluidic isolation of the soma and axon compartment. In this thesis, this property has been used to administer fluorescent neurotrophins just to the soma or axon compartment and to study neurotrophin trafficking through axons in the channel compartment

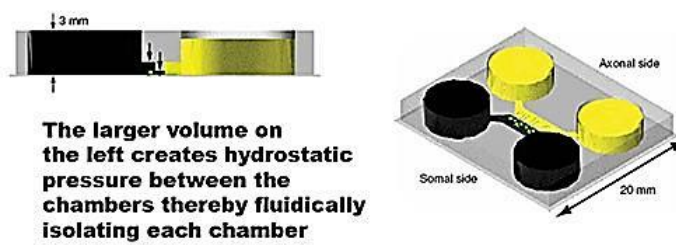

Fig. 4.2. The small hydrostatic pressure prevent soluble compound to diffuse from one compartment to the other. This is achieved by a continuous flow produce by adding less volume on one chamber of the device. Figure taken from *Taylor et al*. 2006[122].

The fluidic isolation can be achieved thanks to the hydrostatic pressure between the two chambers (this pressure arises keeping the volumes in the wells on one side of the

device higher than the one in the other side). As represented in Fig. 4.2, a minute volume difference between the two compartment creates the hydrostatic pressure that fluidically isolates each compartment (50 µl allows chemical microenvironments to be isolated for over 20 hours).

4.1.2 Rat dorsal root ganglion neurons and NGF

Primary neuronal cultures represent a controlled system to study the neurotrophic factor trafficking and signaling. Dorsal root ganglion (DRG) neurons, developing as bipolar neurons from the neural crest, are pseudo-unipolar neurons known to have two very similar processes: a central and a peripheral processes which have structural characteristics of axons[123]. The single axon of the spinal sensory neurons bifurcate in the DRG, sending one branch directly to the spinal cord and the other toward the peripheral tissues directly to their targets (e.g. skin) along a defined set of pathways, as represented in figure 4.3. Sensory DRG neurons depend on NGF for survival during development and for maintenance of aspects of their adult nociceptive phenotype[124]. NGF binds two types of receptor on DRG neurons: the p75 receptor[125] and the TrkA receptor[126], through which NGF exerts its main influence on sensory neurons[127]. NGF derived from the target cells at distal axon sites is carried retrogradely by axonal transport to the cell body. However, from the best of my knowledge, there are not direct evidences of a NGF transport from the cell body of the DRG neuron through the central process direct into the spinal cord.

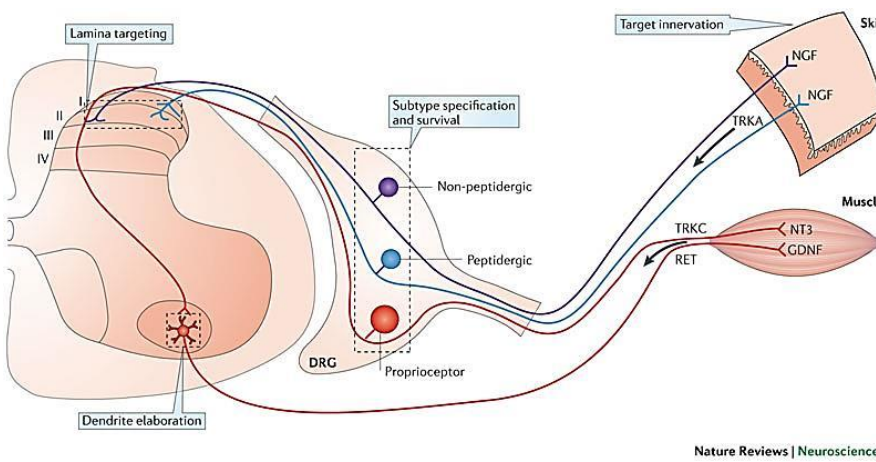

Fig. 4.3. Dorsal root ganglia neurons. Tropic factors, like NGF, are produce in target organ and act to their receptors. Signaling vesicles carry the neurotrophic factor signals to neurons to support and differentiation. Figure taken from *Harrington and Ginty* 2013[128].

Neurons derived from DRG of embryonic, postnatal and adult animals can be easily grown in culture[129]. The use of embryonic neurons has some advantages comparing to postnatal neurons. For example, during their isolation, they allow to obtain a higher content of cells with a higher efficiency and, moreover, they are particularly suitable for compartmentalized cultures[121]. For these reasons, rat embryonic DRG neurons, derived from E14 and E15 rat embryos, have been used in this work, to study proNGF and NGF trafficking.

4.2 fluo-proNGF *versus* fluo-NGF axonal transport

In order to study proNGF and NGF transport in neurons, purified fluorolabeled proNGF and NGF (fluo-proNGF and fluo-NGF) were employed for axonal transport studies in living DRG neurons cultured in a compartmented microfluidic chamber. Each experiment was performed by administering the neurotrophin at 2 nM concentration in the AC or in the SC and measuring the transport of the protein through the axons by epi-fluorescence microscopy and single particle tracking of fluorescent vesicles.

4.2.1 fluo-NGF trafficking in DRG neurons

The first part of this study was aimed at analyzing NGF trafficking. As a consequence, the first set of experiments were conducted administering fluo-NGF in the AC and acquiring video in the CC (Fig. 4.4 A-D).

About 20 minutes after neurotrophin administration, fluo-NGF filled vesicles started to move from the axon tip, where the fluorescent neurotrophin was administered, to the soma of neuron. As previously reported, this lag may be due to a maturation phase that precedes the loading on transport tracks and the moving through the axon[67]. Typical acquisitions with the recorded trajectories are represented in Figure 4.4B. Most of the fluo-NGF vesicles move with the typical stop-and-go dynamics, as previously reported by *Cui et al.*[68], characterized by variable pausing time, as presented in Figure 4.4C. Particle trajectories show a wide distribution of average speed (histograms in Fig. 4.4D). In the plot, positive speeds refer to retrograde movements, while negative to anterograde movement, if not specified otherwise.

The mean speed value is 1.34±0.70 μms^{-1} (the error refers to the standard deviation of the population SD, calculated on n_t=1606 trajectories) for retrograde movement and 1.83±1.11 μms^{-1} (n_t=160) for anterograde movement. The distribution of speeds during active movement, evaluated by subdividing the trajectories in “stop” and “go” parts and considering only the latter ones, are shown as solid lines in Figure 4.4D and their mean values are 2.40±0.70 μms^{-1} and 3.03±1.1 μms^{-1} respectively for retrograde and anterograde movement. These data indicate that vesicles spend about 55% of their time moving.

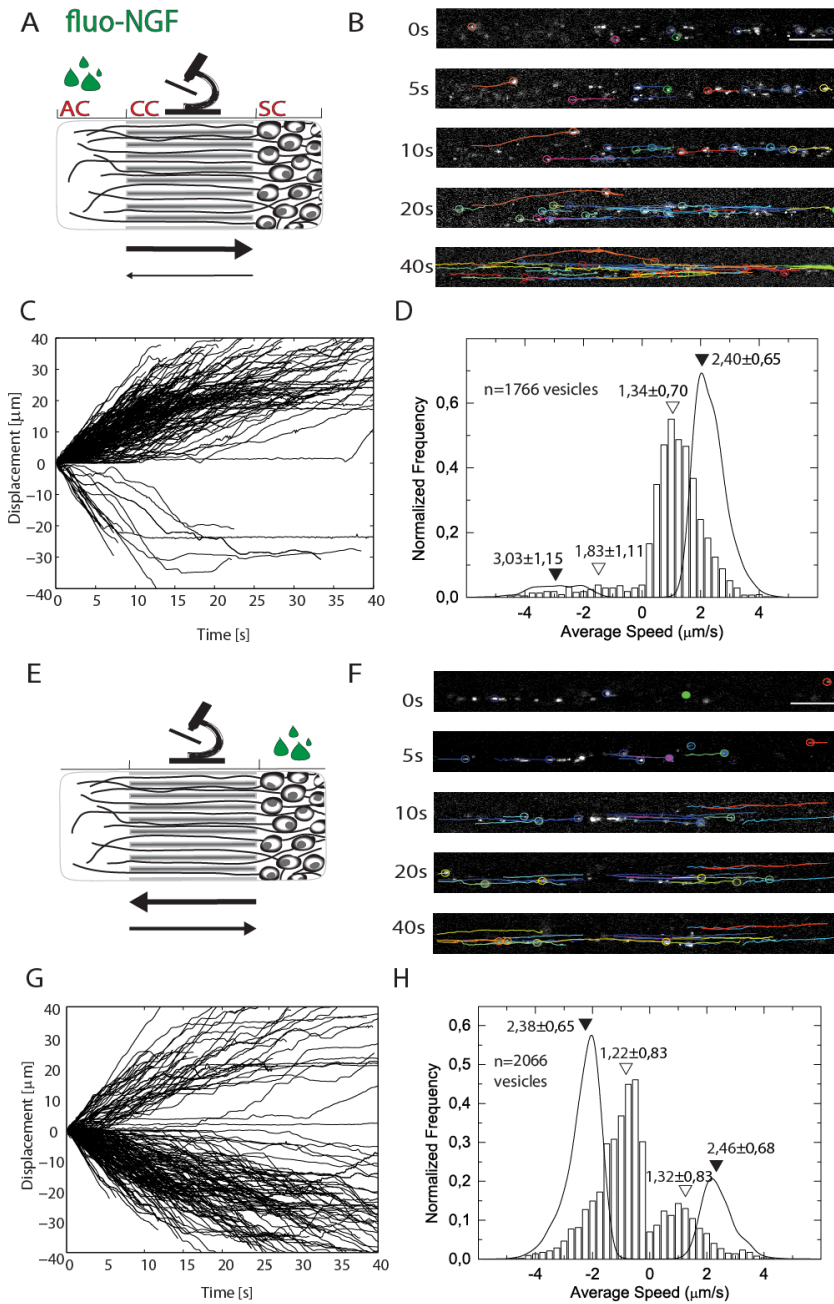
A
fluo-NGF
AC
CC
SC
B
0s
5s
10s
20s
40s
C
Displacement [µm]
Time [s]
D
n=1766 vesicles
1,34±0,70
2,40±0,65
3,03±1,15
1,83±1,11
Normalized Frequency
Average Speed (µm/s)
E
F
0s
5s
10s
20s
40s
G
Displacement [µm]
Time [s]
H
2,38±0,65
1,22±0,83
n=2066
vesicles
2,46±0,68
1,32±0,83
Normalized Frequency
Average Speed (µm/s)

Fig. 4.4. Live axonal transport of fluo-NGF. (A,E) Schematic of the microfluidic device where, in the uppermost panel, the axon compartment (AC), the channel compartment (CC), and the soma compartment (SC) are indicated. The green droplets represent neurotrophin administration compartment (the AC for the upper set of panels; the SC for the bottom set of panels); a stylized microscope indicates the compartment in which fluorescence acquisition is performed; arrows of different dimensions report direction and amount of moving vesicles. (B,F) Representative images of the time lapse videos of moving vesicles travelling through the axon. Each line represents a single vesicle trajectory. (C,G,K,O) Displacement vs time plot of 200 representative vesicles. (D,H) Bars: average speed distribution of moving vesicles. Lines: distribution of speed during active movement. Empty and filled triangles indicate the mean of vesicles average speed and the speed during active movements respectively; uncertainties: standard deviation. The number of acquired trajectories is reported in each panel. Distributions with areas normalized to 1; in C, D, G, H, positive and negative displacements or speeds refer to retrograde and anterograde movements respectively.

Since the separation of trajectories in stop and go parts requires some degree of subjectivity (*e.g.* in the determination of the minimum speed defining a "go" subtrajectory), the most probable velocity for the fastest parts of the trajectories was determined by evaluating the mode of the distribution of times required by vesicles to travel 1 μm. The obtained results yield the values of 2.8 μms^{-1} and, 3.5 μms^{-1}, as shown in Figure 4.5 and discussed in the second chapter of this thesis (see paragraph 2.5of the second chapter).

The second set of experiments were conducted administering fluo-NGF in the SC, to verify if neurotrophins trafficking was measurable in axon also if neurotrophin were given to the SC (Fig. 4.4E). Interestingly, even in this case, fluo-NGF filled vesicles travelled across axon, with the typical stop-and-go dynamics, and they started to move about 20 minutes after neurotrophin administration. Here, the mean speed values is 1.32 ± 0.83 μms^{-1} (n_t=524) and 1.22 ± 0.83 μms^{-1} (n_t=1542) respectively for retrograde (from the AC to the SC) and anterograde (from the SC to the AC) movement. The mean values of speeds during active movement, shown in Fig. 4.4H, is 2.5 ± 0.7 μms^{-1} and 2.4 ± 0.7 μms^{-1}, and the moda of the distribution of times required by vesicles to travel 1 μm (Fig 4.5 C,D), is 3.1 μms^{-1} and 3.2 μms^{-1} respectively for retrograde and anterograde movement.

Then, the velocity of neurotrophin vesicles measured when fluo-NGF was administered to AC and to SC were compared. The high number of trajectories acquired when fluo-NGF is given at the SC allows to statistically compare anterograde *vs* retrograde average speed and to define the former as slightly, but significantly, slower

($p<0.05$, Dunns Test). On the contrary, this observation was not possible in the case of fluo-NGF given to the AC due to the low number of anterograde moving vesicles, but the comparison between the retrograde movement measured by administering fluo-NGF to the AC or to the SC reveals no significant difference in the average speeds. Taken together these results are compatible with the different machinery (two classes of motor proteins: kinesins and dyneins) for the transport in the two directions, with no or small influence from the site of neurotrophin administration.

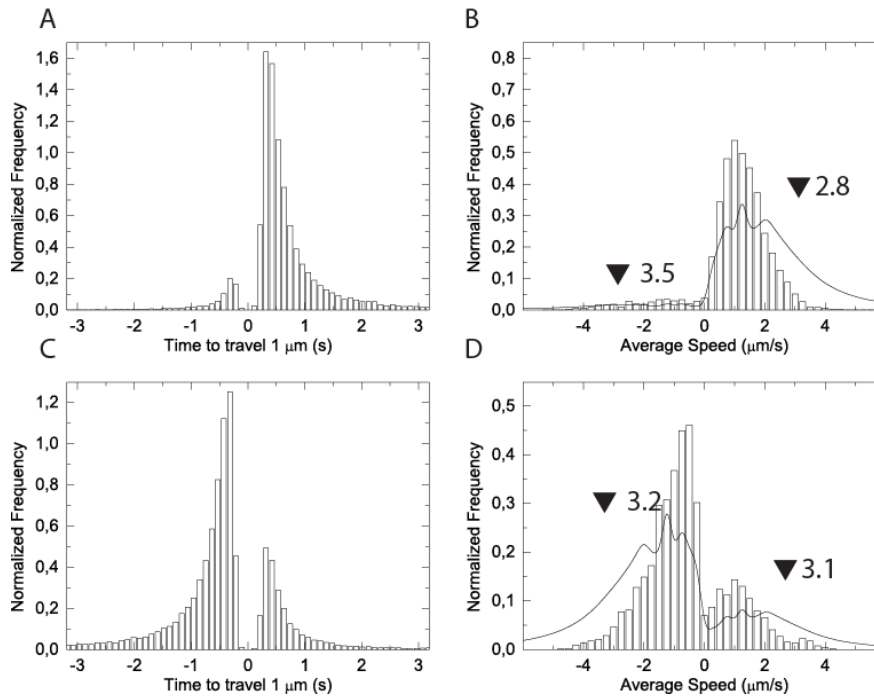

Fig. 4.5. Live axonal transport of fluo-NGF: determination of speed distributions in 1 μm steps of measured trajectories; this kind of distribution will weigh more the speed during active movements. The neurotrophin administration compartment is the AC for the upper set of panels A and B and the SC for the bottom set of panels C and D. (A,C) Bars: histograms of times required for the vesicles to move 1 μm. (B,D) Bars: average speed distribution of moving vesicles (same data of Fig. 4.4, for comparison). Lines: distribution of speeds for steps of 1 μm, obtained by the corresponding time distributions in panels A and C. Distributions with areas normalized to 1.

Notably, in the case of fluo-NGF administered at the AC, about 10 minutes after the first measurable retrogradely moving vesicle, anterogradely moving vesicles have also been observed. This anterograde population seems to increase during time from the start to the end of acquisition, with an average value of 9% of moving vesicles (Fig. 4.6A). This movement, that is different from the short anterograde displacement seen during vesicles transport as frequently observed here and previously reported[68], persists for large displacements (even more than 90 μm) and for a long time (more than 60 sec). Furthermore, when fluo-NGF is given to the SC, about 20 minutes after the appearance of the first moving vesicles, we observe the appearance of a robust transport back to the SC. In this case the amount of vesicles transported back to the administration compartment is significantly higher than what observed for administration of NGF to the AC (25 % of the cases compared to 9 %) and, once started, this retrograde flux to the soma persists quite constantly for hours (Fig. 4.6B).

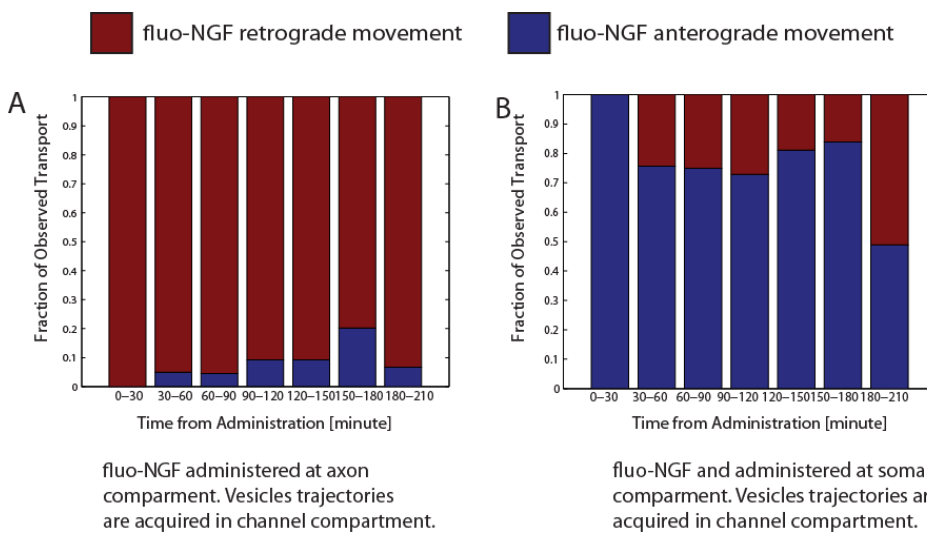

Fig. 4.6. Fraction of retrograde and anterograde trajectories vs time. (A) Bar graph of the fraction of anterograde *vs* retrograde recorded trajectories when fluo-NGF is administered to the AC and time lapse imaging performed in the CC. (B) Same as (A) when fluo-NGF is administered to the SC and time lapse imaging performed in the CC.

4.2.2 fluo-proNGF trafficking in DRG neurons

In order to investigate proNGF vesicular trafficking, under the same experimental conditions described in the previous paragraph, fluo-proNGF was administered to the AC. Also in this case, a retrograde flux of fluo-proNGF vesicles moving from the AC to the SC was recorded (Fig. 4.7 A-D).

Fluo-proNGF moving vesicles display the characteristic stop and go movement, similarly to fluo-NGF ones (Fig. 4.7C). The measured average speed of fluo-proNGF (calculated on n_t=952 trajectories) is 1.26±0.83 μms^{-1} and 1.32±0.87 μms^{-1} respectively for retrograde and anterograde movement, while the mean values of speed during active movement is 2.39±0.74 μms^{-1} and 2.76±1.13 μms^{-1}. The moda of the distribution of times required by vesicles to travel 1 μm was also analyzed, showing the value of 3.0 μms^{-1} and 2.9 μms^{-1} respectively for retrograde and anterograde movement, as reported in Fig. 4.7D and 4.8B.

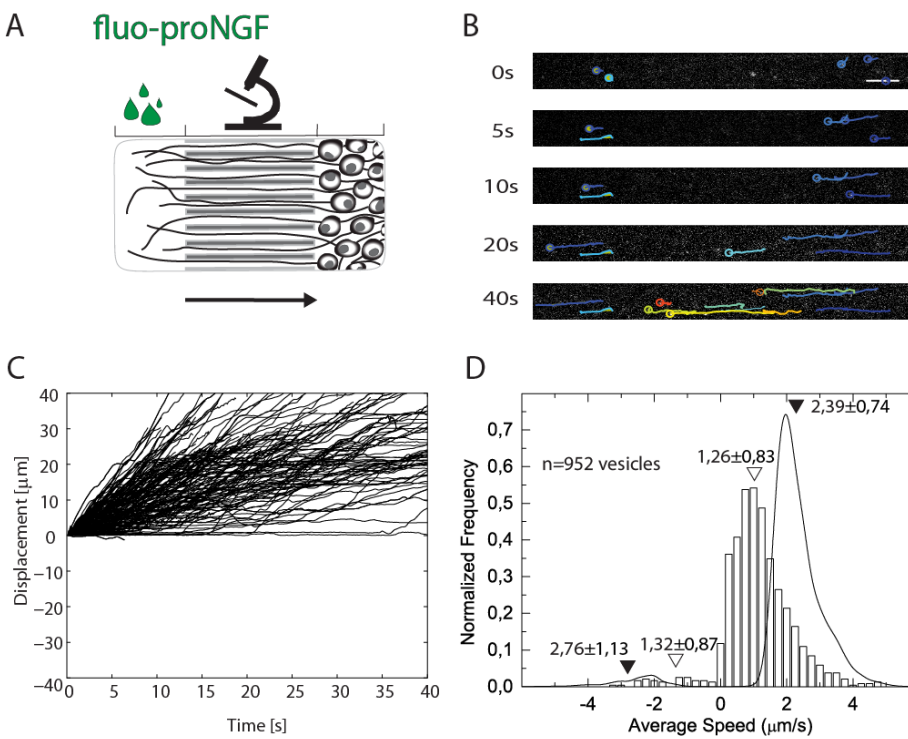

Fig. 4.7. Live axonal transport of fluo-proNGF. (A) Schematic of the microfluidic device where, the green droplets represent neurotrophin administration compartment; an arrows report direction of moving vesicles. (B) Representative images of the time lapse videos of moving vesicles travelling through the axon. Each line represents a single vesicle trajectory. (C) Displacement vs time plot of 200 representative vesicles. (D) Bars: average speed distribution of moving vesicles. Lines: distribution of speed during active movement. Empty and filled triangles indicate the mean of vesicles average speed and the speed during active movements respectively; uncertainties: standard deviation. The number of acquired trajectories is reported in the panel. Distributions with areas normalized to 1; in C, D, positive (negative) displacements or speeds refer to retrograde (anterograde) movements.

Notably, if compared to fluo-NGF positive organells, proNGF vesicles exhibit similar distributions of average speeds during active movement.

Moreover, compared to fluo-NGF, proNGF vesicles flux occurs with a slower kinetics: it starts about 35 minutes after neurotrophins administration, compared to 20 minutes in the case of NGF.

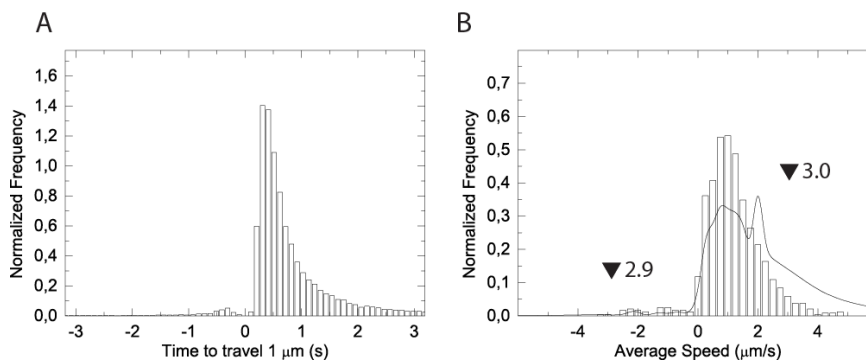

Fig. 4.8. Live axonal transport of fluo-proNGF: determination of speed distributions in 1 μm steps of measured trajectories; (A) Bars: histograms of times required for the vesicles to move 1 μm. (B) Bars: average speed distribution of moving vesicles (same data of Fig. 4.7, for comparison). Lines: distribution of speeds for steps of 1 μm, obtained by the corresponding time distributions in panels A. Distributions with areas normalized to 1.

Next, in another set of experiments, fluo-proNGF was administered to the SC. Strikingly, in this case, no significant anterograde transport through the axons was observed, differently than for fluo-NGF (Fig. 4.9A); however, vesicles trafficking was observed with directed motion inside axons in the SC, with the results reported in Figure

4.9B-D. It is worth noting that, in this case, a positive or negative verse to the movement cannot be automatically assigned (the axons are not in the CC, so it is not clear if the vesicle moves from the soma to the axon tip or vice versa), and therefore only positive speed is reported (Fig. 4.9E-H).

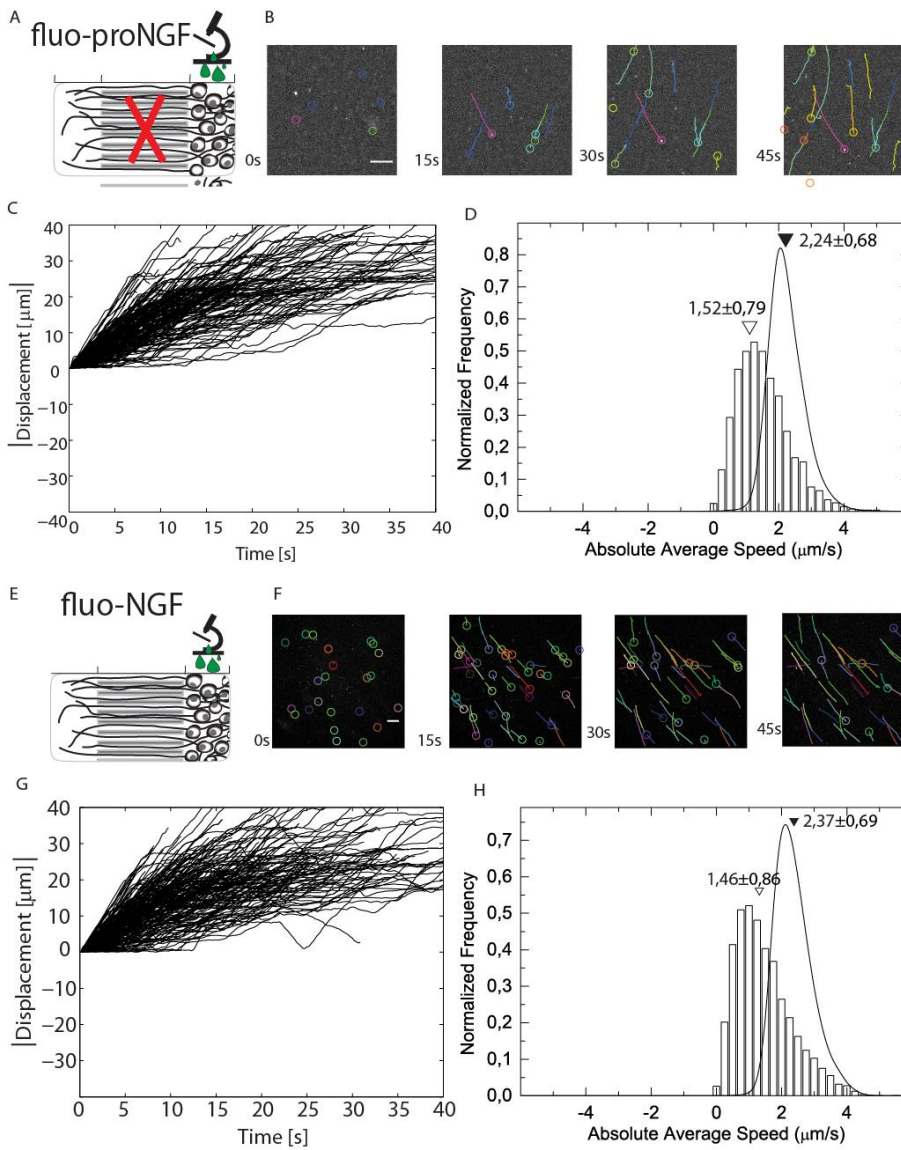

Fig. 4.9. Live axonal transport of fluo-proNGF and fluo-NGf outside the microfluidic channels. (A,E) Schematic drawing of the microfluidic device. The green droplets represent neurotrophin administration compartment; time lapse imaging is performed in SC; (B,F) Representative images of the time lapse videos of moving vesicles travelling through the axon. Each colored line represents a single vesicle trajectory. (C,G) Displacement vs time of 200 representative vesicles. (D,H) Bars: average speed distribution of moving vesicles. Lines: distribution of speed during active movement. Empty (filled) triangles indicate the mean of vesicles average speed (during active movements); uncertainties: standard deviation. Distributions with areas normalized to 1; in this configuration, only the absolute value of displacements and speeds could be determined.

Nevertheless, when fluo-proNGF was given to the AC, a minimum amount of anterogradely moving vesicles (less than 5%) that move just for short displacements (the maximum anterograde displacement acquired is of 25 μm) was observed. These movements can be confidently attributed to small steps backwards while the vesicle moves retrogradely.

These experiments highlight that proNGF and NGF share a similar stop and go retrograde transport when administered at the AC. However, proNGF transport starts later than NGF one upon neurotrophin administration and, differently from NGF, it lacks significant anterograde movements when either administered to the AC and to the SC.

4.3 proNGF vesicles contain the full length precursor NT

As reported in the previous chapter (paragraph 3.2.3), since the fluorescent label is located at the C-terminus of proNGF and NGF, the question could arise whether the observed proNGF vesicles do contain the full length protein, or, rather, its mature cleavage product. To address this question, a time course of proNGF cleavage upon incubation with neurons was performed, over the three-hours' time range of transport data acquisition (for experimental details see Fig. 3.12, paragraph 3.2.3).

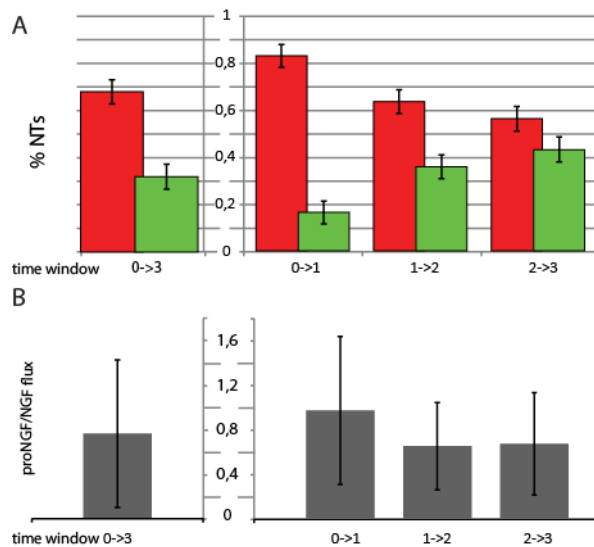

Fig. 4.10. Precursor neurotrophins (NTs) vesicles contain the full length proNGF. Fluo-proNGF is represented in red, and fluo-NGF in green. (A) Histogram of the quantification of the percentage of precursor and mature fluorescent neurotrophins present after fluo-proNGF administration to differentiated PC12 cells. Different time windows were analysed. Data derive from the average of two different experiments. (B) Histogram representing the ratio between proNGF and NGF flux through axon of DRG neurons during single administration experiments. The error bars of both histograms derive from the standard deviation of the data (by standard propagation of uncertainties).

Obtained data were used to measure the amount of fluo-NGF generated during the first, second and third hours of incubation is 16%, 36% and 43% respectively (Fig.4.10).

The average over the three hours period of transport acquisition is about 30%, i.e. 70% of administered fluo-proNGF molecules are on average still present during this period.

In Figure 4.10, it is compared the fluo-proNGF to NGF cleavage kinetics in the three time windows 0-1, 1-2 and 2-3 hours (Fig.4.10A) with the fluo-proNGF/NGF flux ratio in the same time windows (Fig.4.10B, calculated from Fig. 4.15B). In the first hour, the measured flux of proNGF and NGF are equal (their ratio is about 1, Fig. 4.10B). If the bona fide observed transported proNGF vesicles corresponded to cleaved NGF, one would here observe only a 16% (for the 1 hour average cleavage, Fig. 4.10A) of the observed NGF flux.

Thus, at least the 70% of vesicles observed when proNGF is administered to neuron, contains the full length proNGF.

These data evidence that proNGF transport is unlikely to stem only from mature fluo-NGF originated from fluo-proNGF cleavage. Moreover, this finding is also supported by the observation that the axonal transport of these two proteins differs from each other in many aspects that will be described in the following paragraphs.

4.4 Different proNGF and NGF content inside the moving vesicles.

In the previous paragraph it has been described that vesicles, regardless of the form of carried neurotrophin, are transported along the axon with the same characteristic movement and with similar speed, probably because they utilize the same microtubule-dependent motor system. In this context, an in-depth analysis of the number of neurotrophins contained in each vesicle would be useful in the characterization of the physiology of these two proteins that are so related but elicit such different signals.

Moreover, since proNGF and NGF bind to their receptors situated on the nerve terminals and they must be internalized and retrogradely transported along the axon to the cell body in order to exert their functions, and since different amount of neurotrophins correspond to different levels of signaling pathway activation, an important aspect of the neurotrophin trafficking process is represented by the amount of molecules contained in the endocytic vesicles.

Visual inspection of fluorescent NGF and proNGF trafficking suggests that the labelling intensity of trafficking vesicles are substantially different in the two cases. This difference could be due to a different number of neurotrophins transported by a single vesicle in the two cases.

Thus, in this paragraph, thanks to the 1:1 fluorophore:neurotrophin monomer stoichiometry guaranteed by the labeling strategy, this aspect will be analyzed.

Two examples of spots corresponding to representative fluo-NGF and fluo-proNGF vesicles are presented in Fig. 4.11A. The number of neurotrophins carried by each vesicle has been quantified measuring the integral of emitted fluorescence by a Gaussian interpolation of the spots. Moreover, in order to reach a robust interpolation, each vesicle has been re-centered by using the trajectory previously recorded and a temporal moving average of 10 frames was applied (more details are reported in chapter 2, see 2.6 section). The obtained integral intensity was compared to the same intensity measured for immobilized single fluorophores confirmed by single steps photobleaching. The measured number of neurotrophin dimers, each one carrying a couple of fluorophores, has been then used to produce a 2D

histogram in which the number of neurotrophins is plotted *versus* its average speed in Fig.4.11 B.

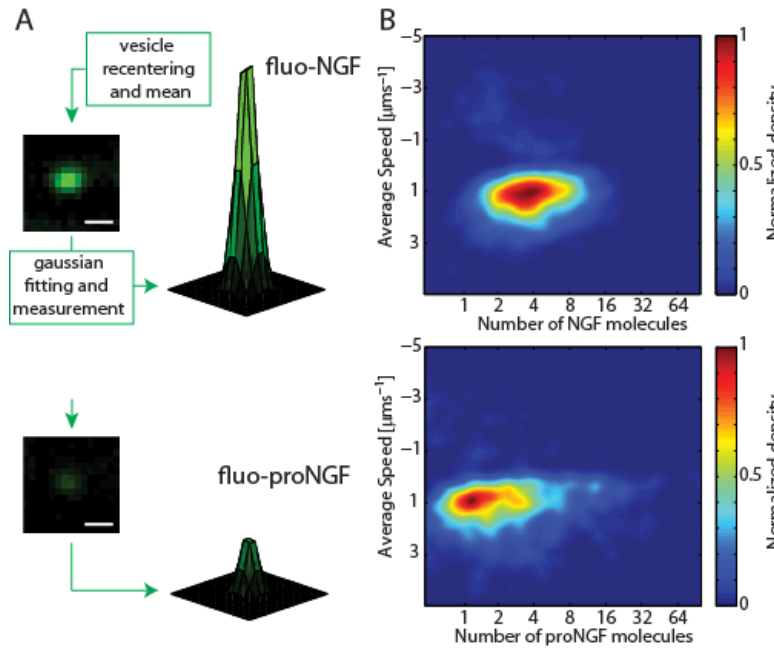

Fig. 4.11. Quantification of neurotrophins number carried by each vesicles. (A) Scheme of neurotrophin number analysis for both fluo-NGF and fluo-proNGF. A representative re-centered vesicle intensity profile with the corresponding Gaussian fit is reported for both neurotrophins. Scale bar 1 μm. (B) 2D histograms of neurotrophin number carried by vesicles vs average speed.

The position on the Y axis confirms that the average speed of the NGF and proNGF vesicles is the same. The X axis show that fluo-NGF vesicles carry a range of NT molecules, spanning from 2 to 8 (full width at half maximum) with a mode of 4 dimers per vesicle, while fluo-proNGF vesicles contain a lower number of NTs, from 1 to 4 proNGF dimers, with a mode value of 1 dimer per vesicle

4.5 NGF competes with proNGF during axonal transport.

In the previous paragraphs, the trafficking of precursor and mature NGF has been analyzed separately. Several aspect of their transport properties has been described by the experiments previously reported. However, since NGF and proNGF coexist *in-vivo* and their interactions are of great interest in the phisio-patological contexts, this section describes the study of the simultaneous axonal transport of the two forms of NGF.

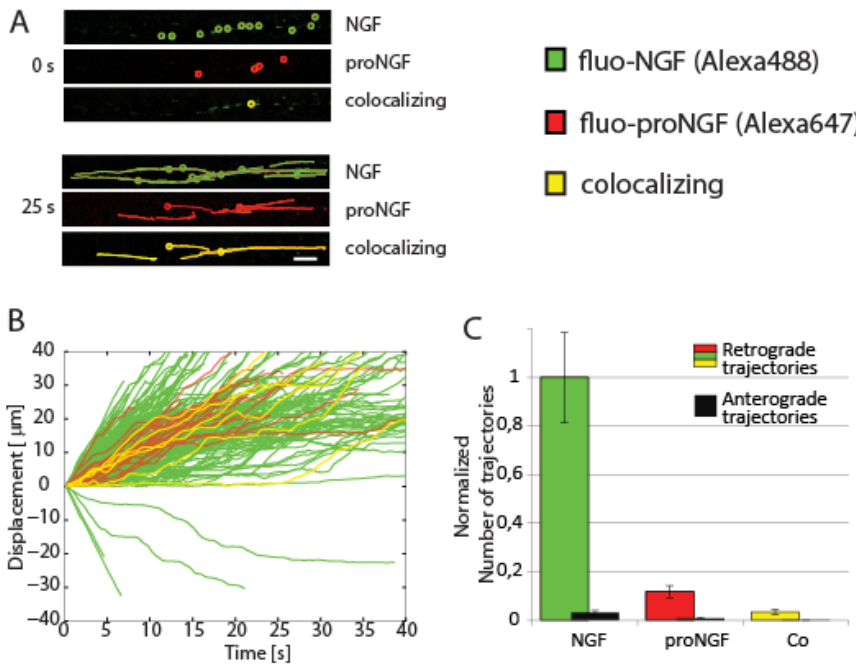

Fig. 4.12. Co-administration of fluo-NGF and fluo-proNGF to the axon compartment. (A) Representative images of the time lapse videos of moving vesicles travelling through the axon, at time 0vs and after 25 s; "colocalizing" (yellow) indicate the vesicles containing both NGF and proNGF. (B) Displacement *vs* time for a representative 10% of all observed vesicles. The color code is the same as in panel A. (C) Histogram of the average number of trajectories measured in different channels of the CC mean±SD for fluo-NGF vesicles (NGF), fluo-proNGF (proNGF) vesicles and for vesicles containing both neurotrophins (Co).

To this aim, proNGF and NGF were conjugated with two spectrally distinct probes, by using two different CoA-fluorophore substrates, CoA-Alexa647 and CoA-Alexa488 respectively. fluo-NGF and fluo-proNGF (Fig. 4.12A *Top*) were co-administered at equimolar concentration to the AC.

A typical dual-color acquisition of the trajectories recorded in the CC is represented in Figure 4.12A, with green and red colors representing NGF and proNGF vesicles respectively. Notably, a population of vesicles carrying the two fluorophores was registered (Fig. 4.12 A-D) indicating that NGF and proNGF could be co-transported. This vesicle population consists of ~25% of proNGF and ~3% of NGF vesicles.

Regarding the velocity of moving vesicles, co-localizing vesicles have a speed that is not significantly distinguishable from those of vesicles carrying the separate neurotrophins (Fig. 4.12B). The measured average speed of retrograde movement is 1,26±0,71 μms^{-1} for vesicles carrying both fluorophores, 1,43±0,87 μms^{-1} for fluo-NGF and 1,24±0,60 μms^{-1} for fluo-proNGF (Fig. 4.13). These last two values were found to be analogue to those detected for the individual incubation of proNGF and NGF.

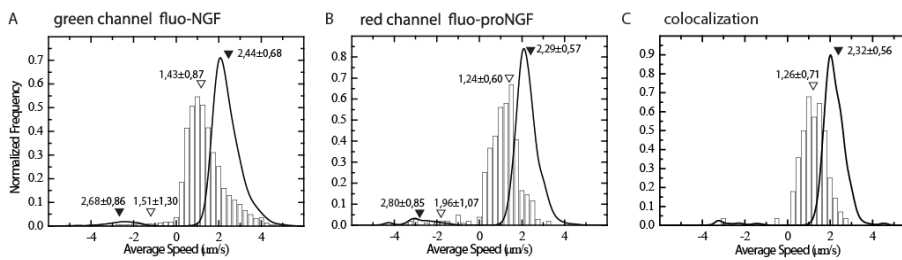

Fig. 4.13. Vesicle dynamics upon co-administration of fluo-proNGF and fluo-NGF. Average speed distribution of moving vesicles (bars) and distribution of speeds during active movement (lines) for vesicles containing fluo-NGF (A), fluo-proNGF (B) and both of them (C).

Additional attention has been given to the analysis of the number of moving vesicles in the two channels, in order to shed light on NGF and proNGF vesicles fluxes. The analysis, conducted by measuring the number of trajectories per axon, shows that the average number of NGF vesicles is ~10-fold higher than proNGF ones (Fig. 4.12C). Actually, the real proNGF flux could be even lower than that

observed due to the possibility of a small fraction of fluo-proNGF being cleaved to its mature counterpart during the acquisition time window (Fig. 3.12 and Fig. 4.10)

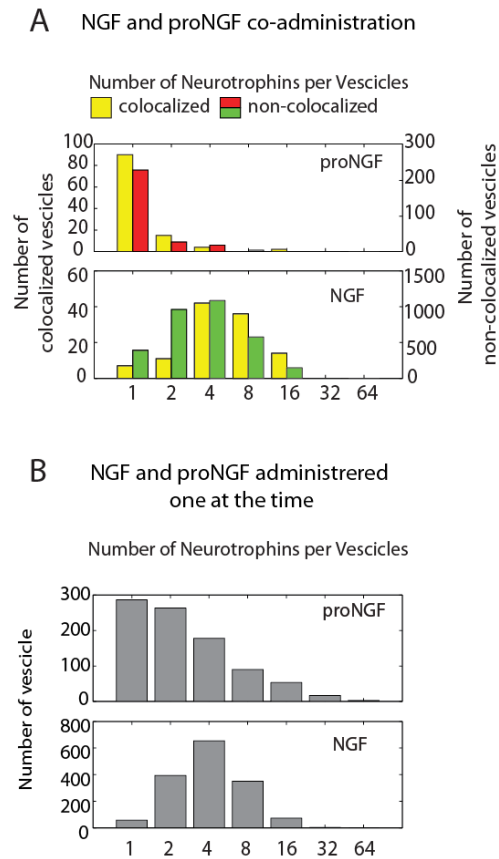

Fig. 4.14. Number of neurotrophins transported by colocalizing and non-colocalizing vesicles (A) fluo-NGF and fluo-proNGF co-administration. Histograms for the numbers of fluo-proNGF and fluo-NGF per vesicle in colocalizing (yellow) and non-colocalizing (proNGF red and NGF green) vesicles. (B) fluo-NGF and fluo-proNGF single administration Histograms for the numbers of fluo-proNGF and fluo-NGF per vesicle in colocalizing (yellow) and non-colocalizing (proNGF red and NGF green) vesicles

Moreover, the number of neurotrophins carried by vesicles putative transporting both precursor and mature NGF has been investigated. In Figure 4.14 A, the two histograms represent the distribution of the number of neurotrophins in vesicles labeled with the two fluorophores (represented in yellow) or in vesicles containing

individual neurotrophins (represented in red and in green). The number of neurotrophins carried by vesicles was investigated in both case, highlighting a slightly higher number of NGF molecules in colocalizing vesicles with respect to the ones containing only NGF. However, both distributions are quite similar to those when only NGF is administered (fig. 4.14). Surprisingly, the number of proNGF molecules contained either in colocalizing and non-colocalizing vesicles was markedly reduced at 1 in the vast majority of cases, as emerged by comparing the panel A and B of Figure 4.14. These findings demonstrate a great preference of vesicles to transport mature NGF instead of the precursor form.

From in-depth study, in which the fraction of moving vesicles was studied as a function of the time after the neurotrophins administration, the time-lapse acquisitions performed up to 180 minutes after administration show that, in the first 30-60 minutes, only NGF vesicles were detected. Fluo-proNGF vesicles have been detected starting from 60 min after administration and their number was found to increase over time from ~ 10% of NGF flux in the 60-90 min to ~ 25% of NGF flux in the 150-180 min interval (Fig. 4.15A). It might be argued that such a reduced proNGF flux could be related to a competition with NGF upon co-administration.

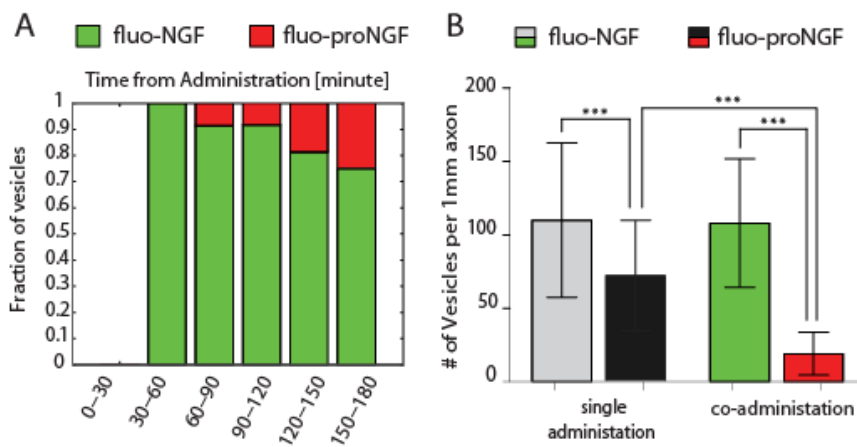

Fig. 4.15. Fluxes of neurotrophins transported by (non-)colocalizing vesicles (A) Distribution of fluo-NGF *vs* fluo-proNGF fraction of vesicles acquired during the three hours' time lapse imaging after neurotrophin administration. (B) Histogram representing mean±SD of the number of vesicles observed per 1mm of axons in the single administration of fluo-NGF and fluo-proNGF case (light grey and dark grey bars) and in case of coadministration (green and red bars). Dunn's Multiple Comparison Test was performed, *** indicates $p<0.001$.

To go into details, the vesicle fluxes, administering fluo-NGF and fluo-proNGF separately or simultaneously at the AC, have been measured and compared. Fig. 4.15B explains that, in the case of single administrations, the number of moving vesicles per 1mm of axon is estimated to be 110±42 and 72±38 (mean ± SD) for fluo-NGF and for fluo-proNGF respectively. This indicates that, when administered alone, proNGF vesicles flux is ~65% of the NGF one. This ratio dramatically drops down to 19±14 vesicles per 1 mm of axon (i.e. ~18% of NGF flux) when the two neurotrophin forms are given together, while fluo-NGF vesicles flux remains similar to that of the individual neurotrophin administration. Moreover, from the temporal point of view, both fluxes start some minutes later in the co-administration case than in the cases of single administrations.

Thus, upon co-administration of the two neurotrophin forms, the proNGF flux, both in term of vesicles number and number of neurotrophin carried by vesicles, is reduced, and this finding hint at the existence of a competition mechanism regulating mature and precursor neurotrophin uptake, transport and signaling.

4.6 Precursor and mature forms exhibit their own peculiar properties.

In this chapter, the study of proNGF and NGF axonal transport in living DRG neurons was described by single molecule fluorescence microscopy. The experiments have been conducted by adding fluo-proNGF or fluo-NGF to the SC or the AC of a microfluidic device where neurons were plated, and by registering fluorescent particles moving through the axons.

To the best of my knowledge, the obtained results have showed, for the first time, that proNGF is retrogradely transported inside vesicles like its mature counterpart. Such proNGF transport is unlikely to stem only from mature fluoNGF originated from fluo-proNGF cleavage (Fig. 4.10). The cleavage-resistant forms of proNGF so far proposed in literature was not used, because these variants display significant different biological features[43,14], and because they are not completely resistant to cleavage, as it has been shown by the Neet group[130]. We are of the opinion that the use of modified proNGF molecules may confound the interpretation of results.

proNGF vesicles display the same stop-and-go movements, that was also detected for the mature neurotrophin. Furthermore, the analysis of the vesicle trajectories recorded shows that proNGF displays an average speed distribution similar to that of NGF. These data suggest that the endocytic pathway and the related engaged molecular motors are conserved between proNGF and NGF, and that both NGF and proNGF signaling vesicles exist in the neurons.

However, besides these similarities, the axonal transport of these two proteins differs from each other in many aspects that will be analyzed in the following section.

4.6.1 proNGF vesicles move exclusively retrogradely, while NGF vesicles exhibit movements in both directions

In this work, it is shown that proNGF vesicles move exclusively from the axon tip to the cell soma of neurons, while NGF vesicles exhibit movements in both directions. In literature, a retrograde trafficking in neurons has been paradigmatically described for mature NGF. However, a bidirectional NGF transport has been previously described in neurite-like processes of PC12 cells, either directly using Cy3.5-NGF[65] or indirectly by studying TrkA trafficking [70,71,128].

Moreover, in the experiments presented here, anterograde movement, when NGF is administered at the AC, accounts for ~10% of the total vesicles analyzed, consistently to what previously reported, for tracked quantum-dot conjugated NGF[68], in the same neurons. The latter study, however, did not quantitatively analyze the 10% anterograde trajectories and did not study proNGF. NGF axonal transport was therefore previously suggested as purely retrograde. Nevertheless, this smaller population of anterogradely moving vesicles should not be neglected for three reasons: 1) it is increased (up to ~75%) when NGF is administered to the SC; 2) it is not observed with fluo-proNGF applied to the AC; 3) it is decreased to ~3% upon the simultaneous administration of proNGF. These finding support that anterograde movements are specific feature of NGF but not of proNGF.

4.6.2 proNGF and NGF signaling vesicles contain a different number of neurotrophins

In this chapter, I also showed that proNGF and NGF signaling vesicles contain a different number of neurotrophins in each vesicle. These results demonstrate that each vesicle mostly hosts 1 or 2 proNGF molecules and between 2 and 8 NGF molecules, when the neurotrophins are administered separately. The number of proNGF molecules is drastically decreased to 1, when neurotrophins are co-administered, both in vesicles carrying the pro-neurotrophins alone or co-transported with NGF. These data suggest that, during co-administration, NGF provides a veto signal for proNGF internalization and transport, maybe due to a competition mechanism that neurotrophins have with their receptors, at the level of receptor engagement or of downstream signaling.

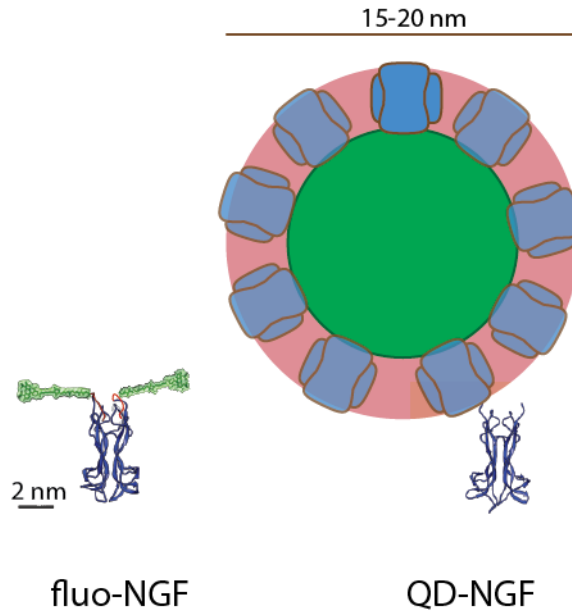

Fig. 4.16. Visual comparison between fluo-NGF and QD-NGF sizes. The two scale bars underline the different dimension of fluorescent NGF labelled with the presented method (*Left*) and one of the methods previously reported in literature[68] (*Right*). In these picture, the impact of the fluorophore on the dimensions of the tagged NGF seems even higher than it is, because the schematic view of NGF and tag structures schematizes only the backbone (with no residuals), while for the Alexa488-maleimide-phosphopantetheinyl the whole structure formula with a linking chain in extended configuration is given.

The high number of mature NGF molecules carried by signaling endosomes contrasts with the recently proposed idea that the typical functional signaling vesicle consists in a single NGF dimer bound to a single pair of TrkA receptors[68]. My data show the existence of a larger complex per vesicle, in which a higher number of NGF molecules, and presumably TrkA or $p75^{TNR}$ receptors, are clustered together. The discrepancy between my work and the one previously reported by *Cui et al.* may be due to the different size and hence steric hindrance, of the two fluorolabels impacting on the NGF structure, as it is represented in Figure 4.16. In fact, *Cui et al.* used QD-conjugated NGF (each QD putatively coupled to a single NGF dimer)[68]. As the QD volume is 7-70 times that of NGF, the QD-NGF conjugate might impair TrkA clustering[103], thus preventing the simultaneous activation of nearby TrkA

receptors. This would finally lead to a decrease in the number of NGF-TrkA complexes internalized and transported per vesicle. Conversely, the use of a much smaller and a less cumbersome organic dye to fluorolabel NGF might allow the clustering of activated NGF-TrkA complexes that could easily find room in the same signaling vesicle.

In this context, the results presented herein are consistent with the work of Campenot and coworkers[131]. Using ^{125}I labeled NGF (^{125}I -NGF) to measure the flux of transported NGF, they argued that, if such vesicles contained only one NGF molecule as supported by *Cui et al*.[68], the total amount of ^{125}I -NGF transported to the soma would require at least two orders of magnitude more vesicles respect to what actually observed.

4.6.3 NGF transport overcomes that of proNGF

Finally, this work revealed that precursor and mature NGF administered to neurons at equal concentrations, display different vesicle fluxes. In particular, when administered separately, the number of proNGF vesicles is slightly lower (~35%) than NGF vesicles.

However, when the two forms of the NT (labeled with two different fluorophores) are co-administrated to the DRG neuron axons, both proNGF flux and number of neurotrophins per vesicles is strongly inhibited and reduced by NGF co-administration. Obtained data suggest a competitive mechanism between the two forms of NGF. Moreover, the presence of vesicles carrying both the two fluorophores lets to hypothesize that mature and precursor NGF could be simultaneously co-transported within the same vesicles. However, it is not possible to exclude that the dual labeled vesicles might contain proNGF cleaved to NGF.

These finding might be related to the faster internalization rate of NGF main receptor, TrkA, versus that of proNGF, p75NTR[90], and to the lower binding affinity of proNGF to TrkA with respect to NGF[103].

Thus, alterations of the NGF proNGF ratio might have direct consequences in the transport fluxes and hence in the availability of the two NTs, in a competitive way, adding a new functional consequence to the emerging importance of the homeostatic regulation of proNGF to NGF metabolism[132,58].

To summarize, the observations described in this chapter shed new light on neurotrophin transport in neurons, suggesting a scenario where precursor and mature forms exhibit their own peculiar properties, both in terms of flux and number of neurotrophins per vesicles. This finding may help to clarify proNGF *versus* NGF signaling mechanisms and could provide an exciting avenue for future investigations.

Chapter

5

NGF and proNGF trafficking in neurons through an innovative site-specific labelling strategy

Concluding remarks

5.1 Functional model of NGF and proNGF transport

The main purpose of this thesis was to develop an innovative site-specific labeling technique for the study of NGF and proNGF trafficking in neurons.

I believe that this work is important as it describes a new powerful methodology to study the trafficking of NGF and proNGF, and, more in general, of mature and precursor neurotrophins, and provides new insight into the transport of proNGF in the neuron. The latter is especially critical, as trafficking of proNGF is still not fully characterized.

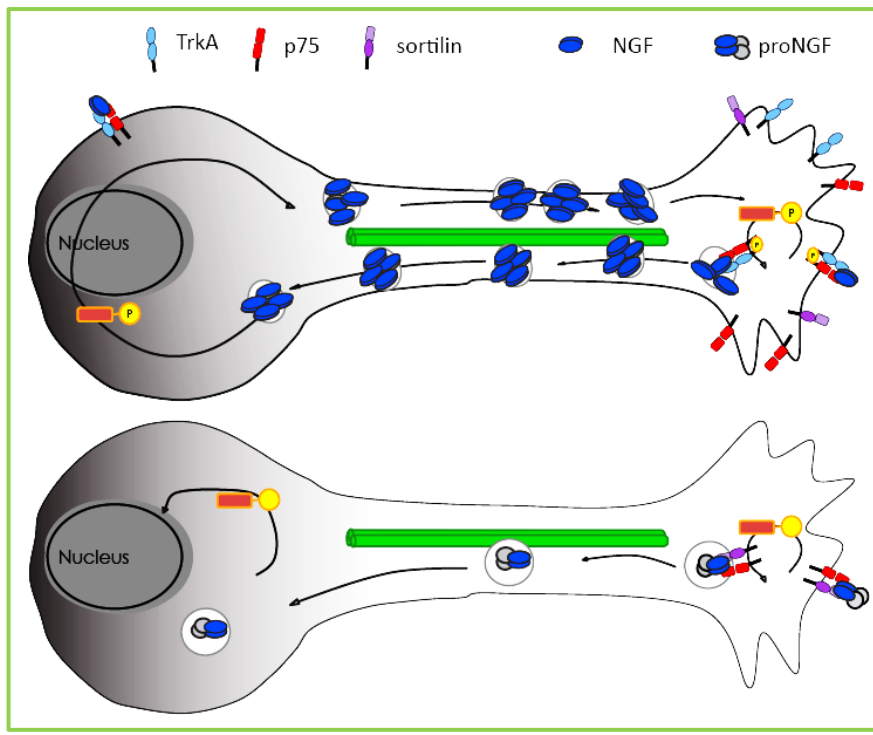

Fig. 5.1. Representation of proNGF and NGF transport through axons. The top figure represents the intracellular trafficking of NGF in DRG neurons: NGF is transported both in retrograde and anterograde direction along the axon. The bottom figure represents the intracellular trafficking of proNGF in DRG neurons: proNGF shows only retrograde trafficking.

Using the developed methodology to site-specific label mature and precursor neurotrophins, several novel and important observations have been made. Figure 5.1 shows the model of proNGF and NGF transport in the neuron based on the results achieved (for more information see paragraph 4.6).

The designed methodology was used to measure, for the first time, the intracellular trafficking of proNGF in DRG neurons, and to compare it with that of mature NGF.

Thanks to the developed strategy, several properties of neurotrophins trafficking were described: NGF was found to be transported both in retrograde and anterograde direction along the axon, whereas proNGF shows only retrograde trafficking.

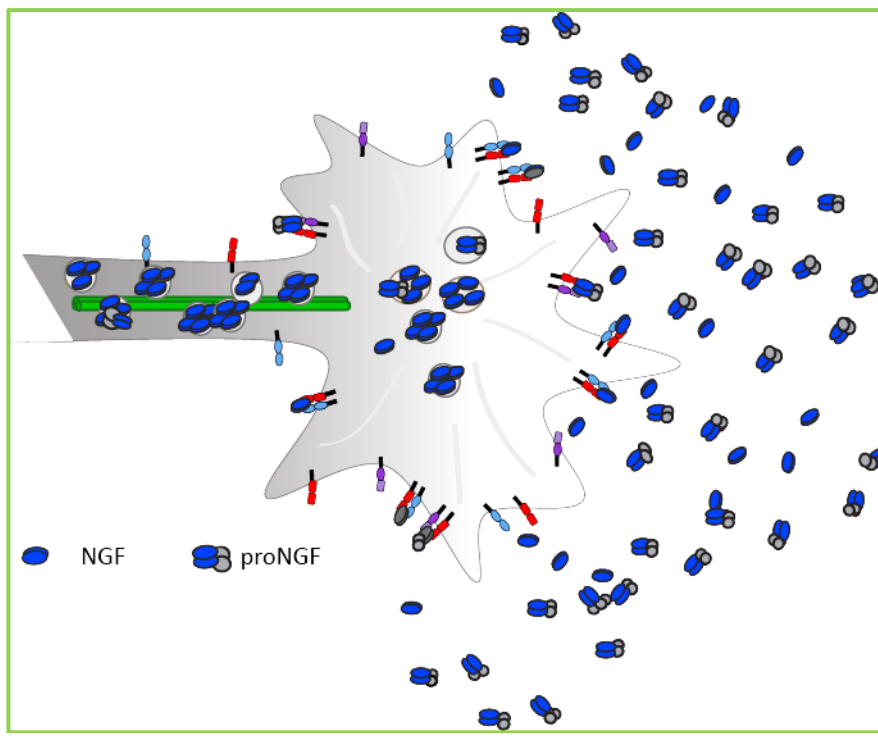

Fig. 5.2. Representation of simultaneously proNGF and NGF transport through axons. The figure represents the intracellular trafficking of NGF and proNGF administered simultaneously to the same DRG neurons: NGF and proNGF can be transported

For the first time, the trafficking of both neurotrophins administered simultaneously to the same neurons has been monitored, by labeling NGF and proNGF with spectrally different fluorophores. Notably, evidence that NGF and proNGF can be transported together has been presented. A competitive mechanism in the transport of both neurotrophins has also been highlighted (Fig. 5.2).

Finally, the site-specific conjugation of fluorophores to NGF and proNGF with a 1:1 stoichiometry has allowed estimating the number of NGF and proNGF molecules in single endosomes, showing that mature NGF vesicles carry a high number of molecules compared to that carried by proNGF vesicles.

The results of this thesis are divided in three chapters.

In **Chapter 2**, I described, step by step, the procedure and the methods developed to: i) insert a sequence coding for a short peptide sequence (from 8 to 12) inside a native DNA. For this purpose, a new mutagenesis method has been developed and described; ii) express and purify recombinant *wt* and tagged proNGF and NGF; iii) label proNGF and NGF with different kinds of molecules; iv) validate the physiological functions of labeled proNGF and NGF; v) grow neurons in microfluidic devices; vi) set up methods for monitoring simultaneous the trafficking of proNGF and NGF in living cells form.

Chapter 3 describes the development and optimization of this labeling method for the study of the trafficking and signaling of neurotrophins in neurons. I successfully identified one short peptide tag that can be linked at the C-terminus of the proNGF, sequence without interfering with the neurotrophin expression and physiology. The chemical tagging technique was conceived in order to allow site-specific conjugation of a biotin ligand, and two different fluorophores, to both precursor and mature NGF. It was demonstrated that, in both cases, the modified neurotrophins retained all the physiological characteristics of the native ones.

Chapter 4 describes the study of precursor and mature NGF transport in living neuron. Taking advantage of the labelling method, described in the previous chapter, I illustrated how the neurotrophins move along axons, the number of neurotrophins carried by each endosome and the velocity of the latter. In particular, it has been shown that the trajectories differ when proNGF or NGF are administered one at a time to neurons, or when they are simultaneously co-administered .

5.2 Future perspectives

The site-specific fluorescent labeling method developed in this thesis work allowed the study of proNGF and NGF trafficking in neurons.

The application of this method could be used to shed light on several aspects of neurotrophin physiology and to address relevant issues about the 'Signaling Endosomes Hypothesis'.

I deem that, thanks to the information acquired, and the optimized protocol described in this thesis, some interesting and unresolved topic could now be investigated. In this section, I will briefly discuss some of the topics and specific biological issues that could be studied thanks to the strategy reported herein.

5.2.1 Endosomes characterization

The first point that could benefit from the production of nearly native fluorescent NGF and proNGF is the characterization of the endosomes carrying the neurotrophins.

According to the outcomes reported in the literature, NGF is transported in signaling endosomes moving along the axons. Several reports support this thesis, showing that NGF is transported in clathrin-coated endosomes[82,80], that upon NGF treatment the axonal transport of p75NTR is triggered in motor neurons[80] and phospho-TrkA is internalized in the endosomes and that its signal colocalize together with Rab5[133] and with Rab11[134] in DRG neurons. Also, NGF–pTrkA complex was demonstrated to be internalized through either clathrin-mediated or non- clathrin-mediated pathways[72,128]. Moreover, it is also known that NGF retrograde signals are carried by early endosomes[79].

However, can this assumption be made also for proNGF? Is proNGF really transported into endosomes along the axon like its mature counterpart? Moreover, if proNGF is carried by endosomes, what kind of endosome transports the precursor neurotrophin? Are these the same signaling endosomes of mature NGF, or different

ones? What are the differences (if any) between endosomes carrying either mature or precursor neurotrophins and those carrying both of them at the same time?

We currently lack a precise molecular definition and characterization of NGF signaling endosomes. In particular, the molecular composition is not completely known, neither it is clear if the traffic of the signaling endosomes is dependent on the transported cargo.

Immunocytochemical experiments need to be performed to test whether fluo-NGF and fluo-proNGF are co-localized with TrkA, p75 and endosomal markers. This can be important to further define if, in terms of trafficking and transport, fluorescently-labelled NGF and proNGF behave in the same way or not.

Moreover, the labeling of precursor and mature NGF with different fluorophores could allow purification of different species of endosomes carrying single or cotransported neurotrophins. Using fluorescence-activated cell sorting (FACS), it could be possible to obtain a pure population of endosomes carrying fluo-NGF and/or fluo-proNGF[135].

Otherwise, the tag that I characterized would allow the site-specific covalent coupling of paramagnetic beads to NGF and/or proNGF, for the purification of the vesicles and subsequent proteomic characterization.

These experiments could be used to performed a proteomic study, in order to obtain a complete characterization of the neurotrophin-transporting endosomes.

5.2.2 Long vs short proNGF

Another argument that could be expanded, using the platform described in this thesis, is the analysis of the different roles of proNGF splicing variants.

It is well known that NGF, like the other neurotrophins, is translated as a preproprotein, and that two splicing variants are produced, leading to the formation of two precursor proteins: a long and a short form respectively (see Fig 5.3). Starting from the existing literature on proNGF, in this thesis the attention has been focused on the short form of proNGF. All characterization experiments of precursor

neurotrophin labelling and trafficking have been conducted using the 25 kDa proNGF.

However, do the long proNGF variants possess the same physiological characteristics of the short ones? And eventually, does the difference between this two forms act like a sort of specification for different properties and intracellular localization?

The analysis and the characterization of the trafficking of a fluo-long form of proNGF could allow obtaining a deeper understanding of the biological role of this form of precursor NGF.

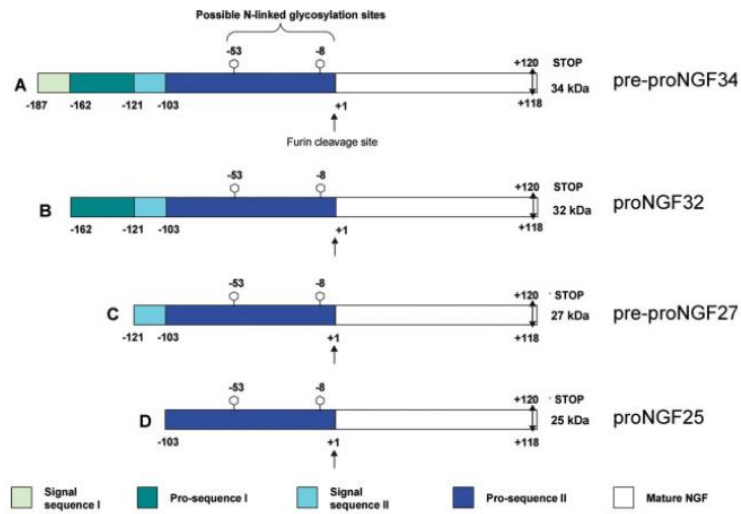

Fig. 5.3. Schematic representation of the major translation products arising from the alternative splicing of the mouse NGF transcript: the long preproNGF form of 34 kDa (A) and the short preproNGF form (C). The two forms differ by the additional prosequence I of 66 amino acids stretch at the N-terminus of the long form A. Upon removal of the signal sequence I for transcript A and signal sequence II for transcript C, the two products give rise to two proNGF proteins: the long form of proNGF of 32 kDa (B) and the short form of proNGF of 25 kDa (D). The arrows mark the cleavage sites for furin, the double headed arrows represent the C-terminal processing site (post translational modification) and the hexagons depict the potential N-glycosylation sites. Figure taken from *Paoletti et al. 2008*[136].

5.2.3 Study of neurotrophin transport in relation to neurodegeneration

Defective axonal transport has been found to play an important role in several neurodegenerative disorders. Hereditary spastic paraplegia[137], Charcot-Marie-Tooth disease[138], AD and tauopathies[139], amyotrophic lateral sclerosis[140] are examples of pathologies characterized by dysfunctions in axonal transport leading to selective damage of the specific neuronal population.

The platform that I developed will allow to study fluorescent neurotrophin transport in relation to neurodegeneration and in different animal models of disease. Understanding the role of axonal transport in neurodegenerative diseases could also be useful to set up chemical or functional genomic screening assays for compounds or genes that regulate positively the velocity of neurotrophin transport.

5.2.4 Biodistribution of NGF after intranasal delivery

Intranasal delivery has already been described as a novel, practical, simple and non-invasive approach to deliver drugs across the Blood Brain Barrier (BBB). This method is extremely promising, thanks to the unique connection that the olfactory and trigeminal nerves provide between the external environments and the brain [141].

Moreover, the passages between the nasal mucosa and the brain provide a unique pathway for the non-invasive delivery of therapeutic agents to the CNS[142]. The olfactory neural pathway provides both an intraneuronal (involving axonal transport) and extraneuronal pathway into the brain (it relies on bulk flow transport through perineural channels, which deliver drugs directly to the brain parenchymal tissue and/or cerebro spinal fluid).

Moreover, NGF is considered as a potential potent therapeutic agent for the treatment of AD [143,144]. Several studies demonstrate the feasibility of a non-invasive intranasal delivery of a “painless” NGF in a mouse model of neurodegeneration. When administered intranasally, this “painless” NGF was shown to prevent the progress of neurodegeneration and behavioral deficits[143]. However, little is known about which route is used by NGF to exert its therapeutic function.

The fluo-NGF developed in this thesis work could help in shedding light on this process, and follow its biodistribution in the brain, after the intranasal delivery.

5.2.5 NGF and proNGF: how do they interact with their receptors?

The intracellular signaling cascades activated by NGF binding to the TrkA and p75NTR receptors have been extensively investigated.

However, a clear description of the dynamics and interactions of the activated neurotrophin receptors, spanning from the initial lateral movements triggered at the plasma membrane to the internalization and transport processes, is still lacking. Moreover, the mechanisms by which proneurotrophins and neurotrophins transduce different signalling outcomes remain to be fully elucidated.

Thanks to the toolbox described here, the study of molecular interactions and dynamics occurring between proNGF, NGF, TrkA and p75NTR receptors could be investigated.

In Cattaneo's group, the short peptide tags technique has been exploited in order to achieve the fluorolabeling of NGF receptors exposed at the surface of living cells. A system allowing for the stable integration of the tagged constructs of TrkA and p75NTR receptors in either immortalized or post-mitotic primary cells has been developed[112]; notably, a doxycycline-dependent low expression of the two receptors was obtained. The tags have been exploited for a dual-color labelling procedure with two spectrally distinct fluorophores; this has made it possible to image single molecules of the two receptors in living neuroblastoma cells by TIRF microscopy[101].

Combining the toolbox developed in this thesis with that described above, it could be possible to achieve a quantitative description of the kinetics, dynamics and stoichiometry of any binary or ternary molecular complex formed at the cell plasma membrane by the proNGF or NGF binding to TrkA and p75NTR receptors.

5.2.6 Fluorescent BDNF

Since the tridimensional structure of neurotrophins is highly conserved[28], the method presented herein could in principle be applied to the other members of this protein family, like BDNF, NT3 and NT4. This project already started in the laboratory: the peptide sequence of YBBR tag is being inserted at the C-terminus of proBDNF sequence, in order to achieve fluorescent precursor and mature BDNF.

Differently from NGF, BDNF is secreted in an activity-dependent manner[145] and its transport in neurons has been described as both anterograde[146] and retrograde[147]. Moreover, activity-dependent conversion of proBDNF to mature BDNF has shown to be fundamental in mediating synaptic competition.

The study of proBDNF and BDNF transport in neurons could be useful in answering to several question regarding their trafficking and related signaling. For example, are the two forms of BDNF transported and secreted in the same manner? Or, is the proBDNF transported mainly in an anterograde way? Is the mature BDNF transported mainly in an retrograde manner? What are the roles of proBDNF secretion and of proteases action in modulating the neurotrophins transport?

The application of the site-specific labeling technique to the other neurotrophins could also allow the simultaneous study of their interaction on cell surface with their receptor.

External contributions

I thank my colleagues Dr. Laura Marchetti, Dr. Giovanni Signore and Carmine Di Rienzo for their support and useful discussions on this thesis work. In particular, I thank Dr. Laura Marchetti for her support in the molecular biology section, Dr. Giovanni Signore for the production of all the Co-A substrate conjugated and for helping me in all the chemical aspects of this work, and Carmine Di Rienzo and Dr. Stefano Luin for the the support in data analysis and microscopy experiments. I also thank Dr. Mariantonietta Calvello for her support in proteins production and purification, and Dr. Sandro Meucci for his help in setting up the microfluidic devices for cell culture.

List of publications

- T. De Nadai, L. Marchetti, C. Di Rienzo, M. Calvello, G. Signore, S. Meucci, A. Viegi, F. Beltram, S. Luin and A.Cattaneo. *Precursor and mature NGF live tracking: one versus many at a time in the axons.* Under revision

- L. Marchetti, S. Luin, F. Bonsignore, T. De Nadai, F. Beltram and A. Cattaneo. *Ligand-Induced Dynamics of Neurotrophin Receptors Investigated by Single-Molecule Imaging Approaches.* Int. J. Mol. Sci. 2015, 16, 1949-1979; doi:10.3390/ijms16011949

- L. Marchetti, T. De Nadai, F. Bonsignore, M. Calvello, G. Signore, A. Viegi, F. Beltram, S. Luin, A. Cattaneo. *Site-specific labeling of neurotrophins and their receptors via short and versatile peptide tags*. PLosOne, 2014.

Bibliography

1. Levi-Montalcini R, Hamburger V. A diffusible agent of mouse sarcoma, producing hyperplasia of sympathetic ganglia and hyperneurotization of viscera in the chick embryo. *J Exp Zool*. 1953;123(2):233-287. doi:10.1002/jez.1401230203.
2. Levi-Montalcini R. Effects of mouse tumor transplantation on the nervous system. *Ann NY Acad Sci*. 1952;55(1):330–343.
3. Hamburger V LMR. Proliferation, differentiation and degeneration on the spinal ganglia of the chick embryo under normal and experimental conditions. *J Exp Zool*. 1949;111: 457.
4. Levi-Montalcini R. The nerve growth factor 35 years later. *Science*1987;26(8):707-716.
5. Levi Montalcini R. THE NERVE GROWTH FACTOR. *Ann N Y Acad Sci*. 1964;118(149–170). doi:10.1111/j.1749-6632.1964.tb33978.x.
6. Barde Y, Edgar D, Thoenen H. Purification of a new neurotrophic factor from mammalian brain. *EMBO J*. 1982;I(5):549-553.
7. Maisonpierre P, Belluscio L, Squinto S, et al. Neurotrophin-3: a neurotrophic factor related to NGF and BDNF. *Science* 1990;247(4949):1446-1451. doi:10.1126/science.2321006.
8. Ibáñez CF, Ernfors P, Timmusk T, Ip NY, Arenas E, Yan- GD. Neurotrophin-4 is a target-derived neurotrophic factor for neurons of the trigeminal ganglion. *Development*. 1993;1353:1345-1353.
9. Acheson A1, Conover JC, Fandl JP, DeChiara TM, Russell M, Thadani A, Squinto SP, Yancopoulos GD LR. A BDNF autocrine loop in adult sensory neurons prevent cell death. *Nature*. 30(;374(6521):450-3.).
10. Wang X, Butowt R. Anterograde Axonal Transport , Transcytosis , and Recycling of Neurotrophic Factors The Concept of Trophic Currencies in Neural Networks. 2001;24:1-28.
11. Skaper SD. Nerve Growth Factor. 2001;24(2):183-199.
12. Edwards RH, Selby MJ, Garcia PD, Rutter WJ. Processing of the native nerve growth factor precursor to form biologically active nerve growth factor. *J Biol Chem*. 1988;263(14):6810-6815.
13. Hempstead BL. Dissecting the diverse actions of pro- and mature neurotrophins. *Curr Alzheimer Res*. 2006;3(1):19-24.

14. Fahnestock M, Yu G, Coughlin MD. ProNGF: a neurotrophic or an apoptotic molecule? *Prog Brain Res*. 2004;146:101-10. doi:10.1016/S0079-6123(03)46007-X.
15. Angeletti RH, Bradshawt RA. Nerve Growth Factor from Mouse Submaxillary Gland : Amino Acid Sequence. *Proc Natl Acad Sci U S A*. 1971;68(10):2417-2420.
16. Sofroniew M V, Howe CL, Mobley WC. Nerve Growth Factor Signaing, Neuroprotection, and Neural Repair. *Annu Rev Neurosci*. 2001.
17. Bruno MA, Cuello AC. Activity-dependent release of precursor nerve growth factor, conversion to mature nerve growth factor, and its degradation by a protease cascade. *Proc Natl Acad Sci U S A*. 2006;103(17):6735-40. doi:10.1073/pnas.0510645103.
18. Shooter EM. Early Days of the Nerve Growth Factor Proteins. *Annu Rev Neurosci*. 2001.
19. Paoletti F, Malerba F, Kelly G, Noinville S, Lamba D, Pastore A. Conformational Plasticity of proNGF. *PLoS One*. 2011;6(7):e22615. doi:10.1371/journal.pone.0022615.
20. Rattenholl A, Ruoppolo M, Flagiello A, et al. Pro-sequence assisted folding and disulfide bond formation of human nerve growth factor. *J Mol Biol*. 2001;305(3):523-33. doi:10.1006/jmbi.2000.4295.
21. Bradshaw RA, Murray-Rust J, Ibáñez CF, McDonald NQ, Lapatto R, Blundell TL. Nerve growth factor: structure/function relationships. *Protein Sci*. 1994;3(11):1901-13. doi:10.1002/pro.5560031102.
22. McDonald NQ1, Lapatto R, Murray-Rust J, Gunning J, Wlodawer A BT. New protein fold revealed by a 2.3-A resolution crystal structure of nerve growth factor. *Nature*. 1991;354(6352).:411-4.
23. Johnson D, Lanahan A, Buck CR, et al. Expression and structure of the human NGF receptor. *Cell*. 1986;47(4):545-554. doi:10.1016/0092-8674(86)90619-7.
24. Sutter A, Riopelle RJ. Nerve growth factor receptors. Characterization of two distinct classes of binding sites on chick embryo sensory ganglia cells. *J Biol Chem*. 1979;254:5972-5982.
25. Marchetti L, Luin S, Bonsignore F, De Nadai T, Beltram F, Cattaneo A. Ligand-Induced Dynamics of Neurotrophin Receptors Investigated by Single-Molecule Imaging Approaches. *Int J Mol Sci*. 2015;16:1949-1979. doi:10.3390/ijms16011949.
26. Casaletto JB, Mcclatchey AI. Spatial regulation of receptor tyrosine. *Nat Rev Cancer*. 2012;12(6):387-400. doi:10.1038/nrc3277.
27. Reichardt LF. Neurotrophin-regulated signalling pathways. *Philos Trans R Soc Lond B Biol Sci*. 2006;361(1473):1545-64. doi:10.1098/rstb.2006.1894.
28. Wiesmann C, Vos AM De. Cellular and Molecular Life Sciences Nerve growth factor : structure and function. *Cell Mol life Sci*. 2001;58:748-759.

29. Wiesmann C, Ultsch MH, Bass SH, de Vos a M. Crystal structure of nerve growth factor in complex with the ligand-binding domain of the TrkA receptor. *Nature*. 1999;401:184-188. doi:10.1038/43705.
30. Wiesmann C, Ultsch MH, Bass SH, de Vos AM. Crystal structure of nerve growth factor in complex with the ligand-binding domain of the TrkA receptor. *Nature*. 1999;401(6749):184-188.
31. Skeldal S, Matusica D, Nykjaer A, Coulson EJ. Proteolytic processing of the p75 neurotrophin receptor: A prerequisite for signalling? *Bioessays*. 2011;33(8):614-25. doi:10.1002/bies.201100036.
32. Roux PP, Barker PA. Neurotrophin signaling through the p75 neurotrophin receptor. *Prog neurobiol*. 2002;67:203-233.
33. Underwood CK, Coulson EJ. The p75 neurotrophin receptor. *Int J Biochem Cell Biol*. 2008;40(9):1664-8. doi:10.1016/j.biocel.2007.06.010.
34. He X-L, Garcia KC. Structure of nerve growth factor complexed with the shared neurotrophin receptor p75. *Science*. 2004;304(5672):870-5. doi:10.1126/science.1095190.
35. Willnow TE, Petersen CM, Nykjaer A. VPS10P-domain receptors - regulators of neuronal viability and function. *Nat Rev Neurosci*. 2008;9(12):899-909. doi:10.1038/nrn2516.
36. Wehrman T, He X, Raab B, Dukipatti A, Blau H, Garcia KC. Structural and Mechanistic Insights into Nerve Growth Factor Interactions with the TrkA and p75 Receptors. *Neuron*. 2007;53:25-38. doi:10.1016/j.neuron.2006.09.034.
37. Chang MS, Arevalo JC, Chao M V. Ternary complex with Trk, p75, and an ankyrin-rich membrane spanning protein. *J Neurosci Res*. 2004;78(August):186-192. doi:10.1002/jnr.20262.
38. Hempstead, B L.; Martin-Zanca, D; Kaplan, D R.; Parada, L F.; Chao M V. High-affinity NGF binding requires coexpression of the trk proto-oncogene and the low-affinity NGF receptor. *Nature*. 1991;350:678-683.
39. Barker P a. High Affinity Not in the Vicinity? *Neuron*. 2007;53:1-4. doi:10.1016/j.neuron.2006.12.018.
40. Covaceuszach S, Konarev PV, Cassetta A, et al. The Conundrum of the High-Affinity NGF Binding Site Formation Unveiled? *Biophys J*. 2015;108(3):687-697. doi:10.1016/j.bpj.2014.11.3485.
41. M Frade, J; Rodríguez-Tébar, A; Barde Y-A. Induction of cell death by endogenous nerve growth factor through its p75 receptor.pdf. *Nature*. 1996;383:166-168.
42. Casaccia-Bonnefil, P; Carter, Bruce D.; Dobrowsky, Rick T.; Chao M V. Death of oligodendrocytes mediated by the interaction of nerve growth factor with its recepto.pdf. *Nature*. 1996;383:716-719.
43. Lee R, Kermani P, Teng KK, Hempstead BL. Regulation of cell survival by secreted proneurotrophins. *Science*. 2001;294(5548):1945-8. doi:10.1126/science.1065057.

44. Nykjaer A, Lee R, Teng KK, Jansen P. Sortilin is essential for proNGF-induced neuronal cell death. *Nature*. 2004;427:15-20. doi:10.1038/nature02289.
45. Feng D, Kim T, Özkan E, et al. Molecular and Structural Insight into proNGF Engagement of p75NTR and Sortilin. *J Mol Biol*. 2010;396(4):967-984. doi:10.1016/j.jmb.2009.12.030.
46. Wyatt S, Davies AM. Regulation of expression of mRNAs encoding the nerve growth factor receptors p75 and trkA in developing sensory neurons. *Development*. 1993;647:635-647.
47. Yoon SO, Casaccia-bonnefil P, Carter B, Chao M V. Competitive Signaling Between TrkA and p75 Nerve Growth Factor Receptors Determines Cell Survival. *J Neurosci*. 1998;18(9):3273-3281.
48. Clewes O, Fahey MS, Tyler SJ, et al. Human ProNGF: biological effects and binding profiles at TrkA, P75NTR and sortilin. *J Neurochem*. 2008;107(4):1124-1135. doi:10.1111/j.1471-4159.2008.05698.x.
49. Suter U, Heymach J V, Shooter EM. Two conserved domains in the NGF propeptide are necessary and sufficient for the biosynthesis of correctly processed and biologically active NGF. *EMBO J*. 1991;10(9):2395-400.
50. Fahnestock M, Michalski B, Xu B, Coughlin MD. The precursor pro-nerve growth factor is the predominant form of nerve growth factor in brain and is increased in Alzheimer's disease. *Mol Cell Neurosci*. 2001;18(2):210-220. doi:10.1006/mcne.2001.1016.
51. Wang Y-J, Valadares D, Sun Y, et al. Effects of proNGF on neuronal viability, neurite growth and amyloid-beta metabolism. *Neurotox Res*. 2010;17(3):257-67. doi:10.1007/s12640-009-9098-x.
52. Al-Shawi R, Hafner A, Olson J, et al. Neurotoxic and neurotrophic roles of proNGF and the receptor sortilin in the adult and ageing nervous system. *Eur J Neurosci*. 2008;27:2103-2114. doi:10.1111/j.1460-9568.2008.06152.x.
53. Fahnestock M, Yu G, Michalski B, et al. The nerve growth factor precursor proNGF exhibits neurotrophic activity but is less active than mature nerve growth factor. *J Neurochem*. 2004;89(3):581-92. doi:10.1111/j.1471-4159.2004.02360.x.
54. Pedraza CE, Podlesniy P, Vidal N, et al. Pro-NGF isolated from the human brain affected by Alzheimer's disease induces neuronal apoptosis mediated by p75NTR. *Am J Pathol*. 2005;166(2):533-43. doi:10.1016/S0002-9440(10)62275-4.
55. Beattie MS, Harrington AW, Lee R, et al. ProNGF induces p75-mediated death of oligodendrocytes following spinal cord injury. *Neuron*. 2002;36(3):375-86.
56. Capsoni S, Ugolini G, Comparini a, Ruberti F, Berardi N, Cattaneo a. Alzheimer-like neurodegeneration in aged antinerve growth factor

transgenic mice. *Proc Natl Acad Sci U S A*. 2000;97:6826-6831. doi:10.1073/pnas.97.12.6826.

57. S. Capsoni A.Cattaneo. On the Molecular Basis Linking Nerve Growth Factor (NGF) to Alzheimer's Disease. *Cell Mol Neurobiol*. 2006;26(4-6,):pp 617-631.
58. Tiveron C, Fasulo L, Capsoni S, et al. ProNGF\NGF imbalance triggers learning and memory deficits, neurodegeneration and spontaneous epileptic-like discharges in transgenic mice. *Cell Death Differ*. 2013;20(8):1017-30. doi:10.1038/cdd.2013.22.
59. Hendry I., Stach R. Characteristic of the retrograde axonal transport system for nerve growth factor in the sympatetic nervous system. *Brain Res*. 1974;82:117-128.
60. Max SR, Schwab M, Dumas M, Thoenen H. Retrograde axonal transport of nerve growth factor in the ciliary ganglion of the chick and the rat. *Brain Res*. 1978;159(2):411-415. doi:10.1016/0006-8993(78)90549-8.
61. Heumann R., Schwab M and Thoenen H. A second messenger required for nerve growth factor biological activity? 1981:Nature 292.
62. Claude P, Hawrot E, Dunis DA CR. Binding, internalization, and retrograde transport of 125I-nerve growth factor in cultured rat sympathetic neurons. *J Neurosci*. 1982;4:431-4.
63. Ure DR, Campenot RB. Retrograde Transport and Steady-State Distribution of I-Nerve Growth Factor in Rat Sympathetic Neurons in Compartmented Cultures. 1997;17(4):1282-1290.
64. Tani T, Miyamoto Y, Fujimori KE, Taguchi T, Yanagida T, Sako Y. Trafficking of a Ligand-Receptor Complex on the Growth Cones as an Essential Step for the Uptake of Nerve Growth Factor at the Distal End of the Axon : A Single-Molecule Analysis. 2005;25(9):2181-2191. doi:10.1523/JNEUROSCI.4570-04.2005.
65. Nomura M, Nagai T, Harada Y, Tani T. Facilitated intracellular transport of TrkA by an interaction with nerve growth factor. *Dev Neurobiol*. 2011;71(7):634-649. doi:10.1002/dneu.20879.
66. Echarte MM, Bruno L, Arndt-Jovin DJ, Jovin TM, Pietrasanta LI. Quantitative single particle tracking of NGF-receptor complexes: Transport is bidirectional but biased by longer retrograde run lengths. *FEBS Lett*. 2007;581(16):2905-2913. doi:10.1016/j.febslet.2007.05.041.
67. Lalli G, Schiavo G. Analysis of retrograde transport in motor neurons and neurotrophin receptor p75 NTR. *JCB Rep*. 2002;156(2):233-239. doi:10.1083/jcb.200106142.
68. Cui B, Wu C, Chen L, et al. One at a time, live tracking of NGF axonal transport using quantum dots. *Proc Natl Acad Sci U S A*. 2007;104(34):13666-13671.
69. Sundara Rajan S, Vu TQ. Quantum dots monitor TrkA receptor dynamics in the interior of neural PC12 cells. *Nano Lett*. 2006;6(9):2049-2059.

70. Jullien J, Guili V, Derrington EA, Darlix JL, Reichardt LF RB. Trafficking of TrkA-green fluorescent protein chimerae during nerve growth factor-induced differentiation. *J Biol Chem*. 2003;278(10):8706-8716. doi:10.1074/jbc.M202401200.Trafficking.
71. N. Hirashima, M.Nishio MN. Intracellular Dynamics of a High Affinity NGF Receptor TrkA in PC12 Cell. *Biol Pharm Bull*. 2000;23(9):1097-1099.
72. Wu C, Ramirez A, Cui B, et al. A functional dynein-microtubule network is required for NGF signaling through the Rap1/MAPK pathway. *Traffic*. 2007;8(11):1503-20. doi:10.1111/j.1600-0854.2007.00636.x.
73. Heerssen HM, Pazyra MF, Segal R A. Dynein motors transport activated Trks to promote survival of target-dependent neurons. *Nat Neurosci*. 2004;7(6):596-604. doi:10.1038/nn1242.
74. Chowdary PD, Che DL, Cui B. Neurotrophin signaling via long-distance axonal transport. *Annu Rev Phys Chem*. 2012;63:571-94. doi:10.1146/annurev-physchem-032511-143704.
75. Schmieg N, Menendez G, Schiavo G, Terenzio M. Signalling endosomes in axonal transport: Travel updates on the molecular highway. *Semin Cell Dev Biol*. 2014;27:32-43. doi:10.1016/j.semcdb.2013.10.004.
76. Restani L, Giribaldi F, Manich M, et al. Botulinum Neurotoxins A and E Undergo Retrograde Axonal Transport in Primary Motor Neurons. *PLoS Pathog*. 2012;8(12). doi:10.1371/journal.ppat.1003087.
77. Lalli G, Schiavo G. Analysis of retrograde transport in motor neurons reveals common endocytic carriers for tetanus toxin and neurotrophin receptor p75NTR. *J Cell Biol*. 2002;156(2):233-9. doi:10.1083/jcb.200106142.
78. Sharma N, Deppmann CD, Harrington AW, et al. Long-distance control of synapse assembly by target-derived NGF. *Neuron*. 2010;67(3):422-34. doi:10.1016/j.neuron.2010.07.018.
79. Delcroix JD, Valletta JS, Wu C, Hunt SJ, Kowal AS, Mobley WC. NGF signaling in sensory neurons: Evidence that early endosomes carry NGF retrograde signals. *Neuron*. 2003;39(1):69-84.
80. Deinhardt K, Reversi A, Berninghausen O, Hopkins CR, Schiavo G. Neurotrophins Redirect p75NTR from a clathrin-independent to a clathrin-dependent endocytic pathway coupled to axonal transport. *Traffic*. 2007;8(12):1736-49. doi:10.1111/j.1600-0854.2007.00645.x.
81. Doherty GJ, McMahon HT. Mechanisms of endocytosis. *Annu Rev Biochem*. 2009;78:857-902. doi:10.1146/annurev.biochem.78.081307.110540.
82. Howe CL, Valletta JS, Rusnak AS, Mobley WC. NGF signaling from clathrin-coated vesicles: Evidence that signaling endosomes serve as a platform for the Ras-MAPK pathway. *Neuron*. 2001;32(5):801-814.

83. Bronfman FC, Tcherpakov M, Jovin TM, Fainzilber M. Ligand-induced internalization of the p75 neurotrophin receptor: a slow route to the signaling endosome. *J Neurosci*. 2003;23(8):3209-3220. doi:23/8/3209 [pii].
84. Ye H, Kuruvilla R, Zweifel LS, Ginty DD. Evidence in support of signaling endosome-based retrograde survival of sympathetic neurons. *Neuron*. 2003;39(1):57-68.
85. Shao Y, Akmentin W, Toledo-Aral JJ, et al. Pincher, a pinocytic chaperone for nerve growth factor/TrkA signaling endosomes. *J Cell Biol*. 2002;157(4):679-691. doi:10.1083/jcb.200201063.
86. Weible MW, Hendry I a. What is the importance of multivesicular bodies in retrograde axonal transport in vivo? *J Neurobiol*. 2004;58(2):230-43. doi:10.1002/neu.10318.
87. Harrington AW, Hillaire CS, Zweifel LS, Glebova NO. Recruitment of actin modifiers to TrkA endosomes governs retrograde NGF signaling and survival. *Cell*. 2012;146(3):421-434. doi:10.1016/j.cell.2011.07.008.Recruitment.
88. Frazier WA, Boyd LF, Bradshaw A. Properties of the Specific Binding of 125 I-Nerve Growth Factor to Responsive Peripheral Neurons Properties of the Specific to Responsive Peripheral Binding Neurons * of ‘ 251-Nerve Growth Factor. *J Biol Chem*. 1974;249:5513-5519.
89. Rosenberg MB, Hawrot, Edward and XOB. Receptor Binding Actiy ities of Biotinylated Derivatii es of P-Nerve Growth Factor. *J Neurochem*. 1986.
90. Bronfman FC, Tcherpakov M, Jovin TM, Fainzilber M. Ligand-induced internalization of the p75 neurotrophin receptor: a slow route to the signaling endosome. *J Neurosci*. 2003;23(8):3209-3220.
91. Shibata SC, Hibino K, Mashimo T, Yanagida T, Sako Y. Formation of signal transduction complexes during immobile phase of NGFR movements. *Biochem Biophys Res Commun*. 2006;342(1):316-22. doi:10.1016/j.bbrc.2006.01.126.
92. Xie Y, Ye L, Zhang X, et al. Transport of nerve growth factor encapsulated into liposomes across the blood-brain barrier: In vitro and in vivo studies. *J Control Release*. 2005;105:106-119. doi:10.1016/j.jconrel.2005.03.005.
93. Vu TQ, Maddipati R, Blute T a, Nehilla BJ, Nusblat L, Desai T a. Peptide-conjugated quantum dots activate neuronal receptors and initiate downstream signaling of neurite growth. *Nano Lett*. 2005;5(4):603-7. doi:10.1021/nl047977c.
94. Mowla SJ, Pareek S, Farhadi HF, et al. Differential sorting of nerve growth factor and brain-derived neurotrophic factor in hippocampal neurons. *J Neurosci*. 1999;19(6):2069-2080.
95. Kawaja MD, Smithson LJ, Elliott J, et al. Nerve growth factor promoter activity revealed in mice expressing enhanced green fluorescent protein. *J Comp Neurol*. 2011;519(13):2522-2545. doi:10.1002/cne.22629.

96. Sung K, Maloney MT, Yang J, Wu C. A novel method for producing mono-biotinylated, biologically active neurotrophic factors: An essential reagent for single molecule study of axonal transport. *J Neurosci Methods*. 2011;200(2):121-128. doi:10.1016/j.jneumeth.2011.06.020.
97. Yin J, Straight PD, Mcloughlin SM, et al. Genetically encoded short peptide tag for versatile protein labeling by Sfp phosphopantetheinyl transferase. *Proc Natl Acad Sci U S A*. 2005;102(44):15818-15820.
98. Yin J, Lin AJ, Golan DE, Walsh CT. Site-specific protein labeling by Sfp phosphopantetheinyl transferase. *Nat Protoc*. 2006;1(1):280-5. doi:10.1038/nprot.2006.43.
99. Zhou Z, Cironi P, Lin AJ, Xu Y, Hrvatin S, Golan DE. Genetically encoded short peptide tag for versatile protein labeling by Sfp phosphopantetheinyl transferase. *Acs Chem Biol*. 2007;2(5):337-346.
100. Zhou Z, Koglin A, Wang Y, McMahon AP, Walsh CT. An eight residue fragment of an acyl carrier protein suffices for post-translational introduction of fluorescent pantetheinyl arms in protein modification in vitro and in vivo. *J Am Chem Soc*. 2008;130(30):9925-30. doi:10.1021/ja802657n.
101. Marchetti L, De Nadai T, Bonsignore F, et al. Site-Specific Labeling of Neurotrophins and Their Receptors via Short and Versatile Peptide Tags. *PLoS One*. 2014;9(11):e113708. doi:10.1371/journal.pone.0113708.
102. Paoletti F, Konarev P V, Covaceuszach S, et al. Structural and functional properties of mouse proNGF. *Biochem Soc Trans*. 2006;34(Pt 4):605-606.
103. Marchetti L, Callegari A, Luin S, et al. Ligand signature in the membrane dynamics of single TrkA receptor molecules. *J Cell Sci*. 2013;126(Pt 19):4445-56. doi:10.1242/jcs.129916.
104. Greene L a, Tischler a S. Establishment of a noradrenergic clonal line of rat adrenal pheochromocytoma cells which respond to nerve growth factor. *Proc Natl Acad Sci U S A*. 1976;73(7):2424-8..
105. Mosmann T. Rapid colorimetric assay for cellular growth and survival: application to proliferation and cytotoxicity assays. *J Immunol Methods*. 1983;65(1-2):55-63. Available at:
106. Park JW, Vahidi B, Taylor AM, Rhee SW, Jeon NL. Microfluidic culture platform for neuroscience research. *Nat Protoc*. 2006;1(4):2128-2136. doi:10.1038/nprot.2006.316.
107. Parthasarathy R. Rapid, accurate particle tracking by calculation of radial symmetry centers. *Nat Methods*. 2012;9(7):724-6. doi:10.1038/nmeth.2071.
108. Griffin B a. Specific Covalent Labeling of Recombinant Protein Molecules Inside Live Cells. *Science* 1998;281(5374):269-272. doi:10.1126/science.281.5374.269.
109. Beckett D, Kovaleva E, Schatz PJ. A minimal peptide substrate in biotin holoenzyme synthetase-catalyzed biotinylation. *Protein Sci*. 1999;8(4):921-9. doi:10.1110/ps.8.4.921.

110. Chen I, Howarth M, Lin W, Ting AY. Site-specific labeling of cell surface proteins with biophysical probes using biotin ligase. *Nat Methods*. 2005;2(2):99-104. doi:10.1038/NMETH735.
111. Yin J, Liu F, Li X, Walsh CT. Labeling proteins with small molecules by site-specific posttranslational modification. *J Am Chem Soc*. 2004;126(25):7754-5. doi:10.1021/ja047749k.
112. Callegari A, Luin S, Marchetti L, Duci A, Cattaneo A, Beltram F. Single particle tracking of acyl carrier protein (ACP)-tagged TrkA receptors in PC12nnr5 cells. *J Neurosci Methods*. 2012;204(1):82-86. doi:10.1016/j.jneumeth.2011.10.019.
113. Zhou Z, Cironi P, Lin AJ, Xu Y, Hrvatin S, Golan DE. Genetically Encoded Short Peptide Tags for Orthogonal Protein Labeling by Sfp and Acp Phosphopantetheinyl Transferases. *Acs Chem Biol*. 2007;2(5):337-346.
114. Rattenholl A, Lilie H, Grossmann A, Stern A, Schwarz E, Rudolph R. The pro-sequence facilitates folding of human nerve growth factor from Escherichia coli inclusion bodies. 2001;3303:3296-3303.
115. Zou LMY. TF-1 Cell Proliferation Assay Method for Estimating Bioactivity of Nerve Growth Factor. 2013;5154:32-37.
116. Pagadala P. Structural and Functional Studies of Pro-Nerve Growth Factor. 2008. Thesis Degree of Doctor of Philosophy in the School of Graduate and Postdoctoral Studies Rosalind Franklin University of Medicine and Science UMI Number: 3304174 UM
117. Howard L, Wyatt S, Nagappan G, Davies AM. ProNGF promotes neurite growth from a subset of NGF-dependent neurons by a p75NTR-dependent mechanism. *Development*. 2013;140(10):2108-17. doi:10.1242/dev.085266.
118. Lebrun-Julien F, Bertrand MJ, De Backer O, et al. ProNGF induces TNFalpha-dependent death of retinal ganglion cells through a p75NTR non-cell-autonomous signaling pathway. *Proc Natl Acad Sci U S A*. 2010;107(8):3817-3822. doi:10.1073/pnas.0909276107.
119. Tani T, Miyamoto Y, Fujimori KE, et al. Trafficking of a ligand-receptor complex on the growth cones as an essential step for the uptake of nerve growth factor at the distal end of the axon: a single-molecule analysis. *J Neurosci*. 2005;25(9):2181-91. doi:10.1523/JNEUROSCI.4570-04.2005.
120. Wombacher R, Cornish VW. Chemical tags: applications in live cell fluorescence imaging. *J Biophotonics*. 2011;4(6):391-402. doi:10.1002/jbio.201100018.
121. Campenot RB. Local control of neurite development by nerve growth factor Cell Biology :1977;74(10):4516-4519.
122. Taylor AM, Rhee SW, Tu CH, Cribbs DH, Cotman CW. Microfluidic Multicompartment Device for Neuroscience Research. Langmuir. 2003;19(5):1551-1556. doi:10.1021/la026417
123. Yip HK, Johnson EM. Developing dorsal root ganglion neurons require trophic support from their central processes: evidence for a role of

retrogradely transported nerve growth factor from the central nervous system to the periphery. *Proc Natl Acad Sci U S A*. 1984;81(19):6245-9.
124. Goedert M, Otten U, Hunt SP, et al. Biochemical and anatomical effects of antibodies against nerve growth factor on developing rat sensory ganglia. *Proc Natl Acad Sci U S A*. 1984;81(5):1580-4.
125. Casaccia-Bonnefil P, Gu C, Khursigara G, Chao M V. P75 Neurotrophin Receptor As a Modulator of Survival and Death Decisions. *Microsc Res Tech*. 1999;45(4-5):217-24. doi:10.1002/(SICI)1097-0029(19990515/01)45:4/5<217::AID-JEMT5>3.0.CO;2-5.
126. Barbacid M. The Trk family of neurotrophin receptors. *J Neurobiol*. 1994;25(11):1386-403. doi:10.1002/neu.480251107.
127. Fang X, Djouhri L, McMullan S, et al. trkA is expressed in nociceptive neurons and influences electrophysiological properties via Nav1.8 expression in rapidly conducting nociceptors. *J Neurosci*. 2005;25(19):4868-78. doi:10.1523/JNEUROSCI.0249-05.2005.
128. Harrington AW, Ginty DD. Long-distance retrograde neurotrophic factor signalling in neurons. *Nat Rev Neurosci*. 2013;14(3):177-87. doi:10.1038/nrn3253.
129. Melli G, Höke A. Dorsal Root Ganglia Sensory Neuronal Cultures: a tool for drug discovery for peripheral neuropathies. *Expert Opin Drug Discov*. 2009;4(10):1035-1045. doi:10.1517/17460440903266829.
130. Pagadala PC, Dvorak L a, Neet KE. Construction of a mutated pro-nerve growth factor resistant to degradation and suitable for biophysical and cellular utilization. *Proc Natl Acad Sci U S A*. 2006;103(47):17939-43. doi:10.1073/pnas.0604139103.
131. Campenot RB. NGF Uptake and Retrograde Signaling Mechanisms in Sympathetic Neurons in Compartmented Cultures. *Results Probl Cell Differ*. 2009:141-158. doi:10.1007/400.
132. Iulita MF, Do Carmo S, Ower AK, et al. Nerve growth factor metabolic dysfunction in Down's syndrome brains. *Brain*. 2014;137(Pt 3):860-72. doi:10.1093/brain/awt372.
133. Cui B, Wu C, Chen L, et al. One at a time , live tracking of NGF axonal transport using quantum dots. Proc. Natl. Acad. Sci. U. S. A. 104, 13666–13671 (2007).
134. Yu T, Calvo L, Anta B, et al. Regulation of trafficking of activated TrkA is critical for NGF- mediated functions. *Traffic*. 2011;12(4):521-534. doi:10.1111/j.1600-0854.2010.01156.x.Regulation.
135. Deinhardt K, Salinas S, Verastegui C, et al. Rab5 and Rab7 Control Endocytic Sorting along the Axonal Retrograde Transport Pathway. *Neuron*. 2006;52:293-305. doi:10.1016/j.neuron.2006.08.018.
136. Paoletti F, Covaceuszach S, Konarev P V, et al. Intrinsic structural disorder of mouse proNGF. *Proteins*. 2009;75(4):990-1009. doi:10.1002/prot.22311.

137. Edgar JM, McLaughlin M, Yool D, et al. Oligodendroglial modulation of fast axonal transport in a mouse model of hereditary spastic paraplegia. *J Cell Biol*. 2004;166:121-131. doi:10.1083/jcb.200312012.
138. Chapman AL, Bennett EJ, Ramesh TM, De Vos KJ, Grierson AJ. Axonal Transport Defects in a Mitofusin 2 Loss of Function Model of Charcot-Marie-Tooth Disease in Zebrafish. *PLoS One*. 2013;8(6). doi:10.1371/journal.pone.0067276.
139. Gunawardena S, Goldstein LSB. Disruption of axonal transport and neuronal viability by amyloid precursor protein mutations in Drosophila. *Neuron*. 2001;32:389-401. doi:10.1016/S0896-6273(01)00496-2.
140. Bilsland LG, Sahai E, Kelly G, Golding M, Greensmith L, Schiavo G. Deficits in axonal transport precede ALS symptoms in vivo. *Proc Natl Acad Sci U S A*. 2010;107(47):20523-20528. doi:10.1073/pnas.1006869107.
141. Talegaonkar S, Mishra PR. Intranasal delivery : An approach to bypass the blood brain barrier. *Indian J Pharmacol* 2004;36(3) 140-147.
142. Malerba F, Paoletti F, Capsoni S, Cattaneo A. Intranasal delivery of therapeutic proteins for neurological diseases. *Expert Opin Drug Discov*. 2011;8(10):1277-1296.
143. Capsoni S, Marinelli S, Ceci M, et al. Intranasal "' painless '" Human Nerve Growth Factors Slows Amyloid Neurodegeneration and Prevents Memory Deficits in App X PS1 Mice. *PLoS One*. 2012;7(5):e37555. doi:10.1371/journal.pone.0037555.
144. Capsoni S, Cattaneo A. On the Molecular Basis Linking Nerve Growth Factor (NGF) to Alzheimer ' s Disease. *Cell Mol Neurobiol*. 2006;26(August):619-633. doi:10.1007/s10571-006-9112-2.
145. Je HS, Yang F, Ji Y, Nagappan G, Hempstead BL, Lu B. Role of pro-brain-derived neurotrophic factor (proBDNF) to mature BDNF conversion in activity-dependent competition at developing neuromuscular synapses. *Proc Natl Acad Sci*. 2012;109:15924-15929. doi:10.1073/pnas.1207767109.
146. Butowt R, Von Bartheld CS. Anterograde axonal transport of BDNF and NT-3 by retinal ganglion cells: Roles of neurotrophin receptors. *Mol Cell Neurosci*. 2005;29:11-25. doi:10.1016/j.mcn.2005.02.004.
147. Xie W, Zhang K, Cui B. Functional characterization and axonal transport of quantum dot labeled BDNF. *Integr Biol*. 2012;4:953. doi:10.1039/c2ib20062g.

Acknowledgements

I would like to express my gratitude to the following people for their support and assistance during this research experience.

My first acknowledgements go to my advisor, Professor Antonino Cattaneo: I had the luck of working with him during these years of PhD study. I would like to thank him for giving me the opportunity to work in the BioLab and NEST research centers: his constant support and precious suggestions stimulated me many times in improving my work and in succeeding in this research project.

I would also like to thank Antonella Calvello, Laura Marchetti, Giovanni Signore and Carmine Di Rienzo for their good friendship and for closely helping me in organizing the measurements and in interpreting experimental results. During these years I also benefited from stimulating discussions with Simona Capsoni, Stefano Luin, Francesca Malerba and Francesca Paoletti, and I get this chance to thank them.

Of course I would say a real big “thank you!” to all the people I had the pleasure to meet at the NEST and BioLab laboratories and at Scuola Normale Superiore, who helped me in many ways.

Last but not least, a mention goes to all my friends and my family: they did not contribute directly to this work but they were part of my everyday life, giving me the strength to face many difficulties.